

**QUANTUM CHEMICAL INVESTIGATION OF REACTIONS OF  
ATOMIC CARBON WITH WATER AND METHANOL**

**A THESIS SUBMITTED TO  
THE GRADUATE SCHOOL OF NATURAL AND APPLIED SCIENCES  
OF  
MIDDLE EAST TECHNICAL UNIVERSITY**

**BY**

**YAVUZ DEDE**

**IN PARTIAL FULFILLMENT OF THE REQUIREMENTS FOR  
THE DEGREE OF DOCTOR OF PHILOSOPHY**

**IN**

**CHEMISTRY**

**NOVEMBER 2007**

Approval of the thesis:

**QUANTUM CHEMICAL INVESTIGATION OF REACTIONS OF ATOMIC  
CARBON WITH WATER AND METHANOL**

submitted by **YAVUZ DEDE** in partial fulfillment of the requirements for the degree  
of **Doctor of Philosophy in Chemistry Department, Middle East Technical  
University** by,

Prof. Dr. Canan ÖZGEN  
Dean, Graduate School of Natural and Applied Sciences

\_\_\_\_\_

Prof. Dr. M. Ahmet ÖNAL  
Head of Department, Chemistry

\_\_\_\_\_

Prof. Dr. İlker ÖZKAN  
Supervisor, Chemistry Dept., METU

\_\_\_\_\_

**Examining Committee Members:**

Prof. Dr. Engin U. Akkaya  
Chemistry Dept., Bilkent University

\_\_\_\_\_

Prof. Dr. İlker Özkan  
Chemistry Dept., METU

\_\_\_\_\_

Assoc. Prof. Dr. Ulrike Salzner  
Chemistry Dept., Bilkent University

\_\_\_\_\_

Prof. Dr. Metin Zora  
Chemistry Dept., METU

\_\_\_\_\_

Asst. Prof. Dr. M. Fatih Danişman  
Chemistry Dept., METU

\_\_\_\_\_

Date:

\_\_\_\_\_

I hereby declare that all information in this document has been obtained and presented in accordance with academic rules and ethical conduct. I also declare that, as required by these rules and conduct, I have fully cited and referenced all material and results that are not original to this work.

Name, Last name : Yavuz DEDE

Signature:

## ABSTRACT

### QUANTUM CHEMICAL INVESTIGATION OF REACTIONS OF ATOMIC CARBON WITH WATER AND METHANOL

DEDE, Yavuz  
Ph.D., Department of Chemistry  
Supervisor: Prof. Dr. İlker Özkan

November 2007, 176 pages

Reactions of singlet ( $^1S$  and  $^1D$ ) and triplet ( $^3P$ ) carbon atoms with water, and  $^1D$  and  $^3P$  carbon atoms with methanol were studied computationally. In the water and methanol systems, the carbon vapor containing a mixture of  $C(^1S)$ ,  $C(^1D)$ , and  $C(^3P)$  atoms, is predicted to react by primarily interacting with the oxygen, OH bond and CH bond of the substrate mainly with the  $^1D$  state. While  $C(^1S)$  was proven to be unreactive  $C(^3P)$  can hardly be supported to be reactive, and can safely be defined as unreactive. The major product, CO forms as a result of oxygen abstraction, which is observed as a fast, energetically quite favorable process. The scheme of this oxygen abstraction is promising to be applicable to substrates with the general formula  $R_1-O-R_2$  i.e. water, alcohols, and ethers. OH insertion, both for water and methanol, yields trappable carbenes; the carbene being a key species on the distribution of the end products. Water matrix trapping the carbene opens the path to the formation of formaldehyde; and exhibits a prototype reaction for the formation of dialkoxymethanes. Gas phase product spectrum from the reactions are broader,

due to the accessibility of the routes originating from the otherwise trapped intermediates; and the excess energy of the reactions being carried by them. In the condensed phase the very early and rapid reactions seem to have chance, the subsequent rearrangements are hard to occur. The conclusions thus far apply to the reactions in the gas phase as well as in condensed phases involving inert matrices; and the experimental isolation of the species is highly dependent on the ability of the medium to trap the intermediates via effective transfer of excess energy. Due to the large excess energies of intermediates involved, subsequent reactions are fast; of the order  $10^{13} s^{-1}$  from kinetic rate calculations. In the absence of efficient transfer of non-fixed energies to the surrounding medium, all of the reaction paths will conclude with irreversible dissociation reactions. Plausible mechanisms for all the experimentally observed products are predicted. The results are in agreement with the available experimental data.

**Keywords:** Atomic Carbon, Water, Methanol, Multi Reference Perturbation Theory (MRMP), Coupled Cluster Singles Doubles (CCSD).

## ÖZ

### ATOMİK KARBONUN SU VE METANOLLE TEPKİMELERİNİN KUVANTUM KİMYASAL YÖNTEMLERLE İNCELENMESİ

DEDE, Yavuz  
Doktora, Kimya Bölümü  
Tez Yöneticisi: Prof. Dr. İlker Özkan

Kasım 2007, 176 sayfa

Tekli (1S and 1D) ve üçlü (3P) haldeki atomik karbonun su ve metanolla tepkimeleri kuramsal kimya metotları ile incelendi. Su ve metanol sistemlerinde, C(1S), C(1D), and C(3P) türlerini içeren karbon buharının asıl olarak C(<sup>1</sup>D) hali ile, sübstrat molekülündeki oksijen, OH bağı ve CH bağı ile etkileşime girerek tepkime verdiği anlaşıldı. C(<sup>1</sup>S) atomlarının reaktif olmadığı ve C(<sup>3</sup>P) halinin ise reaktifliğinin şüpheli olduğu ortaya çıkarıldı. Ana ürün olan CO'nun çok hızlı ve enerjetik olarak oldukça elverişli bir yol olan oksijen abstraksiyonu sonucu oluştuğu bulundu. Bu oksijen abstraksiyonu mekanizması R<sub>1</sub>-O-R<sub>2</sub> genel formülündeki tüm maddeler (su, alkoller ve eterler) için uygulanabilir olması açısından umut vericidir. OH girişi hem su hem de metanol tepkimelerinde ortamda tutulabilme yatkınlığında bulunan karbenleri oluşturmaktadır ve bu karbenlerin davranışları son ürünlerin çeşitlilik ve dağılımları açısından oldukça önemlidir. Su ortamı karbeni deaktive ederek formaldehit oluşumunu sağlamakta ve su ile olan tepkimelerde ortaya çıkarılan

prototip dihidroksimetan oluşumu dialkoksimetanların oluşum mekanizmalarına ışık tutmaktadır. Gaz fazında gerçekleşen tepkimelerde ürün dağılımları daha fazla çeşitlilik göstermekte olup bunun sebebi yoğun fazdaki tepkimelerde bazı ara ürünlerin ortmada tutularak bir takım ürünlere olan geçişlerin kapalı hale gelmesidir. Yoğun fazda tepkimenin hemen başlangıcında gerçekleşen hızlı yolların operatif olduğu anlaşılmıştır. Bu incelemeler sayesinde elde edilen sonuçlar hem yoğun fazda hem de gaz fazındaki tepkimelerde uygulanabilir durumdadır. Bir ürününün deneysel olarak gözlemlenmesi ise onun fazla enerjisini ortamda etkin bir şekilde kaybederek deaktive olmasından kaynaklanmaktadır. Karbon atomu tepkimelerinin ara ürünlere yüklediği yüksek enerjiler nedeniyle tepkimeler oldukça hızlı gerçekleşmekte, kinetik hesaplamalardan elde edilen hız sabitleri  $10^{13} s^{-1}$  mertebesinde görünmektedir. Ortama etkin enerji transferi söz konusu olmayan durumlarda incelenen tepkimelerin, geri dönüşsüz ayrışma reaksiyonları olduğu ortaya çıkarılmıştır. İncelenen tepkimeler göstermektedir ki su ve metanolün atomik karbon ile oluşturduğu tüm ürünleri açıklayabilen mekanizmalar önerilmiştir ve elde edilen sonuçlar deneysel veriler ile tatmin edici bir uyum içerisindedir.

**Anahtar Kelimeler:** Atomik Karbon, Su, Metanol, Çok Referanslı Perturbasyon Teorisi (MRMP), Tekli ve İkili Eşleşmiş Küme (CCSD).

*To Yasemin...*

*To real friends, if there exists any...*

## ACKNOWLEDGEMENTS

I thank to all past and present members of the Computational Chemistry Laboratory for their friendship and moral support. Dr. Armağan KINAL, and Uğur BOZKAYA are gratefully acknowledged.

Secretary General of Turkish Standards Institute, Rasim YILMAZ is gratefully acknowledged for unconditionally supporting my scientific studies. I am indebted to him.

Prof. Dr. Fatma SEVİN DÜZ of Hacettepe University kindly shared information and answered my questions about her experimental studies concerning carbon arc reactions. I appreciate her help.

It is a pleasure to complete this study with Dr. Fatih DANIŞMAN, being a jury member. He helped me a lot in a limited time.

I want to express my thanks to Prof. Dr. Metin ZORA for being helpful and friendly, during my graduate studies at METU.

I sincerely thank to Prof. Dr. Engin U. AKKAYA for his motivative existence nearby, whenever I need; and I needed quite often. It is a pleasure to study with him.

I very much appreciate the helps, comments, suggestions and friendly behavior of Assoc. Prof. Dr. Ulrike SALZNER. In the lonely world of theoretical/computational chemists in Turkey her presence was a chance for me.

I am grateful to my supervisor Prof. Dr. İlker ÖZKAN for the completion of this study. Without his private communications, for which he wasted lots of hours for me, I would not achieve an understanding of the background material and the computation processes. His continuous advice, criticism, support and guidance throughout the study deserves special appreciation. I admire his style of interpreting the data and facts with one of the finest criticism I have ever seen.

## TABLE OF CONTENTS

ABSTRACT .....	iv
ÖZ.....	vi
ACKNOWLEDGEMENTS .....	ix
LIST OF TABLES .....	xiii
LIST OF FIGURES.....	xiv
LIST OF ABBREVIATIONS .....	xvii
CHAPTER I INTRODUCTION .....	1
1.1 What is the Motivation to Study Carbon Atom Reactions.....	1
1.2 Electronic Structure of Carbon Atoms .....	3
1.3 Examples of Important Systems with Carbon Atom Reactions .....	4
1.3.1 Interstellar and Solar Chemistry.....	4
1.3.2 Pre-Biotic Terrestrial Environment, Carbohydrates and Amino- Acids.....	5
1.3.3 CVD, Fullerenes, and Carbon Nano-tubes.....	5
1.3.4 Chemistry of Carbenes and Reactive Intermediates.....	6
1.4 Atomic Carbon (C) and Carbon Cluster (C <sub>n</sub> ) Generation Techniques ...	6
1.4.1 Carbon Arc, and Resistive Heating of Graphite.....	7
1.4.2 The Nuclear Recoil Carbon Atom.....	8
1.4.3 Chemical and Photochemical Methods .....	8
1.4.4 Laser Ablated Carbon.....	9
1.5 Primary Reaction Mechanisms of Atomic Carbon.....	9
1.5.1 CH Insertion .....	10
1.5.2 OH Insertion .....	10
1.5.3 $\pi$ Bond Addition .....	11
1.5.4 Deoxygenation of Oxygen Containing Compounds by Atomic Carbon.....	12
1.5.5 Thermochemical Data About Reactions of Atomic Carbon with Oxygen Containing Compounds .....	12
1.6 Literature Analysis of Reactions of Atomic Carbon with Water and Methanol.....	14
CHAPTER II THEORETICAL AND MATHEMATICAL BACKGROUND	18
2.1 Remarks about Theoretical/Computational Chemistry .....	18

2.2	History and Overview of Quantum Chemistry.....	20
2.3	Theoretical Calculation Methods .....	22
2.3.1	The Schrödinger Equation.....	22
2.3.2	The Born-Oppenheimer Approximation (BO).....	24
2.3.3	Modeling Potential Energy Surfaces.....	26
2.3.4	The Hartree-Fock Theory.....	29
2.3.5	The Basis Set Approximation.....	31
2.3.6	Electron Correlation Methods .....	34
2.3.6.1	Configuration Interaction (CI).....	34
2.3.6.2	Multi-configuration Self-consistent Field (MCSCF) Theory....	35
2.3.6.3	Many Body Perturbation Theory (MBPT).....	37
2.3.6.4	Coupled Cluster (CC) Theory .....	38
2.3.6.5	Density Functional Theory.....	40
2.4	The Computational Chemistry Suites Employed .....	42
2.5	Further Reading.....	42
CHAPTER III RESULTS AND DISCUSSION .....		44
3.1	Reactions of 1S, 1D, and 3P Carbon Atoms with Water.....	44
3.1.1	Computational Details.....	45
3.1.2	Approach of Carbon to the Water Molecule.....	50
3.1.3	Remarks on the Methodological Details of Excited State Calculations .....	55
3.1.4	Carbon-Water Complex 1.....	57
3.1.5	Exit Channels from Complex 1.....	61
3.1.6	Energetics of the System.....	64
3.1.7	Reaction Products.....	67
3.1.8	Effect of Reaction Medium.....	70
3.1.9	Conclusions.....	74
3.2	Reactions of 1D and 3P Carbon Atoms With Methanol .....	76
3.2.1	Computational Details.....	76
3.2.2	Conditions of Typical Experiments.....	79
3.2.3	Energetics of the Singlet PES.....	81
3.2.4	Primary CO Formation Paths On the Singlet PES .....	82
3.2.5	OH Insertion and Dissociation Paths on the Triplet PES.....	95
3.2.6	CH Insertion Path on the Singlet PES.....	108
3.2.7	CH Insertion Path on the Triplet PES.....	111
3.2.8	Intermolecular Dimethoxymethane Formation Path .....	113
3.2.9	Conclusions .....	116
CHAPTER VI CONCLUSION.....		119
REFERENCES .....		122
APPENDICES		
A.	Electronic and Zero Point Energies Of Stationary Structures at Various Levels in Reactions of Atomic Carbon with Methanol.....	130

B. Singlet PES, CCSD/6-311g(D,P) Optimized Geometries and Cartesian Coordinates of Minima in Reactions of Atomic Carbon with Methanol....	137
C. Singlet PES, CCSD/6-311g(d,p) Optimized Geometries and Cartesian Coordinates of Transition Structures in Reactions of Atomic Carbon with Methanol.....	144
D. Triplet PES, UCCSD/6-311G(d,p) Optimized Geometries and Cartesian Coordinates of Minima in Reactions of Atomic Carbon with Methanol ....	153
E. Triplet PES, UCCSD/6-311G(d,p) Optimized Geometries and Cartesian Coordinates of Transition Structures in Reactions of Atomic Carbon with Methanol.....	158
F. CCSD/6-311G(d,p) Optimized Geometries and Cartesian Coordinates of Some Radicalic Species in Reactions of Atomic Carbon with Methanol .....	170
G. The Apparatus Used in Arc Carbon Reactions as Described by Skell.....	170
CURRICULUM VITAE.....	176

## LIST OF TABLES

Table 1.1. Proportions of C <sub>n</sub> fragments in carbon vapor generated with electrical arc and heating.....	7
Table 1.2. Enthalpies of reactions of C with some (oxygen containing) substrates.....	13
Table 1.3. Main products from reactions of C with aliphatic alcohols.....	17
Table 3-1 Full-valence CI absolute energies (hartrees) of the lowest three terms of carbon atom using three basis sets of increasing size.....	49
Table 3-2. CCSD(T)-FC absolute energies (hartrees) for the lowest triplet and singlet terms of carbon atom versus basis set.....	49
Table 3-3. Full-valence CI energies (kcal/mol) of the two lowest singlet terms relative to the ground term 3P of carbon atom versus basis set.....	49
Table 3-4. Difference (kcal/mol) between ccsd(t)-FC and CI-FC energies for the lowest triplet and singlet terms of carbon atom versus basis set.....	50
Table 3-5 Approximate Electronic State Functions (unnormalized) of C+H <sub>2</sub> O System at $\alpha=0$ and Large r.a.....	52
Table 3-6. Partial List of Abbreviations .....	52
Table 3-7. Occupation Numbers of px, py, pz Orbitals in Singlet States at r=1.744 angstrom.....	55
Table 3-8. Occupation Numbers of Natural Orbitals 8 and 9 at Relevant Stationary Points on PES .....	58
Table 3-9. Enthalpies (at 0 K, in kcal/mol, and relative to formaldehyde) of Species at Initial Stages in the Reactions of Singlet and Triplet Carbon Atoms with Water as Calculated by Different Methods .....	65
Table 3-10. Representation of the singlet and triplet species investigated.....	79
Table 3-11. Relative 0K enthalpies of the singlet minima at the levels as specified. ....	81
Table 3-12. Relative 0K enthalpies of the singlet TSs at the levels as specified.....	82
Table 3-13. Relative 0K enthalpies of the triplet minima the levels as specified. ....	96
Table 3-14. Relative 0K enthalpies of the triplet TSs at the levels as specified. ....	96

## LIST OF FIGURES

Figure 2.1. A simplified PES in three dimension.....	27
Figure 2.2. Potential energy surface for a linear triatomic system AB + C reacting to give A + BC.....	29
Figure 2.3. Effect of polarization functions. Addition of p function greatly enhances the flexibility of an s-type orbital (above); Addition of a d function greatly enhances the flexibility of a p-type orbital (below).....	33
Figure 2.4. Pople diagram showing the dependence of the performance of an ab initio method on the basis set and the amount of electron correlation.....	40
Figure 3.1. Schematic representation of the complexation of carbon with water and the primary routes as exit channels from the complex in C + water system.....	45
Figure 3.2. Definition of PES probe parameters $\alpha$ and $r$ . $\alpha=0$ corresponds to a $C_{2v}$ symmetric structure in which all atoms lie on the yz plane.....	51
Figure 3.3. CAS(12,12)/6-311G(d,p) energies of the singlet states relative to $C(^3P)+H_2O$ at $\alpha=0$ ( $C_{2v}$ ) as a function of $r$ .....	53
Figure 3.4. Electronic states of complex 1 at $r=1.744$ angstrom in planar $C_{2v}$ structure.....	54
Figure 3.5. Optimized geometries of minima at various theoretical levels as indicated.....	59
Figure 3.6. Optimized geometries at various theoretical levels of transition states leading from complex 1 to hydroxymethylene 2.....	60
Figure 3.7. Optimized geometries at various theoretical levels of OH-fission transition states leading from complex 1 to isoformyl radical 5.....	63
Figure 3.8. Schematic energy diagram for the early phase in the reactions of $^1D$ and $^3P$ carbon atoms with water molecules. All enthalpies are relative to formaldehyde.....	66
Figure 3.9. Unimolecular reaction pathways of hydroxymethylene $S_0$ , $S_1$ , and $T_1$ states. Energies (kcal/mol) relative to the ground state of formaldehyde (inclusive of ZPVEs) are indicated.....	69
Figure 3.10. Reactions between: A) ground-state hydroxymethylene and water, B) ground-state isoformyl and water.....	71

Figure 3.11. H-bonded complexes of hydroxymethylene and isoformyl radical with a water molecule.....	73
Figure 3.12. Selected geometric parameters of CCSD/6-311G(d,p) geometries of some key species on the singlet PES.....	84
Figure 3.13. Relative 0K enthalpy ( $\Delta H_0$ ) surface corresponding to the processes in Equation. 3.1.....	85
Figure 3.14. Relative 0K enthalpy ( $\Delta H_0$ ) profile corresponding to the processes in Equation 3.2 of singlet carbene 19.....	87
Figure 3.15. Relative 0K enthalpy ( $\Delta H_0$ ) profile corresponding to the processes in eon 3.3 of trans-methoxycarbene 4.....	89
Figure 3.16. Relative 0K enthalpy ( $\Delta H_0$ ) profile corresponding to the processes in Equation 3.4 of cis-methoxycarbene 4'.....	91
Figure 3.17. Relative 0K enthalpy ( $\Delta H_0$ ) profile of processes in Equation 3.5.....	93
Figure 3.18. Relative 0K enthalpy ( $\Delta H_0$ ) profile corresponding to the processes in Equation 3.6. Enthalpy values are given relative to that of acetaldehyde (species 6) calculated at CCSD(T)/cc-pVTZ//CCSD/6-311g(d,p) level using ZPVE obtained at CCSD/6-311g(d,p) level.....	95
Figure 3.19. Selected geometric parameters of some key stationary points on the triplet PES calculated at CCSD/6-311G(d,p) level of theory.....	98
Figure 3.20. Relative 0K enthalpy ( $\Delta H_0$ ) profile of processes Relative 0K enthalpy ( $\Delta H_0$ ) profile corresponding to the processes on the triplet PES, originating from 1T as schematized via Equation 3.7.....	99
Figure 3.21. Relative 0K enthalpy ( $\Delta H_0$ ) profile of processes on the triplet PES, originating from 4T as schematized via Equation 3.8.....	101
Figure 3.22. Relative 0K enthalpy ( $\Delta H_0$ ) profile corresponding to the processes on the triplet PES, originating from 6T as schematized via Equation 3.9.....	103
Figure 3.23. Relative 0K enthalpy ( $\Delta H_0$ ) profile of processes on the triplet PES, originating from 13T as schematized via Equation 3.10.....	105
Figure 3.24. Relative 0K enthalpy ( $\Delta H_0$ ) profile corresponding to the processes on the triplet PES, originating from 19T as schematized via Equation 3.10.....	- 107
Figure 3.25. Selected geometric parameters of some key stationary points on the singlet CH insertion path calculated at CCSD/6-311G(d,p) level of theory.....	109
Figure 3.26. Relative 0K enthalpy ( $\Delta H_0$ ) profile of processes on the singlet CH insertion path, schematized via Equation 3.10.....	110
Figure 3.27. Relative 0K enthalpy ( $\Delta H_0$ ) profile of processes on the triplet CH insertion path, schematized via Equation 3.13.....	112

Figure 3.28. Relative 0K enthalpy ( $\Delta H_0$ ) diagram for the intermolecular dimethoxymethane formation path on the singlet PES computed at {CCSD(T)/cc-pVTZ//B3LYP/6-31G(d,p)} level of theory.....	114
Figure 3.29. Relative 0K enthalpy ( $\Delta H_0$ ) diagram for the overall operative paths in the condensed phase.....	117

## LIST OF ABBREVIATIONS

A	Angstrom.
AO	Atomic orbital.
AU	Atomic units.
B3LYP	Becke's three parameter exchange hybrid functional with Lee, Yang, Parr (LYP) correlation functional.
CASSCF	Complete active space self consistent field theory.
CAS(n,m)	n-electron m-orbital complete active space self consistent field theory.
CAS(n,m)-MRMP	Single-state multireference Moller-Plesset second-order perturbation theory using CAS(n,m) reference wave function.
CC	Coupled cluster theory.
CCSD(T)	Coupled cluster theory with single and double excitations and non-iterative inclusion of triple excitations.
CI	Configuration interaction.
$\Delta H_0$	Reaction enthalpy at 0K.
DFT	Density functional theory.
FC	Frozen core.
GTO	Gaussian type orbital.
HF	Hartree-Fock Theory.
IRC	Intrinsic reaction coordinate.
MBPT	Many body perturbation theory.
MCSCF	Multi-configurational self consistent field theory.
MCQDPT	Multi configuration quasi degenerate perturbation theory.

MO	Molecular orbital.
PES	Potential energy surface.
$\Psi$	Wave function.
SCF	Self consistent field.
$\langle S^2 \rangle$	Average value of the total spin operator.
TS	Transition structure.
(U)	Unrestricted methodology.
ZPVE	Zero point vibrational energy.

## CHAPTER I

### INTRODUCTION

*We can't define anything precisely. If we attempt to, we get into that paralysis of thought that comes to philosophers... one saying to the other: "you don't know what you are talking about!". The second one says: "what do you mean by talking? What do you mean by you? What do you mean by know?"*

*Richard P. Feynman  
The Feynman Lectures on Physics*

#### 1.1 What is the Motivation to Study Carbon Atom Reactions

Properties, and reactions of carbon, being the fourth most abundant element in the universe, and the basis of all known life<sup>1</sup>, are fascinating for scientists.<sup>2,3,4,5</sup> Atomic carbon (C) chemistry is central to the explanation of the chemistry of a vast number of phenomena, including the reactions in interstellar medium;<sup>6</sup> organic molecule formation in the pre-biotic terrestrial environment;<sup>7</sup> polycyclic aromatic hydrocarbon (PAH), soot, and carbonaceous material formation in the combustion processes and the related atmospheric pollution;<sup>8</sup> chemical vapor deposition (CVD) and diamond film growth;<sup>9,10</sup> cluster, nanotube, and fullerene production;<sup>11</sup> tracing molecules in nuclear medicine;<sup>12</sup> and a wide variety of reactions that involve mostly non-isolable carbene-like energetic intermediates.<sup>13</sup> The aforementioned facts suffice to inquire every detail in the chemical properties of carbon atoms.

Led by the facts above, scientists studied reactions<sup>14,15,16</sup> of atomic carbon and carbon clusters with basic classes of most organic and inorganic molecules, and attempted to enlighten the main reaction mechanisms. The chemical, photochemical, electrical arc, thermal, laser ablation, and nuclear production techniques of C and higher order clusters; were among the preferred methods used in experimental studies to react different energetic states of carbon species with the substrates under investigation.<sup>17</sup>

Carbon atoms have very high heats of formation, 171, 201, and 233 kcal/mol for C(<sup>3</sup>P), C(<sup>1</sup>D), and C(<sup>1</sup>S) electronic states respectively. (More detailed information about these states will be given in the following sections.) This is the reason of the possibility of examining very unusual species in the reactions of atomic carbon, as it brings very high energy to the medium, allowing many unexpected paths energetically favorable. Consequently it is reasonable to anticipate most of the reactions of carbon atoms be highly exothermic. (Selected examples of thermodynamic data of C reactions is given in the following sections)

In addition to the presence of two kinds of carbon atoms, differing in their electronic states, currently used techniques of C generation fail to give a sharp spectrum of carbon species. Thus the presence of higher order carbon clusters; C<sub>n</sub> (n > 1), one of which brought the Nobel Prize to its founders<sup>18</sup>, can not be eliminated. This results in a potential complexity of tracing the route of the formation of end products. For instance the reaction of a species with C, two subsequent times, and C<sub>2</sub> once may give the same product.

Another complicating factor arises from the medium of the reactions, most of them being carried in the solid phase, and interpretation of the experimental findings should carefully account for the effect of the reaction medium in order not to end with wrong explanations. Data reported from gas phase reactions of C, may totally differ from the reactions of C with a bulk of condensed substrate. Much of the available experimental data are from the studies carried by the

separate research groups of Skell, in the sixties, and seventies; and Shevlin in eighties and nineties; where -usually- arc generated carbon atoms were preferred to collide with a substrate in the solid phase. There are also studies due to MacKay, Wolf, and Wolfgang where the carbon atoms were generated with the chemically poorly interpreted very high energy nuclear recoil techniques. Application of concepts central to chemical phenomena such as the orbital approximation and the chemical bond breaking, and formation, to the description of the behavior of such high energy particles, may result in erroneous interpretations. This is one reason why the reactions of (nuclear) recoil carbon atoms were generally out of our scope in this thesis.

Mechanistic investigation of C reactions, with various intermediates being present, and the reactive species under investigation accompanied by different electronic and molecular matches, is a difficult task when solely based on experimental data. However with the help of state of the art theoretical chemistry methods, one can better analyze such complex phenomena. Being routine nowadays, standard tools, implemented in publicly available quantum chemistry packages allows one to trap a reactive intermediate not in an energetic well, but on the hazard-free, virtual experimentation on a computer screen, and it is similar for the experimentally non-isolable transition structure (TS). Employing the advances of up to date computational chemistry tools for the mechanistic investigation of carbon atom reactions with different substrates, it is possible to analyze a single type of  $C_n$  fragment with a specified electronic state, and identify all the intermediates, and transition states, the connectivity of the reaction paths, and the relative energies of these species within errors of a few kcal/mol.

## 1.2 Electronic Structure of Carbon Atoms

The electron configuration for the ground state of the carbon atom is designated as  $1s^2 2s^2 2p^2$ , from which three terms arise; namely,  $^1S$ ,  $^3P$ , and  $^1D$ , for  $L=0, 1,$

and 2 respectively. The ground state is a triplet,  $^3P$ , while the other two are singlet  $^1D$  and  $^1S$  states at 29.1 and 61.9 kcal/mol, respectively, above the ground state. The latter singlets are metastable states with very long radiative lifetimes (69 min for  $^1D$  and 1.6 s for  $^1S$ ).<sup>19</sup>

To achieve a full understanding of carbon atom reactions, it is desirable to consider the contribution of each carbon species to the formation of the observed products. However some authors<sup>20</sup> assume chemical generation of carbon atoms not to serve as effective  $C(^1S)$  producers. Thus under low energy conditions the reactions of  $C(^1S)$  may be excluded from discussions. On the other hand depending on the production technique used  $C(^1S)$  may not be insignificant. Nevertheless the presence of the two low lying states with 29.1 kcal/mol separation in between, is a complication for the mechanistic studies, since there exists possibility of contributions to the reactions from states with different spin symmetry. Unfortunately, proportions of reacting carbon atoms in these states are usually not known. Consequently a quantitative assessment of the relative participation of each spin species, in the formation of end-products becomes a difficult task.

### **1.3 Examples of Important Systems with Carbon Atom Reactions**

#### **1.3.1 Interstellar and Solar Chemistry**

Chemistry of carbon atoms in the interstellar medium is an interesting subject, as C, being ubiquitous in the interstellar medium serves to be one of the main sources of chemical reactions in space, and this has numerous manifestations in the physical sciences. A nice review due to Kaiser<sup>1</sup> is available for a detailed presentation of the subject. Behavior and properties of carbon atoms, and small clusters, as assumed to be the precursors of hydrogen deficient hydrocarbon radicals in the interstellar medium, provide valuable information for the formation of organic matter<sup>21,22</sup> in the space.

### **1.3.2 Pre-Biotic Terrestrial Environment, Carbohydrates and Amino-Acids**

Similar to its attractive interstellar chemistry, atomic carbon also served as a reactive species in the pre-biotic terrestrial environment of our planet. This subject, in its relation to origin of life on earth, attracted substantial attention. In its reactions with ammonia and water, C is reported to yield amino acids and carbohydrates, the key bio-molecular building blocks of life. Shevlin et al.<sup>23,24</sup> reported the observation of amino acids in experiments where arc generated carbon atoms were co-condensed with ammonia at  $-196^{\circ}\text{C}$ , followed by hydrolysis. Glycine, alanine, N-methylglycine, Beta-alanine, aspartic acid, and serine were the detected amino acids. In a carbon arc study<sup>7</sup> Flanagan, Ahmed, and Shevlin reported formation of straight chain aldoses up to five carbons, where C atoms were co-deposited with water at liquid nitrogen cooled reactor surface.

### **1.3.3 CVD, Fullerenes, and Carbon Nano-tubes**

Chemical vapor deposition (CVD), being an increasingly used technique for the synthesis of single and multi walled carbon nanotubes (SWCNT, MWCNT), and thin films of synthetic diamond, utilizes carbon atoms and small carbon clusters usually generated from hydrocarbon precursors at elevated temperatures.<sup>25,9</sup> The properties and possible mechanistic behavior of carbon atoms, and carbon clusters towards carbon atoms in a polymeric network of carbons are of central importance to achieve a better understanding of the (polymeric) growth process and to obtain improved synthetic procedures.

The discovery of fullerenes<sup>18</sup> in 1985 was awarded the 1996 Nobel Prize in Chemistry, and the investigation of the mechanism of fullerene formation<sup>26,27</sup> is a hot subject ever since. PAHs in hydrocarbon flames are one important precursor of neutral and charged fullerenes.<sup>28</sup>

Among the many proposed mechanisms for different experimental conditions, fullerene formation in the carbon arc, and from PAH molecules involve  $C_n$  fragments in their mechanisms as reactive intermediates. The close relation of these routes to atmospheric pollution, by means of carbonaceous material and soot formation<sup>29</sup> in the combustion processes, is among the reasons that make the chemistry and properties of small carbon clusters and/or radicalic  $C_n$  fragments intriguing.

#### **1.3.4 Chemistry of Carbenes and Reactive Intermediates**

Atomic carbon, although tetravalent, is regarded as the simplest carbene,<sup>30,3</sup> and many discussions about carbene chemistry starts with the chemistry of carbon atoms. It is well known that the perception about carbene species<sup>31</sup> is very valuable in studying the chemistry of reactive intermediates. It is well known that carbenes play key roles in the chemistry of a large number of very important processes such as organic synthesis<sup>32,33,34,35,36,37,38</sup> and organo-catalysis.<sup>39</sup> It may be quite difficult to improve synthetic procedures without understanding these mechanisms, and computational methods are crucial for a detailed investigation of mechanistic reactive intermediate chemistry, as experimental isolation and analysis of most of the species involved pose high challenges.<sup>40</sup> So besides other benefits gained in the study of atomic carbon reactions, and the specific scientific aim of this study which will be solidified in the following sections, solely from an educational view, a through survey of carbon atom reactions have high importance for reactive intermediate chemistry.

#### **1.4 Atomic Carbon (C) and Carbon Cluster (C<sub>n</sub>) Generation Techniques**

The most widely used atomic carbon generation techniques, in the carbon atom reaction experiments are; arc generation, resistive heating of graphite, nuclear generation of carbon atoms by particle recoil techniques, chemical/photochemical methods, and laser ablation of graphite. The early

studies usually made use of arc generated or nucleogenic carbon atoms, whereas the new literature shows a noticeable shift to laser techniques.

#### 1.4.1 Carbon Arc, and Resistive Heating of Graphite

In the experiments due to Skell<sup>60</sup> the composition and properties of carbon vapor have been widely investigated. The carbon arc was used as a source of carbon vapor. Carbon vapor was produced by alternating arcing between graphite electrodes and co-condensed on the liquid nitrogen cooled walls with a large excess of substrate. The authors expected most of the reactions to occur during the co-deposition at  $-196^{\circ}\text{C}$  (i.e. in the frozen matrix) rather than upon warm-up. They measured the proportions of  $\text{C}_n$  fragments, both mass spectrometrically, and chemically –via reactions with chlorine-. In

Table 1.1 the proportions of small carbon clusters prepared with arcing and resistive heating of graphite are given.

**Table 1.1.** Proportions of  $\text{C}_n$  fragments in carbon vapor generated with electrical arc and heating.

$\text{C}_n$	Arc	Resistive Heating
C (%)	66	55
$\text{C}_2$ (%)	28	11
$\text{C}_3$ (%)	6	34
$\text{C}_4$ (%)	1	-

Data taken from “Skell, P. S.; Havel, J. J.; McGlinchey, M. J. *Acc. Chem. Res.* 1973, 6, 97.”

The carbon vapor formed by resistive heating of graphite showed the domination of  $\text{C}_3$  species, and the  $\text{C}_1$  produced was expected to be mostly in the ground state. On the other hand  $\text{C}_1$  was the major species in arc techniques, and due to the bombardment of graphite with electrons at high temperatures (of ca.

2500°C) the  $^1D$  state of atomic carbon was expected to dominate, whereas the higher excited states were assumed to decay.

#### 1.4.2 The Nuclear Recoil Carbon Atom

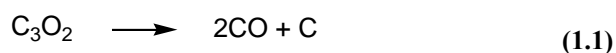
In studies due to Wolf<sup>41</sup> and Wolfgang<sup>42</sup> the description of the method was presented. In these reactions radioactive carbon, usually  $^{11}C$  (half life 20.4 min), was produced in very low concentrations ( $\sim 10^7$  atoms), by recoil techniques. For example  $^{12}C$  atoms subject to gamma radiation produce  $^{11}C$ . A sharp dominance of  $C_1$  species can be achieved due to the low concentration, as the probability of inter-atomic aggregation yielding clusters is decreased. The very high energy of the conditions, allows the carbon atoms to be in the excited states, but the chemical reactions are expected to occur after they decay to the ground or metastable states.<sup>3</sup> A major advantage of utilizing recoil carbons is the ability to detect very low yield products by their radioactivity.

#### 1.4.3 Chemical and Photochemical Methods

The chemical generation technique of C atoms employ the pyrolysis of diaza compounds. Chemical production of C from pyrolysis of diazatetrazole was used by Shevlin et al.<sup>43</sup> at relatively lower temperatures  $\sim 100$  °C when compared to arc conditions, and the products are verified to be the characteristic products of C atom reactions. However the mechanism may be more complex than proposed in the original study.

Bergeat and Loison<sup>44</sup> studied C atom reactions with hydrocarbons where they obtained the ground state carbon atoms by the successive abstractions of halogen atoms from  $CBr_4$  using atomic potassium vapour.

Photolysis of carbon suboxide with the proposed<sup>45</sup> mechanism of



can be given as an example of photochemical methods of C generation. Irradiation of  $C_3O_2$  has been used to study products of C atom reactions in rare gas matrices.<sup>46,47,48,49</sup>

#### 1.4.4 Laser Ablated Carbon

Laser ablation of graphite as a source of  $C_1$  with the specific  $^3P$  electronic state is being increasingly used in carbon atom reactions.<sup>14,12d,50</sup> The laser pulses with short temporal durations generate free carbon atoms. The experiments<sup>51,52,53,54</sup> employ a carrier inert media such as a noble gas to remove the excess energy from the carbon vapor. What remains a challenge seems as the production of only one of the metastable states, as there is no current method to generate an excited carbon without the production of the lower lying states.

It is important to note that all the methods pose complicating factors. Most techniques require the arbitrary input of high energy resulting in an uncontrolled perturbation applied to the system. As Shevlin stated: the ideal method would utilize a highly selective reaction to produce a carbon atom whose concentration could be continually monitored by a convenient analytical technique. In the absence of such a method, the chemistry of atomic carbon must be discussed with an awareness of the shortcomings of the methods by which the carbon atom has been produced.<sup>2</sup>

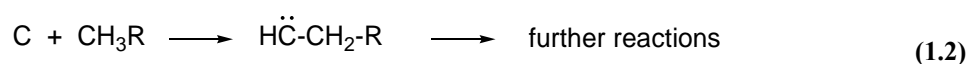
### 1.5 Primary Reaction Mechanisms of Atomic Carbon

Atomic carbon is reported to abstract hydrogen from CH bonds,<sup>55</sup> insert into CH<sup>56</sup> and OH<sup>71</sup> bonds, add to C-C multiple bonds,<sup>57,58</sup> insert into aromatic rings,<sup>59</sup> and yield CO with carbonyl compounds, ethers, and alcohols.<sup>2,60,71</sup> The pioneering works of Skell<sup>60</sup> and coworkers; about reactions of arc generated carbon vapor including C,  $C_2$ ,  $C_3$ , and  $C_4$ ; with different classes of organic compounds; including alcohols, carbonyl compounds, ethers, and epoxides,

presents many suggestions for the reaction mechanisms, most of which are results of isotope labeling studies. This section will give a brief information about some generally proposed mechanisms of atomic carbon reactions that are relevant to our studies.

### 1.5.1 CH Insertion

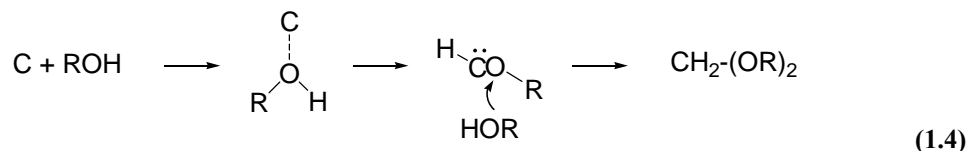
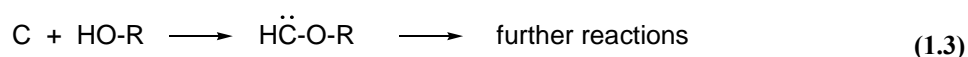
A primary reaction of C with saturated hydrocarbons or any substrate bearing a CH<sub>n</sub> group is CH insertion where the incoming carbon inserts between the C and H atoms of the substrate and yields a carbene as in equation 1.2.



Skell, and Harris<sup>71</sup> observed products from carbon atoms inserting into every CH bond of a series of alcohols. The kinetic data from Husain, and Kirsch<sup>72</sup> about second order rate constants of the disappearance of <sup>3</sup>P, and <sup>1</sup>D carbon atoms with methane as a substrate indicates that the singlet carbon atoms react some 10<sup>4</sup> times faster. This implies <sup>3</sup>P carbon atoms to be practically inert (at least in the presence of <sup>1</sup>D carbons) towards CH insertion. This is also verified<sup>61,15</sup> with <sup>3</sup>P carbons to have barriers for CH insertion and <sup>1</sup>D carbons entering the CH<sub>n</sub> structure in an energetically downhill<sup>62</sup> reaction.

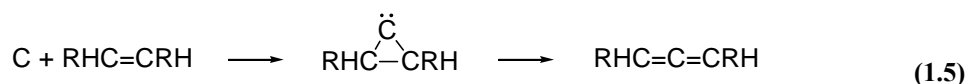
### 1.5.2 OH Insertion

With the substrates bearing an OH function, atomic carbon is reported to insert into OH bonds to yield alkoxy-carbenes. OH insertion is reported<sup>60</sup> to be 5 to 8 times faster than CH insertion with the same substrate. OH insertion was also reported in reactions of nucleogenic <sup>11</sup>C atoms with methanol.<sup>63,64,65</sup> Equation 1.3 shows the proposed OH insertion mechanism for water and aliphatic alcohols. With isotope labeling studies employing arc generated carbon within condensed medium Skell and Harris confirmed<sup>71</sup> the formation of dialkoxy-carbenes with a series of aliphatic alcohols from two consecutive OH insertions as given in equation 1.4.

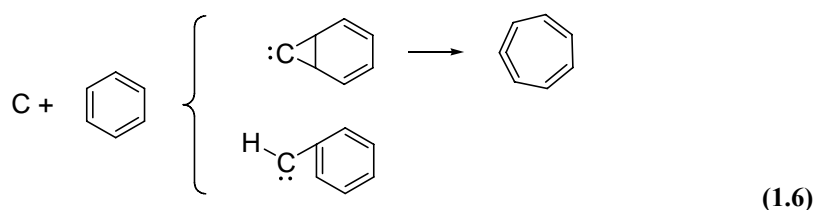


### 1.5.3 $\pi$ Bond Addition

The reactions of carbon atoms with unsaturated systems were also extensively investigated.<sup>66,13a,59b</sup> Addition of carbon to a CC double bond yields cyclopropylidene intermediates, which rearranges to cumulene structures as shown in equation 1.5.



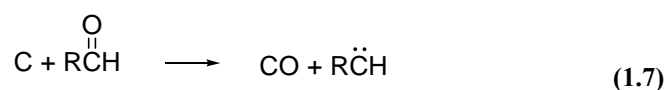
In a joint experimental and theoretical study, Kaiser reported<sup>67</sup> addition of <sup>3</sup>P carbon atoms to double bonds of radicalic hydrocarbon species. The reactions of atomic carbon with aromatic systems such as benzene (Equation 1.6) were also investigated; where preference of CH insertion over double bond addition (DBA) was experimentally verified.<sup>59</sup>



On the seemingly contrary report of Bettineger et al.<sup>13</sup> computational evidence was in favor of DBA for ground state carbon atoms, without ruling out the possibility of CH insertion. The apparent contradiction can be explained by the experimental study using arc generated carbons, hence domination of <sup>1</sup>D carbon atoms, and their mechanism being different than <sup>3</sup>P carbons reported by Bettineger et al.

#### 1.5.4 Deoxygenation of Oxygen Containing Compounds by Atomic Carbon

With compounds containing oxygen, atomic carbon is reported to produce high yields of carbon monoxide. Ethers were reported to react with C, yielding CO<sup>68,69</sup> with a predicted mechanism of direct oxygen loss (Ref. 69 reports C, stripping off oxygen; a result predicted from MINDO/3 calculations.) But the deoxygenation mechanisms of ethers by the explicit treatment of <sup>3</sup>P and <sup>1</sup>D carbon atoms, lacks state of the art theoretical explanation. The proposed mechanism for ethers involves the direct abstraction of oxygen by the incoming carbon. With aldehydes and ketones, Skell and Plonka<sup>70</sup> found that a stripping type reaction was occurring for the carbonyl oxygen, and this route can be used to generate carbenes, as shown in equation 1.7.



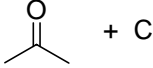
With water and alcohols, either in the inert rare gas matrices, or the reactive solid matrices, high yields of CO obtained in the experiments lacked a mechanistic explanation.

Skell and Harris<sup>71</sup> reported the major products from the reactions of arc generated C with different alcohols as CO and dialkoxymethanes that retain the alkyl groups of the substrate alcohols. Although all alcohols produced CO upon C attack, as either the first or second product by yield, there was no fully described suggestion for CO generation mechanism, neither in the original study -to the best of our knowledge- nor till then.

#### 1.5.5 Thermochemical Data About Reactions of Atomic Carbon with Oxygen Containing Compounds

As mentioned in the previous sections the reactions of carbon atoms are highly exothermic. Its reactions with substrates that contain oxygen are no exception. Table 1.2 lists enthalpies of some reactions of C with (oxygen containing) substrates that are relevant to this work.

**Table 1.2. Enthalpies of reactions of C with some (oxygen containing) substrates.**

Overall Reaction			$\Delta H_{298}$ (kcal/mol)
$O_2 + C$	$\longrightarrow$	$CO_2$	-295
$CH_4 + C$	$\longrightarrow$	$H_2 + C_2H_2$	-129
$H-OH + C$	$\longrightarrow$	$CO + 2H$	-55
$CH_3-OH + C$	$\longrightarrow$	$CO + CH_3 + H$	-162
$CH_3-O-CH_3 + C$	$\longrightarrow$	$CO + C_2H_6$	-203
 + C	$\longrightarrow$	$CO +$ 	-163
 + C	$\longrightarrow$	$CO + C_2H_4$	-202

C ( $^1D$ ) is the reactive species; the enthalpies are calculated from 298K heat of formations; data taken from "P. W. Atkins, Physical Chemistry, Oxford University Press, 5<sup>th</sup> ed. 1995"

Up to here it is clarified that, there is general agreement in the literature for the reactive atomic carbon species being  $^1D$ , rather than  $^3P$ . So carbon atom reactions should be studied by comprehending the behavior of  $^1D$  state. In any substrate bearing available sites, the complicating factor of concurrent multi-type reactions such as instantaneous CH, and OH insertions should be taken into account. So apart from selecting a single  $C_n$  species, and a specific spin symmetry, the immediate routes, like OH and CH insertion, followed by the reactive carbon atom must be analyzed simultaneously. We should also note that no experimental evidence imply CO production being a result of CH or OH insertion, so a different mechanism should be operative for most if not all of the oxygen containing compounds generating CO upon C attack.

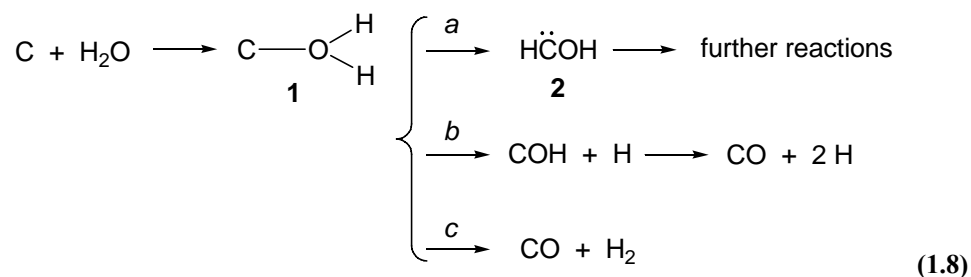
## 1.6 Literature Analysis of Reactions of Atomic Carbon with Water and Methanol

Pioneering work by Skell and coworkers shed much insight into the mechanisms of carbon atom reactions with a variety of oxygen containing organic compounds including alcohols,<sup>71</sup> carbonyl compounds, ethers, and epoxides.<sup>60</sup> All of these reactions produce appreciable amounts of carbon monoxide. Reactions of atomic carbon with alcohols are particularly interesting. Whereas the initial stage of the reaction between carbon and a carbonyl compound appears to generate CO and a carbene intermediate in a 1:1 ratio as in equation 1.7, the situation with alcohols is not as clear; a competition between CO and carbene formation might be involved in the latter case.

Husain and Kirsch have investigated the reactivity of carbon atoms with H<sub>2</sub>O in the gas phase at 300 K.<sup>72</sup> They reported overall second order rate constants of  $k_2(^1\text{D})=1.7\times 10^{-11}$  and  $k_2(^3\text{P})=3.6\times 10^{-13}$  cm<sup>3</sup> molecule<sup>-1</sup> s<sup>-1</sup> for the reactions of <sup>1</sup>D and <sup>3</sup>P carbons, respectively. The value of  $k_2(^1\text{D})$  is roughly one-tenth of the gas kinetic limit, and suggests that no or very small activation energy is required in the reaction of C(<sup>1</sup>D). The <sup>3</sup>P carbons are less reactive than <sup>1</sup>D by a factor of 47 which translates into an activation energy difference  $\Delta E_a$  of 2.3 kcal/mol between the two reactions.<sup>73</sup> Data on the reactivity of <sup>1</sup>S carbons with water is not available, but there is some evidence from other systems that chemical reactivity of this species is negligible.<sup>72</sup>

Galland et al.<sup>74</sup> carried out a similar study for the reaction of C(<sup>3</sup>P) with H<sub>2</sub>S, the latter molecule being valence isoelectronic with H<sub>2</sub>O and therefore expected to behave similarly. They reported  $k_2(^3\text{P})=2.1\times 10^{-10}$  cm<sup>3</sup> molecule<sup>-1</sup> s<sup>-1</sup> for the overall second order rate constant at room temperature. They also performed *ab initio* calculations at CCSD(T)/cc-pVTZ//QCISD/cc-pVDZ level. Consistent with their measured value of  $k_2(^3\text{P})$ , they found that the insertion transition structure (TS) leading to HSCH(T<sub>1</sub>) (sulfur analogue of path *a* in equation 1.8) is lower in energy than C(<sup>3</sup>P)+H<sub>2</sub>S; i.e. no activation energy is required in the

reaction of C(<sup>3</sup>P) with hydrogen sulfide, which contrasts the behavior of this species with H<sub>2</sub>O.



Details about the reaction paths of atomic carbon with H<sub>2</sub>O have also been studied.<sup>75a-c,76</sup> In a joint experimental and *ab initio* study, Shevlin et al.<sup>75a</sup> reported that the reaction produced 9.5% CO and 2.4% H<sub>2</sub>C=O. Carbon atoms were generated by thermolysis of 5-diazotetrazole. In the theoretical part of their work, they considered paths *a* and *c* of equation 1.8. Employing (U)MP3/6-31G(d,p)//(U)HF/3-21G methodology, they concluded that singlet carbons are responsible for both products, and that CO should be formed through path *c* along with molecular hydrogen. Further, they found that while path *c* evolves from a closed-shell singlet <sup>1</sup>A' state of complex **1**, path *a* leading to hydroxymethylene **2** originates from an open-shell singlet <sup>1</sup>A'' PES of **1**. Additionally, the TS along path *c* was found to be at a higher energy than that along path *a*, at odds with their experimental observation that the deoxygenation is the dominant route. Their explanation was a possible entrapment of the <sup>1</sup>A'' open-shell complex **1** in a substantial energy well and/or intersystem crossing of **1** to the ground <sup>3</sup>A'' state. In another experiment at 10 K where carbon atoms obtained by laser evaporation from a graphite rod were reacted with water in a large excess of Ar, carbon monoxide was the only detectable product.<sup>75c</sup> Thus the reaction of diluted H<sub>2</sub>O with atomic carbon does not produce e.g. formaldehyde in an inert matrix even at very low temperatures.

On the other hand, when carbon vapor was reacted with excess water at 77 K, formaldehyde was the major product, and this time no CO was observed.<sup>75b</sup> These interesting effects of the nature of reaction medium on reaction products will be discussed in more detail later.

In a more recent work, Hwang et al.<sup>76</sup> studied path *a* of equation 1.8 at CCSD(T)/6-311+G(3df,2p)//MP2/6-31G(d,p) level. However, for the crucial singlet PES involving complex 1, their employment of an RHF-based method (thus an approximation to the <sup>1</sup>A' state) is questionable in this particular case where, as pointed out by ref <sup>75a</sup>, two potential energy surfaces (<sup>1</sup>A' and <sup>1</sup>A'') might be involved. Note the contrast between the proposed open-shell <sup>1</sup>A'' (ref 75a) vs. the implied closed-shell <sup>1</sup>A' (ref 76) surfaces as the likely routes leading from 1 to 2.

Schreiner and Reisenauer<sup>55</sup> very recently reported the laser ablated triplet carbons being unreactive towards water, where they also employed high level *ab initio* calculations for the singlet and triplet PESs at the CCSD(T)/cc-pVTZ level. This study however focuses more on the non-reaction of <sup>3</sup>P carbons than the reaction of <sup>1</sup>D carbons, and the experimentally observed products. The TS from the initial (<sup>3</sup>P)C – water complex to triplet hydroxymethylene (OH insertion TS) was found to be higher in energy than the total initial energy of the (<sup>3</sup>P)C + water system, hence led to the theoretical conclusion of <sup>3</sup>P carbon atoms being unreactive towards water. The failure to observe the expected products from the OH insertion was also reported, being an experimental verification of the non-reaction.

The experimental data we are interested in, available about C + Methanol system, is due to Skell and Harris. We also previously noted the presence of experimental studies which used carbon atoms generated with nuclear recoil techniques due to Voigt<sup>63,64,65</sup> and coworkers; but these were kept out of our scope as reasoned in the previous sections. What is clear from the experiments about the C + Methanol system is:

- (i.) The arc reactor used, generated higher proportions of  $^1\text{D}$  carbon atoms, than  $^3\text{P}$  carbons.
- (ii.) The intermediates and products with  $\text{C}_2\text{H}_4\text{O}$  stoichiometry were the result of  $\text{C}_1$  added to methanol (and then rearranged).
- (iii.) The substrate is in frozen form, and trapping of some intermediates with effective coupling to the medium was possible.
- (iv.) The intermolecular reactions of two or more intermediates were not likely as the probability of them meeting in a sea of substrate will obviously be negligible.
- (v.) The primary products were CO, dimethoxymethane, and acetaldehyde; (The product yields are shown in Table 1.3) where acetaldehyde is verified – with isotope labeling studies- to be formed from a CH insertion and an intermolecular reaction must have occurred for the dimethoxymethane generation.
- (vi.) Finally, we want to reemphasize that methanol deoxygenation by arc generated atomic carbon lacked a comprehensive mechanistic explanation, and we are not aware of a theoretical and/or computational study in the literature after the experimental work.

**Table 1.3.** Main products from reactions of C with aliphatic alcohols.

<b>Substrate</b>	<b>% CO</b>	<b>% dialkoxy methane</b>	
$\text{CH}_3\text{OH}$	16.8	$\text{CH}_2(\text{OCH}_3)_2$	17.8
$\text{CH}_3\text{CH}_2\text{OH}$	4.3	$\text{CH}_2(\text{OCH}_2\text{CH}_3)_2$	11.5
$\text{CH}_3\text{CH}_2\text{CH}_2\text{OH}$	11.7	$\text{CH}_2(\text{OCH}_2\text{CH}_2\text{CH}_3)_2$	11.5
$(\text{CH}_3)_2\text{CHOH}$	12.8	$\text{CH}_2(\text{OCH}(\text{CH}_3)_2)_2$	10.6
$(\text{CH}_3)_3\text{COH}$	18.8	$\text{CH}_2(\text{OC}(\text{CH}_3)_3)_2$	bdl <sup>a</sup>

<sup>a</sup> Below detection limit.

## CHAPTER II

### THEORETICAL AND MATHEMATICAL BACKGROUND

*We are perhaps not far removed from the time when we shall be able to submit the bulk of chemical phenomena to calculation*

*Joseph Louis Gay Lussac  
De la Societe D'arcueil, 2, 207 (1808)*

*In the Schrödinger equation we very nearly have the mathematical foundation for the solution of the whole problem of atomic and molecular structure, but the problem of the many bodies contained in the atom and the molecule cannot be completely solved without a great further development in the mathematical technique.*

*G. N. Lewis  
J. Chem. Phys. 1, 17 (1933).*

#### 2.1 Remarks about Theoretical/Computational Chemistry

The application of quantum mechanical principles to chemical problems has revolutionized the field of chemistry.<sup>77</sup> Today the understanding of chemical bonding, spectral phenomena, molecular reactivity, and various other fundamental chemical problems, rests heavily on our knowledge of the detailed behavior of electrons in atoms and molecules, which is governed by the rules of quantum mechanics, and is the interest of the popular field of theoretical/computational chemistry.

Theoretical chemistry can be defined as a mathematical description of chemistry, whereas computational chemistry is a set of mathematical methods sufficiently well developed to be automated by implementing in a software. It is interesting to note that as Eyring, Walter, and Kimball,<sup>78</sup> pointed out; chemical questions are problems in applied mathematics as far as quantum mechanics is correct.

Everything in today's world, from the simplest to the very complex, is firstly designed by computer simulations. There is no reason why chemistry should not be part of such a world.<sup>79</sup> Evolution of quantum chemistry after some major steps allowed us to practice chemical research by such simulations. First *ab initio*<sup>a</sup> computations, which predated computers, sought qualitative agreement between experiment and semi-empirical calculations. Computers launched a second age extending the applications to a larger portion of the chemist's interest. Now is the era of quantitative agreement between calculation and experiment.<sup>80</sup> Theoretical approaches to compute structural and electronic parameters are now implemented in very efficient program packages that can be used in computing facilities with rapidly increasing performance.<sup>81,82</sup>

In recent years the field of computational chemistry has attracted substantial attention. Employing theoretical results for the analysis of recorded spectra as well as for the investigation of structure-property relationships and complementation of experimental data allowed computational chemistry to be used as an analytical tool in the same sense that an NMR or X-ray crystallography can be used to rationalize the structure of a molecule. Its true place, however, is as a predictive tool, to be considered before the experiment. Nowadays, depending on the desired accuracy, one can computationally acquire a wealth of information from systems containing several thousands of atoms. A really important problem, and the line which current developments in theoretical/computational chemistry will follow is, the achievement of

---

<sup>a</sup> Latin phrase meaning, "from the beginning"

experimental accuracy.<sup>83</sup> On the other hand, it is desirable to show that computations can do better than a mere reproduction of experimental data; nevertheless this will remain –at least at the short range- as a check tool for the quality of the results for the experimental chemical science.

The continuously increasing number and extent of theoretical/computational chemistry resources publicly available, both provided a driving force for computer aided research, and highlighted the need to better learn the basic principles of computer simulations of chemical interest. It is indispensable to learn the theoretical background of computational chemistry in order to conduct quantum chemical research, thus we included a short list of publicly available computational/theoretical chemistry websites, that contain a wealth of information for the interested reader at different levels. This list together with a record of books on the subject can be found in the *Further Reading* section.

## **2.2 History and Overview of Quantum Chemistry**

The beginning of Quantum Chemistry can be considered as the study of H<sub>2</sub> ground state wave function<sup>84</sup> by W. Heitler and F. London (HL), which also started the valence bond (VB) approximation.<sup>85</sup> The core of the HL idea was; the approximation of the wave function of an n electron system by a product of atomic functions constituting the system.

HL proposal was successful to set a theoretical background for most of the chemically important phenomena such as hybridization and bonding. It also succeeded in utilizing the Lewis electron pair view of the chemical bond, and the Pauli principle.<sup>86</sup> We are familiar with quantum chemistry exercises where HL scheme is superior to its successor, the MO scheme, when explaining the bond formation and bond breaking, for example the homolytic dissociation problem of molecular hydrogen.

Nearly at the same time with Heitler–London work, the concept of determinantal function and of the atomic orbital was introduced by Douglas Rayner Hartree<sup>87</sup> and Vladimir Aleksandrovich Fock.<sup>88</sup> The Hartree–Fock (HF) atomic model appeared to be capable of explaining ionization potentials and atomic spectra. Hund<sup>89</sup>, Herzberg<sup>90</sup>, and Mulliken<sup>91</sup> extended the idea from atoms to molecules both in ground and excited states. Roothaan equations<sup>92,93</sup> proved to be a general, simple, and robust algorithm of using the determinantal model. With the utilization of Boys Gaussian functions,<sup>94</sup> instead of the physically beautiful but analytically unbearable STO exponential functions, a general methodology for computerized *ab initio* calculations was established.

Thanks to the rapid development of computers (for crunching numbers); from a few electrons considered in the early sixties, dozens of electrons can now be properly handled. (Obviously this manageable number of electrons do not stay still and as of these writing they certainly increased) However, a very simple chemical system has tens of atoms, and the need for computational short cuts such as semi-empirical methods is clear. As the computer industry growth allowed larger computations, different mathematical techniques for modeling chemical systems became available.

All the several approaches for obtaining a correct quantum chemical description of a molecular system; fall into one of the two main categories. First is the wave function-based methods, (WFBM). Second one is density based methods (DBM), in particular the Density Functional Theory (DFT). The 1998 Nobel Prize in Chemistry was awarded for pioneering contributions in both areas. The work presented in this thesis employed both methods, with primary utilization of WFBM. The technical and mathematical details of these methods are shortly given in the following sections.

WFBM are applicable to small molecules, of the order of tens of atoms, and the theory gives a detailed insight into the nature of the electron correlation. On the

contrary, DBM supplies little information about the nature of electron correlation, but the methods can be applied to larger systems.

The electronic structure of the system consisting of  $n$  electrons and  $N$  nuclei can be represented by the wave function  $\Psi(\mathbf{r},t)$ , or -in DFT- by the electron density  $\rho(\mathbf{r})$ . The wave function belongs to the complex  $3n$ -dimensional space, and is a non-visualizable concept. It does not represent any observable. On the contrary, the electron density belongs to the real three-dimensional space, and is a physical observable.

The ground state energy of atoms and molecules are of primary interest for the theoretical chemist. Wave function theory (WFT) can estimate it by means of the variational principle. Variational ground-state energies ( $E_0$ ) computed at any level give upper bounds to the exact energy of the ground state of a specific symmetry. DFT attempts to find  $E_0$  from ground state electron density.

WFT methods can be classified into single or multi-configuration formalisms whether the electronic wave function is represented by a single Slater determinant or by a linear combination of Slater determinants. Single Slater determinants can describe electronic states near equilibrium geometries in the PES. However, more than one Slater determinant is necessary to describe the electronic structure of compounds containing multivalent elements or specifying the dissociation fragments of a molecule.

## **2.3 Theoretical Calculation Methods**

### **2.3.1 The Schrödinger Equation**

The Schrödinger equation enables us to study the wave function which fully characterizes the state of a quantum mechanical system. The solutions of the Schrödinger equation are called stationary states and the state with the lowest energy is called the ground state. Stationary states with higher energies correspond to so-called excited states. By solving the Schrödinger equation for

the ground state it is possible to calculate properties such as ionization energies, electron affinities, charge distributions, and dipole moments.

The Schrödinger equation (equation 2.1) is a numerical eigenvalue problem for

$$\hat{H}\Psi = E\Psi \quad (2.1)$$

which multiple solutions can be found. Each of the eigenfunctions is a possible wavefunction for the system. The corresponding eigenvalues are the allowed energies. With the time-dependent formalism of the Schrödinger equation<sup>95</sup> the evolution of the properties of the system in time can also be created. However in a majority of chemically important systems we one is interested in the time independent Schrödinger equation.

$$\hat{H}\Psi(\mathbf{r}) = E\Psi(\mathbf{r}) \quad (2.2)$$

Where the Hamiltonian in atomic units is given as:

$$\hat{H} = -\sum_{i=1}^n \frac{1}{2} \nabla_i^2 - \sum_{a=1}^N \frac{1}{2M_a} \nabla_a^2 - \sum_i \sum_a \frac{Z_a}{r_{ia}} + \sum_i \sum_{j>i} \frac{1}{r_{ij}} + \sum_{a=1}^N \sum_{b>a} \frac{Z_a Z_b}{R_{ab}} \quad (2.3)$$

In equation 2.3 i and j indices run over all the n electrons in the system; and a and b indices over all the N atomic nuclei.  $M_a$  is the ratio of the mass of nucleus a to an electron, and  $Z_a$  is the atomic number of nucleus a.  $r_{ij}$  is the distance between electron i and electron j.  $r_{ia}$  is the distance between the nucleus a and electron i.  $R_{ab}$  is the distance between nucleus a and nucleus b. The first and second terms are the kinetic energy operators of the electrons ( $T_e$ ) and the nuclei ( $T_N$ ), respectively. The third term is the electron nucleus attraction energy operator ( $V_{Ne}$ ), and the fourth and fifth terms represent the energy operator of the electron-electron ( $V_{ee}$ ) and the nucleus-nucleus repulsion ( $V_{NN}$ ), respectively.

Thus the Hamiltonian operator can be separated into parts of electronic kinetic energy, nuclear kinetic energy, nucleus-electron attraction, electron-electron repulsion, and nucleus-nucleus repulsion.

$$\hat{H} = T_e + T_N + V_{Ne} + V_{ee} + V_{NN} \quad (2.4)$$

In only a few simple cases do analytic solutions of the Schrödinger equation exist, and in order to solve this equation for systems of interest, certain approximations need to be made.

### 2.3.2 The Born-Oppenheimer Approximation (BO)

The BO approximation starts by partitioning  $H$  as  $H = T_N + H_{elec}$ , where  $T_N$  is the kinetic energy operator of the nuclei, and  $H_{elec}$  is a hamiltonian describing the motion of the electrons in the field of clamped nuclei. It is called the electronic hamiltonian. In the BO approximation, the total wavefunction is assumed to have a product form,

$$\Psi(\mathbf{r}, \mathbf{R}) = \Psi_{elec}(\mathbf{r}; \mathbf{R}) \Psi_{nuc}(\mathbf{R}) \quad (2.5)$$

where the symbols  $\mathbf{r}$ , and  $\mathbf{R}$ , collectively denote the set of electronic and nuclear variables, respectively. For a molecule containing  $n$  electrons and  $N$  nuclei, the number of these variables is  $3n$  for the electrons, and  $3N-6$  for nuclei in nonlinear molecules. The first factor in eq 2.5 is found by solving the electronic Schrödinger equation,

$$H_{elec} \Psi_{elec} = E_{elec} \Psi_{elec} \quad (2.6)$$

and gives the electronic energy,  $E_{elec}(\mathbf{R})$ , and the associated wavefunction for a particular choice of  $\mathbf{R}$  (i.e. one manually specifies the positions of the nuclei in the molecule, and solves equation 2.6 for the motion of the electrons in the field of fixed nuclei). For a given  $\mathbf{R}$ , equation 2.6 has infinitely many solutions (i.e. infinitely many electronic states). One first decides the electronic state of interest, for example the ground electronic state, and solves equation 2.6 for

that state at the specified geometry  $R$ . This process of solving equation 2.6 for the desired electronic state is repeated for many other choices of  $R$  values (geometries). Thus, the electronic energy  $E_{\text{elec}}(R)$  is not a constant, but a function of  $3N-6$  variables (for a nonlinear molecule). This function is called the electronic potential energy surface (PES). The PES is needed to obtain the second, nuclear function in equation 2.5, by solving

$$[T_N + E_{\text{elec}}(R)] \Psi_{\text{nuc}}(R) = E \Psi_{\text{nuc}}(R) \quad (2.7)$$

This is the second step of the BO approximation, and determines the total energy  $E$  (a constant) together with  $\Psi_{\text{nuc}}$ . Equation 2.9 shows that the electronic PES plays the role of potential energy function for the nuclear motion.

The procedure used in solving equation 2.7 needs some elaboration. In general, a PES will have many stationary points in the  $3N-6$  dimensional space. The chemically important stationary points on a PES are the minima and first-order saddle points. In practice, equation 2.7 is solved locally in a small region around a specified stationary point on PES. For example, let  $R_0$  denote the geometry of the molecule corresponding to the absolute minimum on the ground PES. The electronic energy at this geometry is  $E_{\text{elec}}(R_0)$ , and will be denoted by the symbol  $E^{\circ}_{\text{elec}}$ . It is a constant. Then, one defines an equivalent vibrational potential energy function by

$$V(R) = E_{\text{elec}}(R) - E^{\circ}_{\text{elec}} \quad (2.8)$$

and rearranges eq 2.7 to the form

$$[T_N + V(R)] \Psi_{\text{nuc}}(R) = E_{\text{nuc}} \Psi_{\text{nuc}}(R) \quad (2.9)$$

where  $E_{\text{nuc}} = E - E^{\circ}_{\text{elec}}$ . Eq 2.9 is solved in the vicinity of  $R_0$ , usually adopting the harmonic approximation for  $V(R)$ .

It should now be pointed out that whereas the PES and hence  $V(R)$  depends only on  $3N-6$  variables, kinetic energy of the nuclei,  $T_N$ , and the function  $\Psi_{\text{nuc}}$

in equations 2.5 and 2.6 actually depend on all  $3N$  variables of the nuclei. Of the  $3N$  variables, 3 variables can be taken as center-of-mass variables (called translational degrees of freedom). They are exactly separable from the remaining variables. Thus one sets

$$\Psi_{\text{nuc}}(\mathbf{R}) = \Psi_{\text{vib-rot}} \Psi_{\text{tr}} \quad (2.10)$$

where the first function on the right is a function of  $3N-3$  variables (vibrational plus rotational variables), and the second function is a function of the 3 translational degrees of freedom. While the product form in eq 2.10 is exact, separation of rotational motion from the vibrations can only be done approximately. Three of the  $3N-3$  variables are suitably defined to describe the overall rotations of the molecule. By definition, the remaining  $3N-6$  variables are called vibrational variables (normal coordinates, in the harmonic approximation). Thus, one writes

$$\Psi_{\text{vib-rot}} \approx \Psi_{\text{vib}} \Psi_{\text{rot}} \quad (2.11)$$

Using the relations in equations 2.10 and 2.11 in equation 2.9, one gets 3 Schrodinger equations; one equation for the center-of-mass motion (giving translational energies  $E_{\text{tr}}$ ), one equation for the rotational motion (giving rotational energies  $E_{\text{rot}}$ ), and an equation for the vibrational motion (giving vibrational energies  $E_{\text{vib}}$ ). These energies are then combined with the electronic energy to give approximate values for the total energy,

$$E \approx E_{\text{tr}} + E_{\text{rot}}^{\circ} + E_{\text{vib}}^{\circ} + E_{\text{elec}}^{\circ} \quad (2.12)$$

### 2.3.3 Modeling Potential Energy Surfaces

Many aspects of chemistry can be reduced to questions about potential energy surfaces (PES). A PES displays the energy of a molecule as a function of its geometry. A PES associates an energy with each geometry of a molecule. Energy is plotted on the vertical axis; geometric coordinates (e.g bond lengths,

angles, etc.) are plotted on the horizontal axes. A PES can be thought of as a hilly landscape, with valleys, mountain passes and peaks. Real PESs have many dimensions, but key features can be represented by a 3 dimensional PES, as depicted in Figure 2.1.

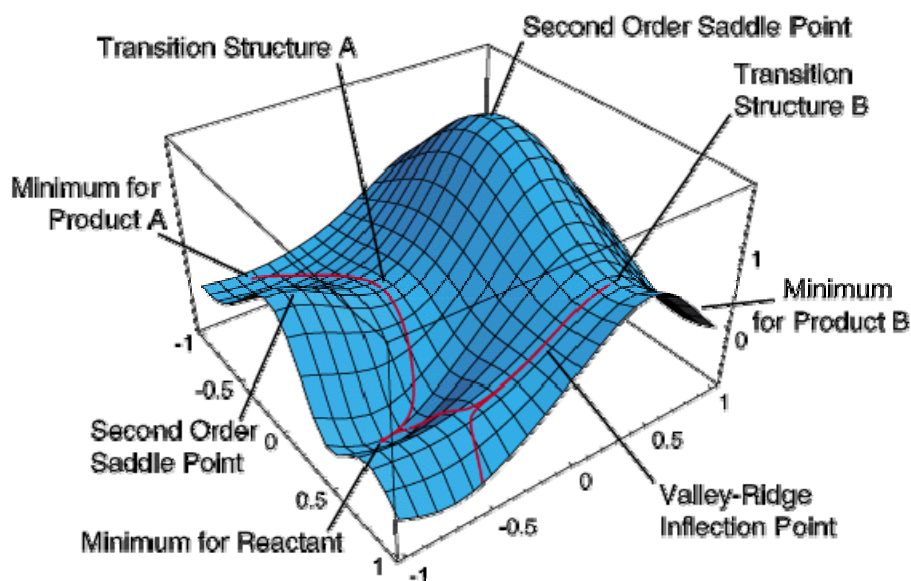


**Figure 2.1.** A simplified PES in three dimension.  
Reprinted from “An Introduction to Theoretical Chemistry” Jack Simons, Cambridge University Press, 2003, pp 105.

The form of a potential energy surface for a specific number of nuclei and electrons, can be calculated by solving the Schrödinger equation for every possible set of atomic coordinates. If the energy is optimized with respect to all coordinates, one obtains “stable” molecules. “Normal molecules” i.e. equilibrium molecular structures, correspond to the positions of the minima in the valleys on a PES. The transition state of a reaction corresponds to a maximum in the reaction coordinate and a minimum in all other coordinates, i.e. the highest point on the lowest energy path being a first-order saddle point. A reaction path connects reactants and products through a mountain pass. Energetics of reactions can be calculated from the energies or altitudes of the minima for reactants and products.

The structure, energetics, properties, reactivity, spectra and dynamics of molecules can be readily understood in terms of potential energy surfaces. Except in very simple cases, the potential energy surface cannot be obtained from experiment. The challenge is to explore potential energy surfaces with electronic structure methods that are efficient and accurate enough to describe the chemistry of interest.

Classical dynamics of a molecule can be visualized as a ball rolling on a potential energy surface. Reaction rates can be obtained from the height and profile of the potential energy surface around the transition structure. The shape of the valley around a minimum determines the vibrational spectrum. Each electronic state of a molecule has a separate potential energy surface, and the separation between these surfaces yields the electronic spectrum. Properties of molecules such as dipole moment, polarizability, NMR shielding, etc. depend on the response of the energy to applied electric and magnetic fields.

In order to gain better insight into the behavior of species involved in a chemical reaction the potential energy surface shown in Figure 2.2 may be useful. The “gully” in the figure represents a minimum energy pathway (MEP) on going from  $AB + C$  to  $A + BC$ . In this particular case this minimum energy pathway, which is a measure of the variations in  $r_{AB}$  and  $r_{BC}$ , is called the reaction coordinate.

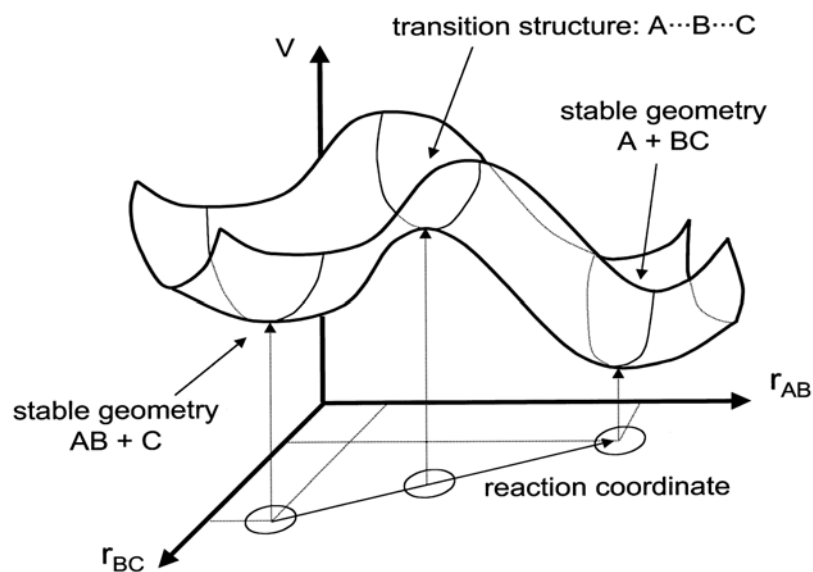


**Figure 2.2.** Potential energy surface for a linear triatomic system  $AB + C$  reacting to give  $A + BC$ .

Reprinted from "Handbook of Radical Polymerization" Krzysztof Matyjaszewski & Thomas P Davis, Wiley & Sons, 2003.

The TS corresponding to the coordinates at the maximum along the reaction coordinate (corresponding to the bond breaking and bond formation) displays a maximum in energy for only one of the coordinates (i.e., the reaction coordinate); whereas it displays a minimum for the others (in this case a coordinate perpendicular to the reaction coordinate). This simple picture can be extended to any system with  $N$  atoms having  $3N - 6$  internal coordinates, and  $(3N - 5)$  - dimensional potential energy surface.

### 2.3.4 The Hartree-Fock Theory

The electronic Schrödinger equation, as the Born-Oppenheimer approximation introduces is still mathematically obnoxious. This is due to the electron-electron interactions. Among the many efforts to alleviate this problem the independent-particle approach of Hartree, where the wavefunction is approximated by a product of orthonormal molecular orbitals (MOs) is of major importance. For an  $n$  electron system the Hartree wavefunction is given as:

$$\Psi = \phi_1(x_1)\phi_2(x_2)\dots\phi_n(x_n) \quad (2.13)$$

where  $x_i$  are the electrons occupying the spin orbitals  $\phi_i$ . This is the view chemists are familiar with, i.e. electrons occupying orbitals.

The Hartree approximation assumes each electron to move independently. It also does not take into account the indistinguishability of the electrons. Electrons are fermions, hence putting labels on them is violation of one of the most fundamental principles of the quantum theory; the Pauli Principle.<sup>96</sup> Therefore, the wave function must satisfy the condition;

$$\Psi(x_1, x_2, x_3, \dots, x_n) = -\Psi(x_2, x_1, x_3, \dots, x_n) \quad (2.14)$$

thus be anti-symmetric upon exchange of the labels of any two of the electrons. Slater<sup>97</sup> using the mathematical antisymmetrizing property of determinants, introduced the determinant with spin molecular orbitals as the entries;

$$\Psi = \frac{1}{\sqrt{n!}} \begin{vmatrix} \phi_1(x_1) & \phi_2(x_1) & \dots & \phi_n(x_1) \\ \phi_1(x_2) & \phi_2(x_2) & \dots & \phi_n(x_2) \\ \dots & \dots & \dots & \dots \\ \phi_1(x_n) & \phi_2(x_n) & \dots & \phi_n(x_n) \end{vmatrix} \quad (2.15)$$

the so called (normalized) Slater Determinant; enabling the formulation of Hartree-Fock<sup>98,99</sup> equations. The HF equations describe a system of electrons which only interact in an average style. Although the model is an independent particle model there is some sort of electron correlation by means of same spin electrons avoiding each other in space. The HF equations are solved iteratively in a self consistent manner, hence are usually termed as self consistent field (SCF) equations.

In the HF model if the space parts of the orbitals are chosen to be equal for each pair of electrons, the wave function is said to be spin-restricted; giving rise to the name Restricted Hartree-Fock (RHF). On the other hand the wave function

can be constructed by using a different space part for each orbital. The resulting wave function is called an Unrestricted Hartree-Fock (UHF) wave function.<sup>100</sup> The UHF wavefunction which may lower the energy below the RHF wave function may suffer from the ill behavior of not being an eigenfunction of the total spin operator,  $S^2$ . This condition is termed as spin contamination, and implies the contributions from higher-lying multiplicities to the state of interest.

### 2.3.5 The Basis Set Approximation

Traditionally, the quantum chemical calculations were performed as Linear Combination of Atomic Orbitals - Molecular Orbitals, LCAO MO, where molecular orbitals are formed as a linear combination of atomic orbitals:

$$\phi_i = \sum_{\alpha} c_{\alpha i} \chi_{\alpha} \quad (2.16)$$

In Equation 2.16  $\phi_i$ s are the molecular orbitals,  $c_{\alpha i}$  are the coefficients of linear combination,  $\chi_{\alpha}$  are the atomic orbitals.

Atomic Orbitals (AO) are solutions of the HF equations for the atom, i.e. a wave function for a single electron in an atom. Early, the Slater Type Orbitals (STOs) were used in place of AOs. Later the terms basis function or contraction were used interchangeably. Slater type orbitals have the form

$$\chi_{\zeta, n, l, m}(r, \theta, \varphi) = N Y_{l, m}(\theta, \varphi) r^{n-1} e^{-\zeta r} \quad (2.17)$$

The  $n$ ,  $l$ , and  $m$  are quantum numbers: principal, angular momentum, and magnetic; respectively.  $\zeta$  is the orbital exponent or screening constant.  $N$  is a normalization constant. The STOs, although physically significant, are unfortunately not suitable for fast calculations of the important two-electron integrals. On the other hand the functions in the form of

$$\chi_{\zeta,n,l,m}(r,\theta,\varphi) = NY_{l,m}(\theta,\varphi)r^{(2n-2-l)}e^{-\zeta r^2} \quad (2.18)$$

are mathematically more convenient. These are the Gaussian Type Orbitals (GTOs). Even if one sums up 4 or 5 GTOs to represent an STO, one will still calculate the integrals much faster than if original STOs were used. In all computational chemistry calculations the unknown MOs are expressed in terms of a set of known basis functions, so the practicing of basis set properties is essential in quantum chemistry.

It is important to realize that the more basis functions one uses, the better one approximates the real vector space, and the more expensive the calculations will be.

The smallest number of functions used in the definition of the basis set yields in minimal basis sets. A Double Zeta (DZ) basis set utilizes twice as many functions when compared to the minimal basis set. A triple Zeta (TZ) as thrice and so on. The name “Zeta” originates from the exponent  $\zeta$  in the formulation of STOs and GTOs. The generally used split-valence basis sets supplements only the valence orbitals with more functions.

A significant improvement is made if the flexibility is enhanced by addition of polarization functions to the basis set. The distribution of electron density beyond isolated atoms can be more efficiently described in this way. The effect of the addition of p-type functions to s-type functions, and of d-type functions to p-type functions is shown in Figure 2.3.

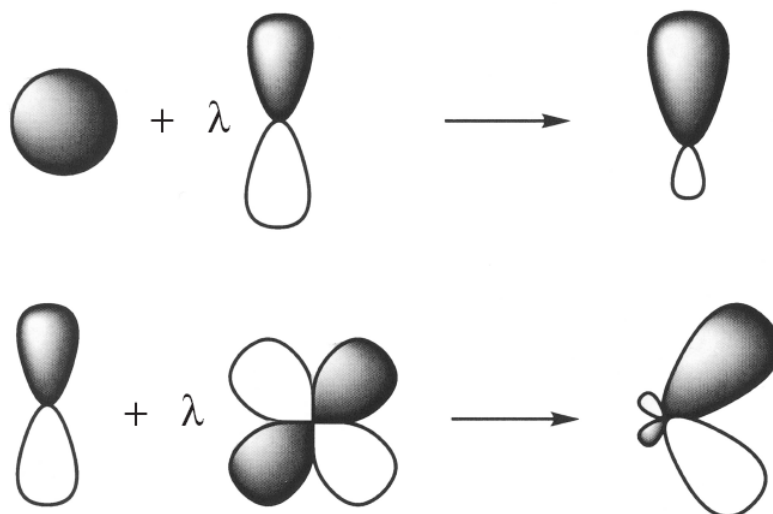


**Figure 2.3.** Effect of polarization functions. Addition of p function greatly enhances the flexibility of an s-type orbital (above); Addition of a d function greatly enhances the flexibility of a p-type orbital (below).

Reprinted from “Ab Initio Molecular Orbital Theory” W. J. Hehre, L. Radom, P. v. R. Schleyer, and J. A. Pople, Wiley, New York, 1986.

Adding diffuse functions (denoted by +) allows the spatial distribution of the basis sets to be much more dispersed. This effect may in particular be needed in simulating the behavior of anions.

Another larger class of basis sets is the correlation consistent (cc-) basis sets. They were specifically designed for recovering as much as possible the correlation energy of the valence electrons. The designations of cc-pVDZ<sup>101</sup>, cc-pVTZ<sup>102</sup>, cc-pVQZ<sup>103</sup>, denote the degree of splitting for the valence electrons. Various augmentations to these basis sets have also been developed. These include the addition of diffuse functions to better describe anions and weakly interacting molecules (aug-cc-pVnZ), as well as special basis sets designed for describing the effects of correlating the core electrons (cc-pCVnZ and cc-pwCVnZ).

In summary, the quality of the approximate solution to the Schrödinger equation improves when the flexibility to where the electrons “are allowed to go”

increases. This increases the size of the basis set, making the calculations computationally more demanding.

### **2.3.6 Electron Correlation Methods**

Currently the most challenging problem for the theoretical chemist is the accurate description of the correlation energy (CE).<sup>104</sup> Electron correlation (EC) refers to the adjustment of electron motion to the instantaneous –instead of spatial averaged– positions of all the electrons in a many-electron system due to the Pauli Exclusion Principle (exchange correlation) and the electrostatic repulsions (Coulomb correlation). It shows the tendency of electrons to correlate their motions in order to keep as far apart as possible. In WFBM, CE is defined as the difference between the HF energy and the exact energy.

Hartree–Fock (HF) theory treats interacting electrons as being independent particles within a self-consistent field (SCF). The HF method recovers ~99% of the total energy of a molecule but the remaining ~1% is in the range of chemical reaction energy. Consequently the appropriate and accurate formulation of CE is vital for theoretical predictions.

There are many techniques for including electron correlation, sometimes termed as going beyond HF. These include Configuration Interaction (CI), Multi-configuration Self Consistent Field (MCSCF) Theory, Many Body Perturbation Theory (MBPT), Coupled Cluster (CC) Theory, and Density Functional Theory (DFT).

#### **2.3.6.1 Configuration Interaction (CI)**

The simplest way of introducing EC to the HF scheme is using a linear combination of the Slater determinants instead of a single determinant. Replacing occupied MOs in the HF determinant with unoccupied MOs, and terming the singly, doubly, triply... replaced determinants as single, double,

triple excitations; then using the linear combination of these determinants as the new approximate wave function is the spirit of the method. These sort of new configurations are multiplied by weighing constants, and the constants are varied self consistently for obtaining the minimum energy of the system. Thus greater flexibility is introduced to the wave function by Configuration Interaction (CI)<sup>105,106</sup> beyond the HF scheme.

If the excitations in the determinants are restricted to single excitations, the method is CI singles (CIS). Higher order CI is termed as CI doubles, (CID); CI singles doubles (CISD) and so on. If the CI expansion is complete (full CI), the exact correlation energy (within the limitations of the basis set in use) is attained. This is one important point that we previously introduced in short. The WFBMs can systematically be improved as far as one dares to deal with. Full CI is impossible except for very small systems as the total number of determinants is

$$\# \text{ of Slater Det} = \frac{b!}{n!(b-n)!} \quad (2.19)$$

where n is the number of electrons, and b is the number of spin orbitals.

### 2.3.6.2 Multi-configuration Self-consistent Field (MCSCF) Theory

The zeroth order wavefunction for a system which in principle can be modeled by a single determinant, is HF. Typical examples include ground state closed shell singlet atoms and molecules. Many problematic cases such as radicals, excited states, transition structures, may frequently fail to be correctly described by HF. Any system with near degeneracy effects can not be well represented by single configuration wavefunctions. In such cases, the correct zeroth order wavefunction is MCSCF  $\Phi$ .

$$\Phi = \sum c_K \Psi_K \quad (2.20)$$

Where  $\Phi$  is the MCSCF wavefunction  $\Psi_K$  is a configuration wavefunction, that can either be a single determinant or a linear combination of determinants in order to be spin-correct;  $c_K$  are the coefficients. Generally  $\Psi_K$  are called configuration state functions (CSF), meaning spin-correct (i.e an eigenfunction of  $S^2$  operator), symmetry-correct configuration wavefunction.

In MCSCF the determinant coefficients and MOs used for constructing the determinants are optimized simultaneously. In this regard it differs from CI, or it can be treated as a special type of CI with MO optimization. MCSCF methods provide an important tool for studying systems with high spin contamination. The correlation energy recovered by MCSCF methods can be divided into two main categories.

The long-range or non-dynamic or static correlation, arises from large separation of electrons in a pair. It is associated with the interaction of electrons at long distance, and hence, it accounts for a correct molecular dissociation. It is non-local and multicentered.

The short-range or dynamic correlation, arises from short separation of electrons in a pair. It is associated with the absence of interelectronic cusp in HF, and hence, anti-parallel electrons tend to be closer than they should be in reality. In order to include dynamical correlation energy in MCSCF one should include perturbative corrections. (Refer to the following section)

One popular formalism of MCSCF is the Complete Active Space SCF (CASSCF) which enables one to include only the relevant CSFs to the MCSCF wavefunction, decreasing the number of determinants to deal with. CASSCF<sup>107</sup> which is sometimes referred to as Full Optimized Reaction Space (FORS)<sup>108</sup>

enables one to design the core, active, and virtual set of orbitals; among which the active ones experiences a full CI optimization. The notation is CASSCF(n,o); which implies n electrons in o orbitals -which are all picked up

manually- make up the active space. A major drawback of CASSCF is the selection method of active space being non-routine.

### 2.3.6.3 Many Body Perturbation Theory (MBPT)

In perturbation methods the full Hamiltonian is partitioned into two;

$$\hat{H} = \hat{H}_0 + \lambda\hat{H}' \quad (2.21)$$

where  $\hat{H}_0$  is the known, unperturbed (reference) part, and  $\hat{H}'$  is a small perturbation to  $\hat{H}_0$ ,  $\lambda$  is a small parameter defining the extent of the perturbation. Utilizing the Taylor series expansion of the perturbed Hamiltonian, and the corresponding perturbed wave function in powers of  $\lambda$ :

$$\begin{aligned} E &= \lambda^0 E_0 + \lambda^1 E_1 + \lambda^2 E_2 + \lambda^3 E_3 + \dots \\ \Psi &= \lambda^0 \Psi_0 + \lambda^1 \Psi_1 + \lambda^2 \Psi_2 + \lambda^3 \Psi_3 + \dots \end{aligned} \quad (2.22)$$

one can obtain the unperturbed wave function and energy; and the first, second, third... order corrections to them. In Equation 2.22  $E_i$  are the energies and  $\Psi_i$  are the wave functions respectively.

The formulation of Moller and Plesset<sup>109</sup> in 1934, employed the zeroth order Hamiltonian from the HF method, and introduced the now popular, inexpensive Moller-Plesset perturbation theory (MPPT). The MPPT to the second order (MP2) is widely used as a quick tool to go beyond HF. With the inclusion of higher order terms the methods MP3... MPn are also available; while complicated and computationally more demanding.

A major shortcoming of PT methods is, they are not variational. Thus there is no guarantee that the calculated PT energy is an upper bound to the energy of the state of interest.

PT methods when applied to MCSCF wave functions help in recovering the dynamical correlation energy. There are several ways to define a multireference perturbation theory. The most noteworthy are the CASPT2<sup>110</sup> method of Roos' group, the MRMP method of Hirao,<sup>111</sup> the closely related MCQDPT method of Nakano,<sup>112</sup> and the MROPTn methods of Davidson.<sup>113</sup> The MCQDPT method used in this study as implemented in GAMESS is a multistate perturbation theory due to Nakano.

#### 2.3.6.4 Coupled Cluster (CC) Theory

Coupled cluster (CC) method, today regarded as the most powerful of post-HF methods for the majority of the chemical problems was formulated for quantum chemical calculations in the sixties.<sup>96,97,98,114,115,116</sup> The wavefunction in CC theory is written as an exponential ansatz;

$$\Psi_{CC} = e^{\hat{T}} \Phi_0 \quad (2.23)$$

where the cluster operator T has the form

$$\hat{T} = \hat{T}_1 + \hat{T}_2 + \hat{T}_3 + \dots + \hat{T}_N \quad (2.24)$$

and the exponent is expanded in the Taylor series;

$$e^{\hat{T}} = 1 + \hat{T} + \frac{1}{2} \hat{T}^2 + \frac{1}{6} \hat{T}^3 + \dots = \sum_{k=0}^{\infty} \frac{1}{k!} \hat{T}^k \quad (2.25)$$

The  $\hat{T}_i$  in Equation 2.24 acting on the reference wave function generates all  $i^{\text{th}}$  excited Slater determinants, and the powers of these  $\hat{T}_i$  result in higher excitation terms. By this way all excitations of a given type to infinite order, - unlike the all excitations to a specified order in PT methods- are included. When these are written explicitly and the excitations to the same order are grouped. The exponential operator is written as;

$$e^{\hat{T}} = 1 + \hat{T}_1 + (\hat{T}_2 + \frac{1}{2}\hat{T}_1^2) + (\hat{T}_3 + \hat{T}_2\hat{T}_1 + \frac{1}{6}\hat{T}_1^3) + \dots \quad (2.26)$$

which will yield the reference, the singly excited state, the doubly excited state, and so on; for the terms in the sequence. The reference function is usually the HF function, and the truncated CC formalisms are denoted as CCD,<sup>117</sup> CCSD,<sup>115,100,101,102</sup> etc. The popular CCSD(T)<sup>118</sup> method has a formulation where the single and double excitations are calculated in an iterative way, and the triple excitations are included by means of perturbation theory; hence the designative difference (T). A CCSD(T) calculation provides a higher-level treatment of electron correlation beyond MP4.

In principle all cluster operators up to  $\hat{T}_n$  may be included in  $\hat{T}$ , to generate all possible excitations and such a coupled cluster wave function is equivalent to the full CI wave function within the same basis. However in practice the method is computationally expensive, and a fully excited cluster is out of question.

At this point before moving to the density functional theory, we want to re-emphasize the “convergent to the exact solution of the Schrödinger equation” character of *ab initio* methods. This is one difference between WFBM and DFT which is of primary importance. The more one increases the size of the basis, and the more one includes correlation energy to the calculation; the closer one gets to the exact answer of the time independent nonrelativistic Schrödinger equation, within the constraints of the Born-Oppenheimer approximation. (vide infra)

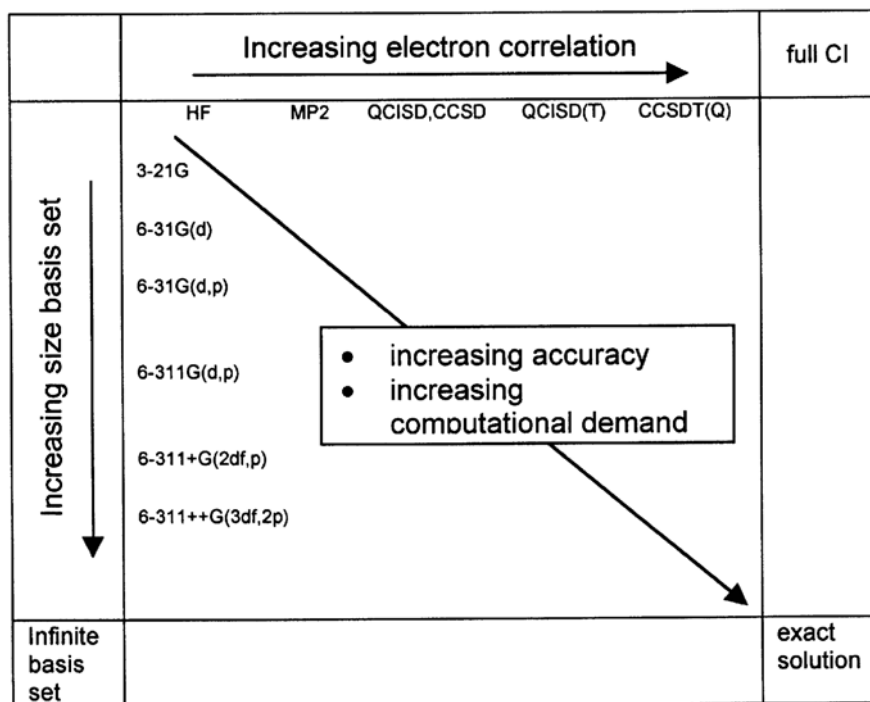


**Figure 2.4.** Pople diagram showing the dependence of the performance of an *ab initio* method on the basis set and the amount of electron correlation.  
 Reprinted from “Ab Initio Molecular Orbital Theory” W. J. Hehre, L. Radom, P. v. R. Schleyer, and J. A. Pople, Wiley, New York, 1986.

### 2.3.6.5 Density Functional Theory

DFT is based on two fundamental theorems. The basic Hohenberg-Kohn<sup>119</sup> theorem ensures the existence of the exact ground state energy of a molecular system as a functional of only the electron density and the fixed positions of the nuclei. Accordingly, for a given nuclear distribution, the electron density uniquely determines the energy and all properties of the ground state, including the electronic Hamiltonian and its ground state wave function. Yet the theorem does not state the explicit formula for this functional dependence of the energy on the electron density. The second Hohenberg-Kohn theorem, in turn, ensures that the exact electron density function is the one that minimizes the energy, in that way giving a variational principle to find the density

Kohn–Sham<sup>120</sup> (KS) theory proves that the electronic energy for a system of  $n$  interacting electrons, can be written as the contributions of; the kinetic energy ( $E_{KE}$ ) of the ground state of non-interacting electrons; the classical Coulomb electron-nuclear attraction  $E_{nN}$ ; the classical Coulomb electron-electron repulsion  $J_{nn}$ ; and a non-classical term accounting for correlation and exchange effects included in the exchange-correlation (XC) energy,  $E_{xc}$ .

$$E_{\text{el}}^{\text{KS-DFT}} = E_{KE}[\rho] + E_{nN}[\rho] + J_{nn}[\rho] + E_{xc}[\rho] \quad (2.27)$$

In the local-density approximation of DFT, the exchange-correlation energy of an inhomogeneous system, such as an atom or a molecule, is estimated by an integral. The integrand of this integral samples the local density  $\rho(\mathbf{r})$  at each integration point  $\mathbf{r}$ .

In the generalized gradient approximation (GGA) of DFT, the exchange-correlation energy of the inhomogeneous system is estimated by an integral, whose integrand depends on the density and its gradient.

Becke successfully introduced semiempirical fitting parameters in the GGA based on the atomization energies of a standard set of molecules. In a subsequent approach founded on the adiabatic connection formalism, Becke<sup>121</sup> further introduced a hybrid method, with an exchange-correlation expression that contains a parameter to include non-locality in the real exchange-correlation hole. This was shortly thereafter combined with the LYP<sup>122</sup> correlation functional to yield the hybrid B3LYP functional;

$$E_{xc}^{\text{B3LYP}} = aE_x^{\text{LSDA}} + (1-a)E_x^{\text{HF}} + b\Delta E_x^{\text{B88}} + c\Delta E_c^{\text{LYP}} \quad (2.28)$$

where  $\Delta E_x^{\text{B88}} = E_x^{\text{B88}} - E_x^{\text{LSDA}}$ ,  $\Delta E_c^{\text{LYP}} = E_c^{\text{LYP}} - E_c^{\text{LSDA}}$  and the empirical values of the parameters are:  $a = 0.80$ ,  $b = 0.72$ , and  $c = 0.81$ .

## 2.4 The Computational Chemistry Suites Employed

The calculations in this work have mostly been performed by using Gaussian 03 (RevD.01)<sup>123</sup> suite of programs, and the GAMESS<sup>124</sup> package. Gaussian 03 was used for the DFT and CC calculations as well as the preliminary CASSCF jobs. GAMESS was used for the CASSCF and MRMP calculations. The details of the calculations for the two sections of the discussion are given separately prior to the discussions, and within the text where necessary.

A graphical interface program<sup>125</sup>, which allows full integration of various packages including Gaussian 98, Gaussian 03, and GAMESS, have been used for the processes of giving input and assessing output, to linux and windows platforms as well as all kind of visualization jobs. Our linux workstations and our in-house PC cluster *ivc* of the Computational Chemistry Laboratory were the primary computer resources in this work.

## 2.5 Further Reading

Below is a list of introductory computational chemistry books, and web sites containing helpful theoretical/computational material. The theoretical and mathematical introduction of this section was written by trying to be consistent with the material presented in the following books.

- ❖ "Ab Initio Molecular Orbital Theory" W.J.Hehre, L.Radom, J.A.Pople, P.v.R.Schleyer, Wiley and Sons, New York, 1986.
- ❖ "Modern Quantum Chemistry: Introduction to Advanced Electronic Structure Theory" A.Szabo, N.S.Ostlund Dover Publications Inc., 1996.
- ❖ "Quantum Chemistry, 5th Edition" I.N.Levine Prentice Hall, 1999.
- ❖ "Introduction to Computational Chemistry" F.Jensen Wiley and Sons, Chichester, 1999.
- ❖ "Introduction to Quantum Mechanics in Chemistry" M.A.Ratner, G.C.Schatz Prentice Hall, 2000.

- ❖ “Handbook of Computational Quantum Chemistry” David B. Cook, Dover Publications Inc., 2005.
- ❖ “Essentials of Computational Chemistry: Theories and Models”, Christopher J. Cramer, Wiley 2004.
- ❖ “Quantum Chemistry: The Development of Ab Initio Methods in Molecular Electronic Structure Theory”, Henry F. Schaefer III, Dover Publications Inc., 2004.
- ❖ “An Introduction to Theoretical Chemistry” Jack Simons, Cambridge University Press, 2003.
- ❖ <http://www.ccl.net/chemistry/index.shtml>
- ❖ <http://www.msg.ameslab.gov/GAMESS>
- ❖ <http://simons.hec.utah.edu/TheoryPage/index.html>
- ❖ <http://www.fz-juelich.de/nic-series/NIC-Series-e.html>
- ❖ [http://zopyros.ccqc.uga.edu/lec\\_top/lectures.html](http://zopyros.ccqc.uga.edu/lec_top/lectures.html)
- ❖ <http://www.smps.ntu.edu.au/modules/>

## CHAPTER III

### RESULTS AND DISCUSSION

*If we knew what it was we were doing, it would not be called research, would it?*

*Albert Einstein*

*Nothing resembles a new phenomenon as much as a mistake.*

*Enrico Fermi*

#### 3.1 Reactions of $^1\text{S}$ , $^1\text{D}$ , and $^3\text{P}$ Carbon Atoms with Water

The purpose in this part was exploring reactions of  $\text{C}(^3\text{P})$ ,  $\text{C}(^1\text{D})$ ,  $\text{C}(^1\text{S})$  atoms with alcohols by computational chemistry methods. Reliable treatment of singlet carbons is problematical. The isolated  $\text{C}(^1\text{D})$  atom is in an excited electronic state that has five-fold spatial degeneracy. On its approach to the oxygen of an alcohol molecule this degeneracy splits, but we still have to deal with two nearly isoenergetic potential energy surfaces (PES). An accurate description of the initial stages of the reaction is critical as it is this part of the reaction path that determines the branching into the CO and carbene paths. Standard *ab initio* or DFT methods based on single-determinantal wave functions may fail to make reliable predictions. Thus MCSCF methods including electron correlation are chosen to verify or clarify the assessments.



CAS(12,10) and CAS(12,10)-MRMP(FC), and in some cases at CAS(12,12)-MRMP(FC) levels.<sup>a</sup>

The TSs on the first excited singlet PESs are located at the state averaged CAS(12,10) level, denoted as CAS(12,10)-avg, using the first two singlets with equal weights. The second singlet is optimized for a saddle point, employing numerical gradients. Likewise, vibrational frequencies are obtained numerically in these cases.

Examination of the CAS(12,10) PES as a function of the carbon-oxygen separation,  $r$ , (see Figure 3.2) indicated that at large  $r$  this active space tended to a 2 electrons in 2 orbitals (2px and 2py) CAS(2,2) for the carbon atom,<sup>b</sup> and an all-electrons CAS(10,8) for the H<sub>2</sub>O fragment where the 1s and 3p<sub>x</sub> AO<sup>c</sup> of oxygen became active in addition to the 6 valence orbitals on water. In order to have a balanced description of all states of complex 1 originating from <sup>1</sup>D, <sup>3</sup>P, and <sup>1</sup>S states of the carbon atom, one needs an active space that retains all three 2p orbitals on carbon when  $r$  gets large (see Table 3-5). Consequently, a larger CAS(12,12) obtained from CAS(12,10) by augmenting the latter with the oxygen 3s and 3p<sub>x</sub> AOs is employed in calculations at various points on the PES. At infinite  $r$ , this (12 electron, 12 orbital) active space gives CAS(4,4) for the carbon atom, and CAS(8,8) for the water molecule.<sup>d</sup> Relative CASSCF and MRMP (at 0 K) enthalpies reported below are obtained by combining the MRMP energies with harmonic zero-point vibrational energies (ZPVE) that are computed at the CAS(12,10) level at CAS(12,10)/6-311G(d,p) optimized

---

<sup>a</sup> The CAS(12,10)-MRMP(FC) and CAS(12,12)-MRMP(FC) optimizations are carried out with numerical evaluation of gradients as implemented in GAMESS program. The 1s core orbitals on carbon and oxygen are excluded from the correlation treatment, (FC).

<sup>b</sup> i.e. as  $r$  gets larger, contribution of carbon 2p<sub>z</sub> to the active space diminishes, eventually exchanging with the 3p<sub>x</sub> of oxygen while carbon 2s moves into the inactive space (core).

<sup>c</sup> x-axis is perpendicular to the plane of water molecule; see Figure 3.2.

<sup>d</sup> Active orbitals for carbon are 2s and 2p; those for water are 2s, 2p, 3s, 3p<sub>x</sub> on oxygen and 1s on each hydrogen. With CAS(12,12), the 1s core orbitals on carbon and oxygen remain inactive at all geometries of complex 1.

geometries. The enthalpies are given at CAS(12,10)-MRMP(FC) and CAS(12,12)-MRMP(FC) levels. In the following, these will be referred to as MRMP-1 and MRMP-2, respectively.

Where appropriate the CASSCF results are compared against predictions by coupled clusters (CCSD) and density functional (B3LYP) methods. The latter calculations are done by the Gaussian98 program.<sup>129</sup> The 6-311G(d,p) basis set is used in geometry optimizations and in obtaining harmonic ZPVE at CCSD level. Energies are then refined by single-point CCSD(T)/aug-cc-pVTZ calculations at CCSD/6-311G(d,p) optimized geometries. Core electrons are excluded from the correlation calculations. The B3LYP computations employed the aug-cc-pVTZ basis set in both geometry optimizations and in performing harmonic vibrational analysis.

Connectivities of stationary points (including those on excited singlet PESs) are verified by intrinsic reaction coordinate (IRC) runs.<sup>130</sup>

Notation scheme for species and PESs is provided in Table 3-6. Partial List of Abbreviations “Table 3-6. A transition structure between two consecutive minima, *A* and *B*, on a PES will be indicated by the designation “*A/B*”.

Coupled-cluster singles and doubles method with a perturbative treatment of triple excitations (CCSD(T)) is a powerful and practical approach for achieving predictions within chemical accuracy ( $\pm 1-2$  kcal/mol). It works best when the (lowest-energy) electronic state of a given spin multiplicity can be reasonably well represented by a single-determinant Hartree-Fock wave function; i.e. CCSD(T) is a single-reference method. Electronic states that are known to require more than one Hartree-Fock determinant for a qualitatively correct description need special attention. For example in the BH molecule, CCSD(T) fails for bond lengths larger than 2.6 Å<sup>131</sup>. There is a similar break down of the method in the HF molecule. The failure is attributable to growing multireference character in the wave function at large bond lengths. The

problem of substantial multireference character is also present in the reactions of singlet C(<sup>1</sup>D) atoms studied in this work. It is therefore necessary to validate the reliability of the CCSD(T) method in the troublesome regions of the singlet PES where multireference character is expected. The most difficult part of the singlet PES involves the initial path of attack of the C(<sup>1</sup>D) atom to the substrate. Indeed, the isolated C(<sup>1</sup>D) atom itself appears to face this problem. The <sup>1</sup>D term has a five-fold spatial degeneracy. If complex orbitals could be used, two of these states, those with  $M_L = \pm 2$ , could each be expressed by a single closed-shell Slater determinant, and CCSD(T) based on such complex reference wave functions should work. However, our computational facilities allow only real orbitals in coupled-cluster calculations. With real orbitals none of the five states can be adequately approximated by a single determinant, and it is not obvious whether CCSD(T) based on a real restricted Hartree-Fock reference will still be reliable.

For a given basis set and a specified electronic spin, exact solutions of the nonrelativistic Schrodinger equation can be obtained by a full configuration interaction (CI) calculation. Carbon atom is a small system for which full CI calculations with relatively large basis sets are feasible. The CCSD(T) method for the same spin state and using the same basis set as in CI provides an approximation to the lowest eigenvalue of the CI matrix. Thus for a given basis set, absolute accuracy of CCSD(T) method for each spin state can be determined by comparing CCSD(T) energy against the lowest eigenvalue of the CI matrix.

Table 1.1 lists the absolute energies of the three terms obtained by full-valence (the core 1s electrons are not correlated) CI calculations with three different basis sets. Table 3-3 compares relative energies of the two singlets against the experimentally known values. Use of cc-pVTZ basis set appears to produce sufficiently high quality results for both singlets. Results of CCSD(T) calculations for the lowest singlet and triplet states are given in Table 3-2. The

singlet calculation employed the spin-restricted coupled-cluster formalism whereas in the triplet, unrestricted CCSD(T) was used (in both, the core 1s orbital was frozen). shows the errors in the CCSD(T) values as a function of basis set size. It is seen that errors in both the singlet and triplet CCSD(T) values are nearly independent of basis set. For the triplet, the CCSD(T) method almost exactly reproduce the computationally much more expensive CI results.

**Table 3-1 Full-valence CI absolute energies (hartrees) of the lowest three terms of carbon atom using three basis sets of increasing size.**

Basis set	<sup>3</sup> P	<sup>1</sup> D	<sup>1</sup> S
6-311g(d,p)	-37.767049	-37.712809	-37.661885
cc-pVTZ	-37.781280	-37.732046	-37.679057
cc-pVQZ	-37.786813	-37.739354	-37.686958

**Table 3-2. CCSD(T)-FC absolute energies (hartrees) for the lowest triplet and singlet terms of carbon atom versus basis set.**

Basis set	<sup>3</sup> P	<sup>1</sup> D
6-311g(d,p)	-37.766669	-37.708155
cc-pVTZ	-37.780762	-37.727207
cc-pVQZ	-37.786540	-37.734696

**Table 3-3. Full-valence CI energies (kcal/mol) of the two lowest singlet terms relative to the ground term <sup>3</sup>P of carbon atom versus basis set.**

Basis set	<sup>1</sup> D	<sup>1</sup> S
6-311g(d,p)	34.0	66.0
cc-pVTZ	30.9	64.1
cc-pVQZ	29.8	62.7
Experiment	29.1	61.9

**Table 3-4. Difference (kcal/mol) between ccSD(t)-fc and CI-FC energies for the lowest triplet and singlet terms of carbon atom versus basis set.**

Basis set	<sup>3</sup> P	<sup>1</sup> D
6-311g(d,p)	0.24	2.92
cc-pVTZ	0.32	3.04
cc-pVQZ	0.17	2.92

It appears that contribution of connected quadruple excitations (omitted in CCSD(T) formalism) to the energy of the triplet is not significant. On the other hand, the error of about 3 kcal/mol in the restricted CCSD(T) values for the singlet state is attributable to these missing quadruple excitations. It can be concluded that spin-restricted CCSD(T) method with real orbitals is reliable in predicting properties of <sup>1</sup>D carbon atom in spite of its five-fold degeneracy.

When a <sup>1</sup>D carbon atom approaches a substrate molecule such as H<sub>2</sub>O, the degeneracy between the  $M_L=+2$  and  $M_L=-2$  states is removed, but the splitting remains very small as indicated by MCSCF calculations. Both states are attractive (the remaining three states being repulsive). At close distances to the substrate molecule, one of these two states evolves into a closed-shell singlet while the other retains an open-shell-singlet character. The spin-restricted CCSD(T) method should be reliable for the description of the closed-shell singlet PES.

### 3.1.2 Approach of Carbon to the Water Molecule.

Initial attachment of carbon atom in various states to the water molecule in its ground state was explored as a function of the out-of-plane bending angle  $\alpha$  and the distance  $r$  between carbon and oxygen (Figure 3.2). The OH<sub>2</sub> part of the system was kept frozen at the CAS(8,8)/6-311G(d,p) optimized geometry of water.<sup>a</sup> The lowest nine PESs in  $C_{2v}$  and  $C_s$  symmetric structures were probed by the CAS(12,12)/6-311G(d,p) method. Table 3-5 lists the asymptotic forms of

<sup>a</sup> R<sub>OH</sub>=0.962 angstroms,  $\angle$ HOH=104 degrees.

the electronic wavefunctions arising from the combination of  $^1S$ ,  $^1D$ , and  $^3P$  carbon atoms with water. As a loose terminology, the  $a^1A_1$ ,  $c^1A_1$ , and  $f^1A_1$  states (under  $C_{2v}$  symmetry) containing doubly occupied orbitals will be referred to as the “closed-shell” states, and the remaining singlets with singly occupied orbitals will be called “open-shell” singlets. Calculations indicate that the former singlets smoothly evolve into approximately single-determinantal forms as  $r$  decreases, whereas the latter singlets are much more resistant to change their open-shell (i.e. two-determinantal) character.

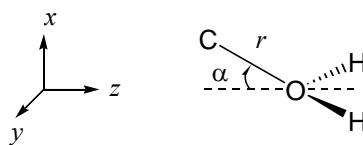


**Figure 3.2.** Definition of PES probe parameters  $\alpha$  and  $r$ .  $\alpha=0$  corresponds to a  $C_{2v}$  symmetric structure in which all atoms lie on the  $yz$  plane. For nonzero  $\alpha$ , symmetry reduces to  $C_s$  ( $xz$  plane is the symmetry plane).

**Table 3-5 Approximate Electronic State Functions (unnormalized) of C+H<sub>2</sub>O System at  $\alpha=0$  and Large  $r$ .<sup>a</sup>**

carbon species	$\Psi$	state label	
		$C_{2v}$	$C_s$
C( <sup>1</sup> S)	$ p_x\bar{p}_x  +  p_y\bar{p}_y  +  p_z\bar{p}_z $	$f^1A_1$	$f^1A'$
C( <sup>1</sup> D)	$ p_x\bar{p}_x  -  p_y\bar{p}_y $	$a^1A_1$	$a^1A'$
	$ p_x\bar{p}_y  -  \bar{p}_x p_y $	$b^1A_2$	$b^1A''$
	$ p_x\bar{p}_x  +  p_y\bar{p}_y  - 2 p_z\bar{p}_z $	$c^1A_1$	$c^1A'$
	$ p_y\bar{p}_z  -  \bar{p}_y p_z $	$d^1B_2$	$d^1A''$
	$ p_x\bar{p}_z  -  \bar{p}_x p_z $	$e^1B_1$	$e^1A'$
C( <sup>3</sup> P) <sup>b</sup>	$ p_x p_y $	$X^3A_2$	$X^3A''$
	$ p_y p_z $	$A^3B_2$	$A^3A''$
	$ p_x p_z $	$B^3B_1$	$B^3A'$

<sup>a</sup> See Figure 3.2. Vertical bars denote Slater determinants;  $p_x$ ,  $p_y$ ,  $p_z$  are orbitals localized mainly on the approaching carbon atom. Horizontal bar on an orbital symbol indicates a  $\beta$  spin orbital. Closed shell parts are not shown, but implied. <sup>b</sup>  $M_S=1$  spin states.

**Table 3-6. Partial List of Abbreviations<sup>a</sup>**

species	C-OH <sub>2</sub>	HOCH	H <sub>2</sub> CO	HCO	COH	CO + 2H	CO + H <sub>2</sub>	CH <sub>2</sub> (OH) <sub>2</sub>
label	<b>1</b>	<b>2</b>	<b>3</b>	<b>4</b>	<b>5</b>	<b>6</b>	<b>7</b>	<b>8</b>

<sup>a</sup> Singlet labeling is used as above, T is used for triplet species throughout the text. PESs of doublets **4** and **5** are marked by symmetry species A' and A'' of the  $C_s$  group.

Figure 3.3. depicts the behavior of the singlet state energies with decreasing  $r$  under  $C_{2v}$  symmetry (i.e.  $\alpha=0$ ). Two of the states originating from the five-fold degenerate <sup>1</sup>D state of carbon, the closed shell  $a^1A_1$  and the open shell  $b^1A_2$ , are weakly attractive while the remaining states are repulsive along this direction of approach. Interestingly, the  $f^1A_1$  state corresponding to <sup>1</sup>S carbon is the most repulsive at all distances considered. Calculations at  $\alpha$  values between 0 and 150° showed a similar pattern. These results suggest that the <sup>1</sup>S carbons are not reactive toward H<sub>2</sub>O.

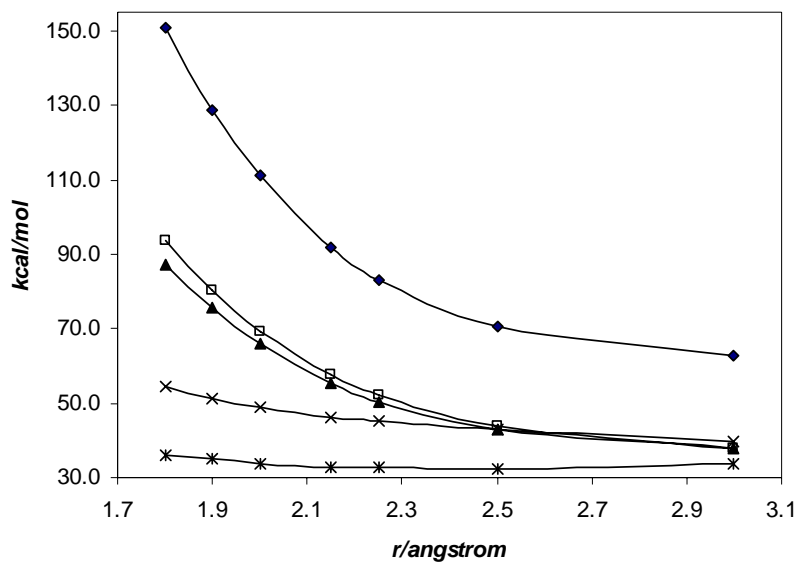


**Figure 3.3.** CAS(12,12)/6-311G(d,p) energies of the singlet states relative to C(<sup>3</sup>P)+H<sub>2</sub>O at  $\alpha=0$  ( $C_{2v}$ ) as a function of r.

<sup>a</sup>Lowest curve is a <sup>1</sup>A<sub>1</sub>; b <sup>1</sup>A<sub>2</sub> is indistinguishable from a <sup>1</sup>A<sub>1</sub> at this scale. Crosses: c <sup>1</sup>A<sub>1</sub>; triangles: d <sup>1</sup>B<sub>2</sub>; squares: e <sup>1</sup>B<sub>1</sub>; diamonds: f <sup>1</sup>A<sub>1</sub>.

<sup>a</sup> CAS(4,4) for C(<sup>3</sup>P), and CAS(8,8) for H<sub>2</sub>O with 6-311G(d,p) basis set.

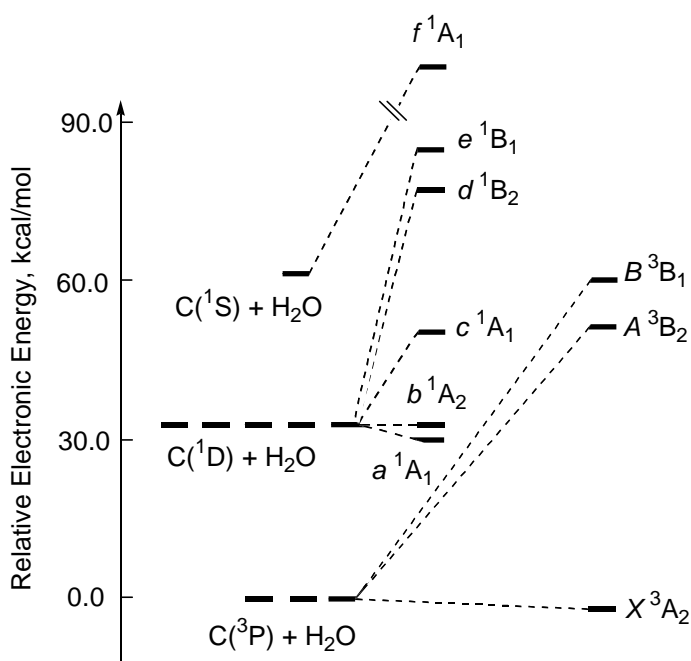


**Figure 3.4.** Electronic states of complex 1 at  $r=1.744$  angstrom in planar  $C_{2v}$  structure. CAS(12,12)-MRMP/6-311G(d,p) relative electronic energies (without ZPVE) are shown.

It may be anticipated that among the three triplet states, only the  $X^3A_2$  ( $C_{2v}$  symmetry) PES is attractive. Figure 3.4 shows the split levels at  $r=1.744$  angstrom.

Occupation numbers of natural orbitals are convenient measures of multireference character in a wavefunction. A singlet state is considered to be adequately represented by a single determinant if all occupation numbers are close to either 2 or zero. Occupation numbers  $n^a$  of  $p_x$ ,  $p_y$ , and  $p_z$  orbitals in all open shell singlets remained at their asymptotic values of 1.0 at all  $r$  and  $\alpha$  values considered (Table 3-7). Note that, for the same reason, in these open shell states charge density distribution is not very sensitive to geometry changes. The three closed shell states are much more responsive in this respect. In the lowest energy singlet state, a  $^1A_1$ , occupation numbers of  $p_x$  and  $p_y$  orbitals gradually change from 1.0 at infinite separation to 0.08 and 1.95 at  $r=1.744$  angstrom ( $C_{2v}$  geometries), for  $n(p_x)$  and  $n(p_y)$ , respectively, the state

<sup>a</sup> All occupation numbers reported in this section are from single-point CAS(12,12)/6-311G(d,p) calculations at the indicated geometries.

approaching a closed shell configuration. In other words, charge density on the carbon atom is more and more polarized along y direction with decreasing r. The second and third (c and f)  $^1A_1$  states also approach closed shell configurations as r decreases, with electrons on the carbon atom polarized along x and z directions, respectively.

**Table 3-7. Occupation Numbers of  $p_x, p_y, p_z$  Orbitals in Singlet States at  $r=1.744$  angstrom**  
<sup>a</sup>

state	$n(p_x)$	$n(p_y)$	$n(p_z)$
$f^1A_1$	0.09 (0.71)	0.09 (0.71)	1.94 (0.71) <sup>b</sup>
$a^1A_1$	0.08 (1.0)	1.95 (1.0)	0.04 (0.0)
$b^1A_2$	1.0 (1.0)	1.0 (1.0)	0.0 (0.0)
$c^1A_1$	1.73 (0.5)	0.33 (0.5)	0.04 (1.0)
$d^1B_2$	0.06 (0.0)	1.0 (1.0)	1.0 (1.0)
$e^1B_1$	1.0 (1.0)	0.06 (0.0)	1.0 (1.0)

<sup>a</sup> CAS(12,12)/6-311G(d,p) occupation numbers at a  $C_{2v}$  symmetric geometry;  $R_{OH}=0.962$  angstrom,  $\angle HOH=104$  degrees. Values in parentheses are those at  $r=\infty$ . <sup>b</sup> Asymptotic values in  $f^1A_1$  state are larger than 2/3 due to some contribution from the carbon 2s orbital. This is also true at  $r=1.744$  angstrom.

### 3.1.3 Remarks on the Methodological Details of Excited State Calculations

We here will discuss only the singlet PES. Our calculations indicate that in addition to the closed-shell singlet, the reaction of  $C(^1D)$  with water (and probably with other alcohols) may also proceed on the excited (open-shell) singlet PES. Same numbers are used to label the species in their ground and excited states. Excited species are distinguished by placing an asterisk to the numbers.

The stationary points (minima and TS) on the excited singlet PES are found by CAS(12,10)/6-311G(d,p) optimizations. Direct use of absolute CASSCF or even CAS-MRMP energies do not give relative energies with sufficient accuracy. This is due to the sensitivity of the results on (unavoidable) small

changes in the active space when comparing energies of species with very different geometries. Qualitatively minor-looking changes in the active orbitals easily cause deviations in energy by 5-6 kcal/mol. Uncertainties of this magnitude are not tolerable especially for the entrance channel of our reaction. In order to obtain presumably more reliable relative energies we proceed as follows.

The closed-shell singlet energy at most geometries of interest can be calculated accurately by `ccsd(t)/cc-pVTZ` method (a good level of theory combined with a relatively large basis set). This is a single-point calculation. If we can obtain a good estimate of the vertical energy separation (gap) between the open-shell singlet and the lower singlet at a given geometry, then we can combine this energy difference ( $\Delta E$ ) with the absolute `ccsd(t)` energy of the closed-shell singlet to get an accurate energy for the upper singlet at this geometry. We calculate  $\Delta E$  by CAS-MRMP and check it with another method EOM-CCSD. The latter method finds  $\Delta E$  directly. We may expect less serious problems with CAS-MRMP now since the geometry is the same for both states. Firstly, there is a better chance of error cancellation when we find  $\Delta E$  by subtraction. Also, by using state-average CAS MOs (MOs optimized for both states) we may expect reasonably well description of the electronic structures in both states (instead of biasing one state over the other in a normal single-state CASSCF). In other words, energies of the two states are calculated using the same set of MOs. Dynamical correlation effects will be partially corrected by MRMP. The geometries we select will be CASSCF optimized stationary points of the open-shell singlet PES. We will denote such points by  $R^*$ . Let  $E(R^*)$  be the `ccsd(t)/cc-pVTZ` energy of the closed-shell singlet PES at geometry  $R^*$ , and let  $\Delta E(R^*)$  be the energy gap at same geometry, calculated by CAS(12,12)-MRMP-avg. Then we estimate  $E^*(R^*)$ , the absolute energy of open-shell singlet state at  $R^*$ , by:  $E^*(R^*) = E(R^*) + [\Delta E(R^*)]$ .

The relative enthalpies will then be obtained as usual, using these values and correcting for ZPVE differences. The ZPVEs of the excited singlet species are calculated at CAS(12,10)/6-311g(d,p) level. For many species on the closed-shell PES we have ZPVE values calculated at both ccSD and CASSCF levels. An inspection of these values indicates that there is only a minor discrepancy between the CCSD and CASSCF ZPVE for a given species. Hence, CASSCF ZPVEs of the excited species can be safely<sup>a</sup> combined with CCSD ZPVE of our reference species (formaldehyde) in obtaining relative enthalpies.

### 3.1.4 Carbon-Water Complex 1.

The minimum energy paths (MEP) for the approach of singlet and triplet carbons to the water molecule are barrierless, both having  $C_s$  symmetry (i.e.  $\alpha > 0$ ). The electronic state along the singlet MEP is the closed shell  $a^1A'$ , but the open shell  $b^1A''$  is nearly isoenergetic in a considerably large region of PES including MEP (these singlet species will henceforth be referred to as **1** and **1\***, respectively). In fact, the two singlet PESs as well as the ground triplet PES **1T** are nearly parallel all the way from large  $r$  to the vicinity of their minima. This is not surprising since these three states originate from asymptotic wavefunctions that do not contain the carbon  $2p_z$  orbital (Table 3-5). At large  $r$ , they have approximately the same one-electron density distribution. Interfragment electron correlation (electrons on carbon with those on the water fragment) is minor at such distances, and the three PESs behave similarly with decreasing  $r$ .

Structures of complex 1 at minima of the three PESs are similar (Figure 3.5). All are bent, with  $C_s$  symmetry. The out-of-plane angle  $\alpha$  is near  $70^\circ$ .

---

<sup>a</sup> The TS  $2^*/4^*$ , H-dissociation TS on the excited PES, was problematic in frequency calculation (optimization was OK). Two of the (numerical) vibrational frequencies were too large, and hence completely unphysical. The ground state analogue,  $2/4$ , was also a difficult case. In calculating  $H_0$  of  $2^*/4^*$ , ZPVE of  $2T/4$  is used. This should not cause a significant error since ZPVE of the singlet TS  $2/4$  is similar to that of the triplet  $2T/4$ , and we may expect a similar value for ZPVE of  $2^*/4^*$ .

Geometry of H<sub>2</sub>O fragment remains essentially same as in isolated water. The C-O distance,  $r_{\min}$ , is the least certain geometric parameter of the complex. It is sensitive to the level of theory employed. For the closed-shell singlet species, 1S-a, CAS(12,10) predicts it to be 2.127 angstrom. Including dynamic electron correlation with CAS(12,10)-MRMP,  $r_{\min}$  decreases to 1.818 angstrom. Using a larger active space with inclusion of correlation, CAS(12,12)-MRMP,  $r_{\min}$  is 1.957 angstrom. Clearly, the closed-shell singlet PES is substantially flat in the neighborhood of its 1 minimum. A similar fluctuation in geometry is found with the ground state triplet complex, 1T. While CAS(12,10)-MRMP and B3LYP predict shorter distances (1.785 and 1.862 angstrom, respectively), CAS(12,10) and CCSD optimizations place  $r_{\min}$  at 2.236 and 2.016 angstrom, respectively. Structure of the complex in its open-shell singlet state, 1\* appears to be more definitive with  $r_{\min}$  = 1.80 angstrom at the correlated level.

**Table 3-8. Occupation Numbers of Natural Orbitals 8 and 9 at Relevant Stationary Points on PES <sup>a</sup>**

species	$n_8$	$n_9$
<b>1</b>	1.34	0.66
<b>1/inv</b>	1.48	0.53
<b>1/5</b>	1.94	0.06
<b>1/2</b>	1.92	0.07
<b>1*</b>	1.00	1.00
<b>1*/inv</b>	1.00	1.00
<b>1*/5*</b>	1.39	0.60
<b>1*/2*</b>	1.12	0.89
<b>2*</b>	1.06	0.95
<b>3</b>	1.93	0.07

<sup>a</sup> CAS(12,12)/6-311G(d,p); these orbitals correspond to HOMO and LUMO of closed-shell molecule.

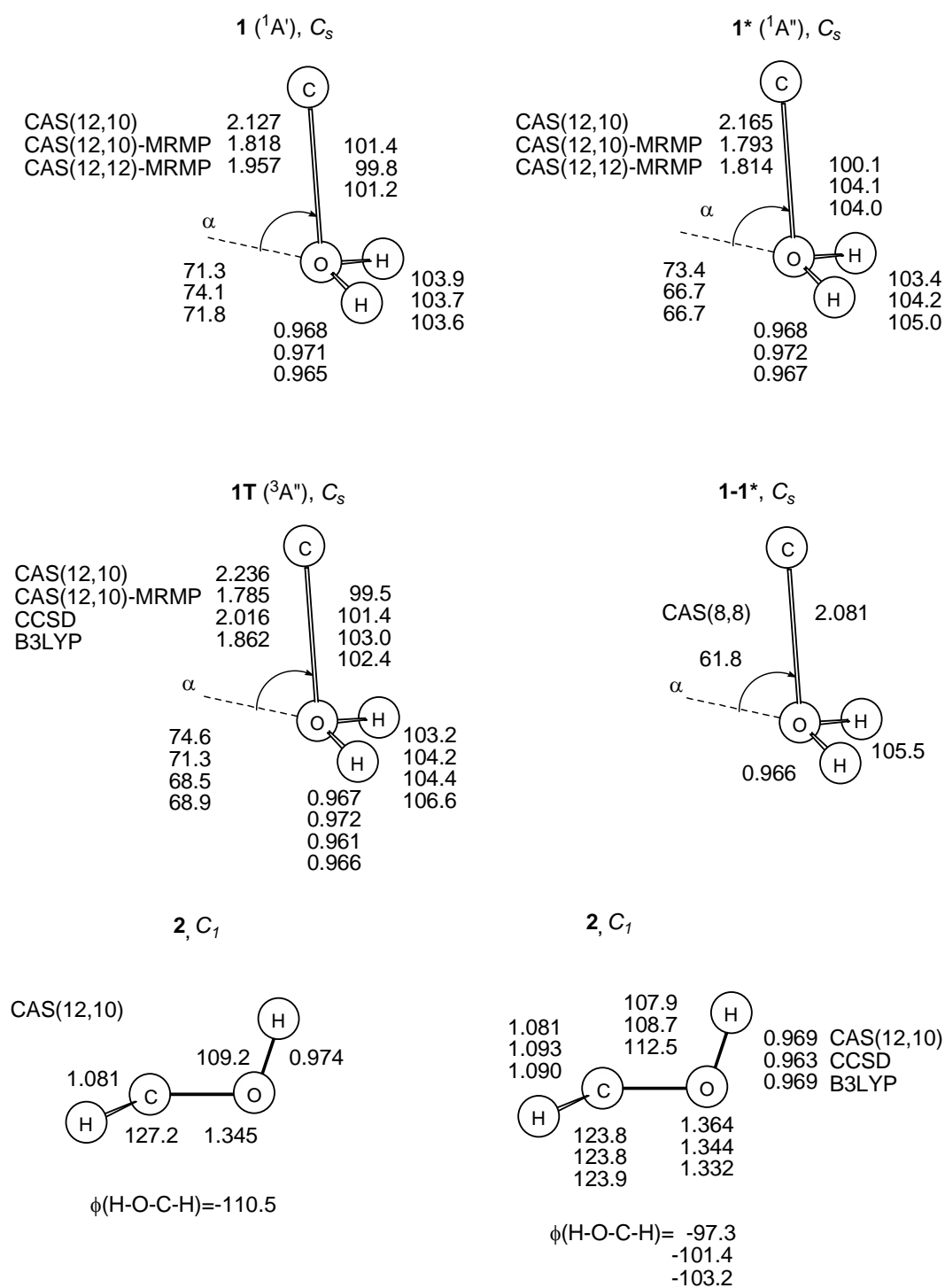


**Figure 3.5.** Optimized geometries of minima at various theoretical levels as indicated. Bond lengths are in angstroms and angles are in degrees.

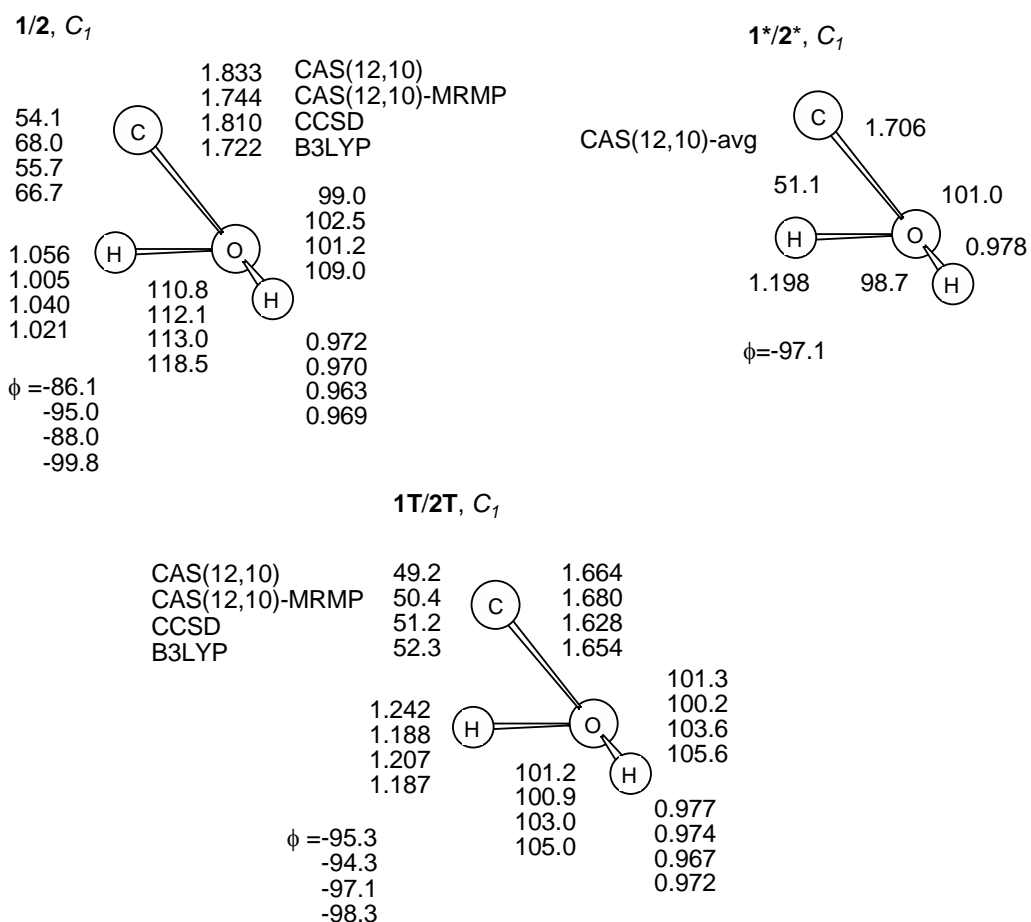


**Figure 3.6.** Optimized geometries at various theoretical levels of transition states leading from complex **1** to hydroxymethylene **2**. Bond lengths are in angstroms and angles are in degrees.  $\phi$  is the dihedral angle, C-O-H\*-H, where H\* is the left hydrogen in the pictures.

As remarked before, the two singlet surfaces are energetically very close in the vicinity of their minima. Geometry of closest approach of the two PESs in this region is determined by carrying out a CAS(8,8)/6-311G(d,p) conical intersection optimization starting with an unsymmetrical geometry.<sup>a</sup> The result is a  $C_s$  symmetric geometry with  $r=2.081$  angstrom and  $\alpha=61.8^\circ$  (species **1-1\*** in Figure 3.5). At this structure, **1** lies lower than **1** by 1.4 and 1.8 kcal/mol at CAS(8,8) and CAS(8,8)-MRMP levels, respectively.

<sup>a</sup> The conical intersection CASSCF calculation is done with GAUSSIAN98.

### 3.1.5 Exit Channels from Complex 1.

No transition structure along path c of Figure 3.1 leading to direct formation of H<sub>2</sub> and CO could be located. It is most likely that path c does not exist.<sup>a</sup> This conclusion is supported by experiments of ref 75b in which no CO was observed as a product. Carbon monoxide is an unreactive species under the conditions of these experiments. If it were formed at some stage during the reaction, it would have been eventually detected. Transition structures in the other two paths are found without much difficulty, and verified at several theoretical levels. Figure 3.6 displays the TSs in the rearrangement of complex 1 to hydroxymethylene 2. The closed-shell 1 PES is connected with the lowest singlet PES, **2**, of 2, whereas the open-shell 1\* PES continues into the first excited singlet state, 2\*, of 2. The latter singlet and the first triplet state, 2T, of hydroxymethylene are obtained from the ground 2 state via n→π\* excitation, and have similar structures (Figure 3.5). Like 1\* state of complex 1, the 2\* state of 2 is an open-shell singlet (Table 4). The three TSs are qualitatively similar (Figure 5), and can be regarded as early TSs. In the open-shell ts(1\*/2\*) and in 1T/2T, the breaking O-H bond stretches by about 25% of its value in complex 1, while the corresponding extension is less than 10% in ts(1/2). CASSCF indicates that the wavefunction of the latter TS is dominated by a single closed-shell determinant (Table 3.4). This observation suggests that spin-restricted, single-determinantal methods such as RCCSD and RDFT may perform adequately in predicting properties of ts(1/2). Geometrical parameters of ts(1/2) as calculated by RCCSD and RB3LYP methods are included in Figure 3.6. Agreement with CASSCF results is satisfactory.

The closed-shell complex 1 and the open-shell one, 1\*, exhibit different chemistry also along the O-H fission pathway that produces isoformyl radical

---

<sup>a</sup> The planar TS reported in ref 75a (species 5a in their Figure 1) appears to be an artifact of the RHF PES. It does not exist with CASSCF, RB3LYP, or RMP2/6-311G(d,p). At RCCSD/6-311G(d,p) level, it is predicted to be a second order saddle point. CASSCF geometry minimizations starting with such structures indicate that they are outside of the local potential well of complex 1.

and atomic hydrogen. While 1 generates a ground state isoformyl (5), 1S-b proceeds to the first excited state, 5\*, of the radical. One would expect the triplet PES 1T to behave similarly to 1\*, but it goes to the lower 5 due to an avoided crossing with the next triplet PES. The TSs are shown in Figure 3.7. The open-shell singlet  $ts(1^*/5^*)$  and the triplet  $ts(1T/5)$  have similar, unsymmetrical geometries. The closed-shell singlet  $ts(1/5)$ , on the other hand, has a planar geometry. Fission occurs in this plane, conserving the state symmetry ( $A'$ ). CASSCF wavefunction at the geometry of  $ts(1/5)$  has a closed-shell character (Table 3.4). Geometries optimized by RCCSD and RB3LYP methods are in reasonable agreement with those of CASSCF (Figure 3.7). Thus, the RCCSD, RB3LYP, and CASSCF PESs appear to be parallel at configurations near the geometry of  $ts(1/5)$ .



(1/inv) in Figure 3.7). Such consecutive TSs along MEPs are also known for other systems.<sup>a</sup>

### 3.1.6 Energetics of the System.

Relative energies (ZPVE corrected) of stationary points with respect to the ground-state energy of formaldehyde are presented in Table 3.5 at various levels of theory.

---

<sup>a</sup> See, for example: Ozkan, I.; Zora, M. J. *Org. Chem.* 2003, 68, 9635, and the references therein.

**Table 3-9. Enthalpies (at 0 K, in kcal/mol, and relative to formaldehyde) of Species at Initial Stages in the Reactions of Singlet and Triplet Carbon Atoms with Water as Calculated by Different Methods <sup>a</sup>**

	MRMP-2	EOM-CCSD <sup>n</sup> vert. Exc.	MRMP <sup>m</sup> vert. Exc.	CCSD(T) <sup>d</sup>	B3LYP <sup>e</sup>	exp.
C( <sup>1</sup> D)+H <sub>2</sub> O	164.9 <sup>g</sup>			169.0		168.2
<b>1</b>	155.7 <sup>h</sup>			159.0		
<b>1*</b>	161.3 <sup>h</sup>	156.5	158.3			
<b>1/inv</b>	158.4 <sup>h</sup>					
<b>1*/inv</b>	164.6 <sup>i</sup>					
<b>1/5</b>	162.1 <sup>h</sup>			160.5	156.1	
<b>1*/5*</b>	172.8 <sup>j</sup>	175.3	177.7			
<b>1/2</b>	164.8 <sup>i</sup>			161.8	164.2	
<b>1*/2*</b>	164.1 <sup>j</sup>	166.8	164.3			
<b>2*</b>	107.9 <sup>k</sup>	108.4	108.0			
C( <sup>3</sup> P)+H <sub>2</sub> O	132.2 <sup>g</sup>			134.0	139.1	139.1
<b>1T</b>	124.5 <sup>i</sup>			135.3 <sup>l</sup>	129.3	
<b>1T/inv</b>	127.3 <sup>i</sup>			129.7 <sup>l</sup>	131.8	
<b>1T/5</b>	151.4 <sup>i</sup>			154.6 <sup>l</sup>	149.1	
<b>1T/2</b>	139.3 <sup>i</sup>			142.0 <sup>l</sup>	141.5	

<sup>a</sup> See note <sup>a</sup>. <sup>b</sup> At CAS(12,10) optimized geometries; 6-311G(d,p) basis set is used in optimizations with CASSCF, and in MRMP. <sup>c</sup> CAS(12,10)-MRMP(FC) optimized geometries. <sup>d</sup> CCSD(T)/cc-pVTZ with CCSD(T)/cc-pVTZ ZPVE. <sup>e</sup> aug-cc-pVTZ basis set in all DFT. <sup>f</sup> Sum of CAS(2,2)-MRMP(full) for carbon atom and CAS(10,8)-MRMP(full) for H<sub>2</sub>O (see note <sup>b</sup>) relative to CAS(12,10)-MRMP(full) for formaldehyde, including ZPVE corrections. <sup>g</sup> Sum of CAS(4,4)-MRMP(full) for carbon atom and CAS(8,8)-MRMP(full) for H<sub>2</sub>O relative to CAS(12,12)-MRMP(full) for formaldehyde, including ZPVE corrections. <sup>h</sup>At CAS(12,12)-MRMP(FC) optimized geometry. <sup>i</sup>At CAS(12,10)-MRMP(FC) optimized geometry. <sup>j</sup>At CAS(12,10)-avg optimized geometry. <sup>k</sup>At CAS(12,10) optimized geometry. <sup>l</sup>CCSD(T)/aug-cc-pVTZ at CCSD/6-311G(d,p) optimized geometries with CCSD/6-311G(d,p) ZPVE. <sup>n</sup>Vertical excitation energy of EOM-CCSD added to ground state CCSD(T) energy. <sup>m</sup> Vertical excitation energy of MRMP added to ground state CCSD(T) energy

<sup>a</sup> Enthalpies relative to formaldehyde using different methods are obtained as follows. Let E(i,m;m') denote the absolute electronic energy of species i as calculated by method m at a geometry optimized by possibly another method m'. Electronic energies relative to formaldehyde are calculated by  $\Delta E(i,m;m') = E(i,m;m') - E(\text{formaldehyde},m;m')$ . Relative enthalpies at 0 K are then obtained by correcting  $\Delta E(i,m;m')$  using ZPVEs for species i and formaldehyde calculated at the same computational level.

<sup>b</sup> The active orbitals in CAS(10,8) of H<sub>2</sub>O are: 1s, 2s, 2p, 3p<sub>x</sub> on O and 1s on each hydrogen.

An energy diagram that contains our best estimates for the energies of the stationary points along the various MEPs will now be constructed. For the triplet species **1T** and the associated TSs, we use the average of CCSD(T) and B3LYP values from Table 3.5. The resulting energy diagram is displayed in Figure 3.8.

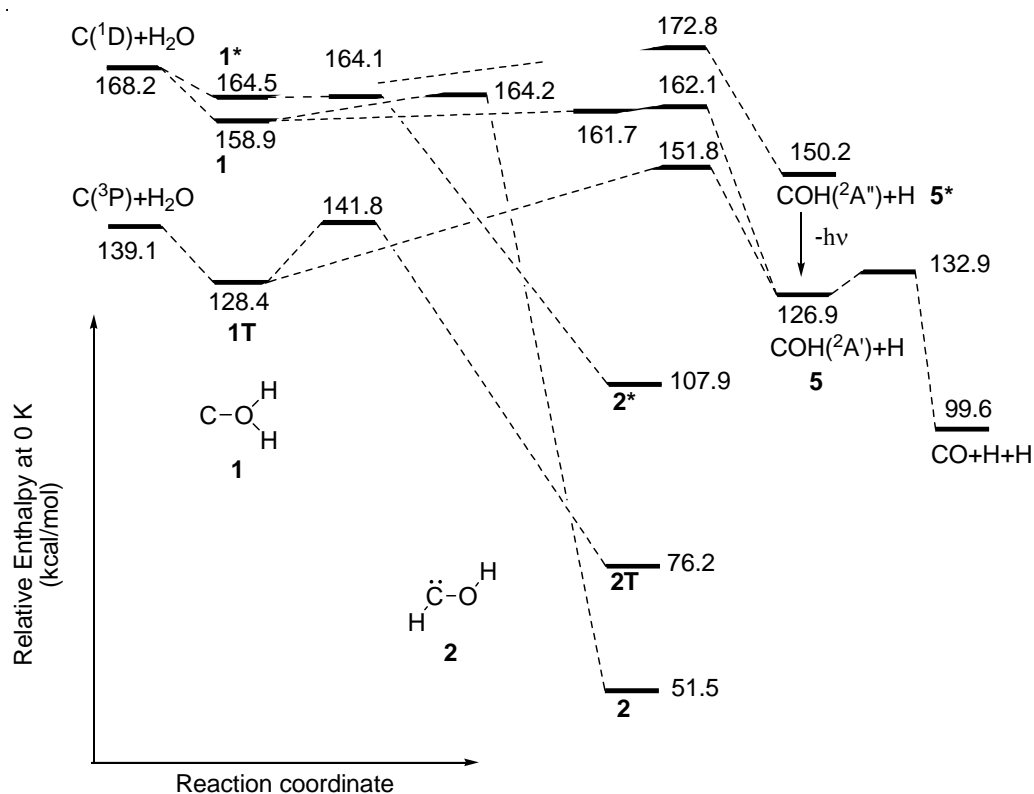


**Figure 3.8.** Schematic energy diagram for the early phase in the reactions of  $^1D$  and  $^3P$  carbon atoms with water molecules. All enthalpies are relative to formaldehyde. Enthalpies of **2**, **2T**, **5**, **CO**, and the TS between the latter two species are computed at CCSD(T)/aug-cc-pVTZ//CCSD/6-311G(d,p) level. Energy of **5A''** is obtained by adding the CAS(11,9)-MRMP/6-311G(d,p) enthalpy difference between **5A''** and **5A'** to the CCSD(T) relative enthalpy of **5A'**. For the remaining values see Table 5, and text.

### 3.1.7 Reaction Products.

In this discussion we will assume that there is no energy transfer from the reacting system to the surrounding medium; we will address this issue later. Relative to formaldehyde, the minimum energy of the singlet reactants is 168.2 kcal/mol while that of triplet reactants is 139.1 kcal/mol. From data in Figure 3.8, one sees that in the reactions of singlet carbon atoms with water molecules, excited isoformyl radicals ( $5A''$ ) may be produced only if additional translational energy ( $E_{\text{coll}}$ ) of carbon atoms (due to the generation technique) is greater than 4.6 kcal/mol. The fission here occurs on the open-shell  $1^*$  PES. The excited isoformyl will then decay into the ground state ( $5A'$ ) by a radiative transition.<sup>a</sup> The latter species is also produced via the closed-shell  $1S$ -a PES without requiring extra energy, and by triplet carbons if  $E_{\text{coll}} > 12.7$  kcal/mol. (a very high additional energy) Regardless of the mode of production, the  $\text{COH}(^2A') + \text{H}$  system will have at least  $151.8 - 126.9 = 24.9$  kcal/mol of non-fixed energy.<sup>132</sup> Part of this energy will be channeled into the translational energies of the dissociated fragments. According to experiments by Kaiser et al. on reaction of  $\text{C}(^3P)$  with  $\text{H}_2\text{S}$ , energy released into translational motion of the products ( $\text{H} + \text{HCS}$ ) is about 40% of the total.<sup>133</sup> Assuming this value is applicable to the present reactions,  $\text{COH}(^2A')$  will be produced with at least 14.9 kcal/mol of non-fixed energy, and it will immediately dissociate into  $\text{CO} + \text{H}$  (barrier is only 6.0 kcal/mol). These results suggest that in the gas-phase reactions of carbon atoms with water, the isoformyl radical intermediate is not a trappable species.

The remaining paths in Figure 3.8 lead to hydroxymethylenes in various electronic states. Hydroxymethylene is formed in its  $S_1$  state via the open-shell complex  $1^*$  while the closed-shell complex  $1$  yields *trans*-HCOH in its  $S_0$

---

<sup>a</sup> The dissociation energies of the excited radical  $\text{COH}(^2A'')$  into  $\text{CO}(^3\pi) + \text{H}$  and  $\text{C}(^3P) + \text{OH}$  are very high, estimated as 91 and 107 kcal/mol, respectively. These values are obtained by combining the computed enthalpy of  $\text{COH}(^2A'')$  with experimental data on  $\text{CO}(^3\pi)$  and  $\text{OH}$  (ref 14). The barrier for the rearrangement of  $\text{COH}(^2A'')$  into the Renner-Teller unstable species  $\text{HCO}(^2\pi)$  is calculated to be 25.2 kcal/mol at CAS(11,9)-MRMP//CAS(11,9)/6-311G(d,p) level. With  $E_{\text{coll}}$  around 8 kcal/mol, excess vibrational energy in  $\text{COH}(^2A'')$  formed from  $1S$ -b will not be enough to surmount the barrier. Hence, only the radiative path remains.

ground electronic state. These processes need no extra energy whereas formation of triplet hydroxymethylene **2T** requires  $E_{coll} > 2.7$  kcal/mol. All three species are highly energized with non-fixed energies of 60.3, 62.9, and 116.7 kcal/mol plus  $E_{coll}$  in **2\***, **2T**, and **2**, respectively. With such excess energies, each species may undergo many further reactions. Possibilities are summarized in Figure 3.9.<sup>134</sup> Radiative and internal conversion (IC) pathways from excited singlets, and intersystem crossing (ISC) paths from triplets are not shown in the figure since their rates are expected to be much smaller than rates of competing unimolecular rearrangements or dissociation reactions at relevant non-fixed energies (vide infra).

The excited formyl radical HCO( $2\pi$ ) formed from **2\*** rapidly decays to the ground state formyl HCO( $2A'$ ) via Renner-Teller coupling.<sup>a</sup> The latter species is also produced by many other processes as indicated in Figure 3.9. As is the case with the isoformyl radical, there is enough non-fixed energy so that the formyl radical is expected to dissociate giving CO and atomic hydrogen as the final products. The reactions will also generate a minor amount of molecular hydrogen arising from one of the two fragmentation routes on the ground-state PESs of formaldehyde and cis-HCOH( $S_0$ ).

---

<sup>a</sup> The energy reported in Figure 3.8 for the excited HCO( $2\pi$ ) is that of the molecule with a linear geometry (actually, a first order saddle point). The conventional state symbol is  $A^2A''$ . Due to the electronic degeneracy this species exhibits Renner-Teller instability; decay rate constants are of order  $10^{12}$ - $10^{13}$  s<sup>-1</sup>. See e.g., (a) Loettgers, A.; Untch, A.; Keller, H.-M.; Schinke, R.; Werner, H.-J.; Bauer, C.; Rosmus, P. J. Chem. Phys. 1997, 106, 3186. (b) Werner, H.-J.; Bauer, C.; Rosmus, P.; Keller, H.-M.; Stumpf, M.; Schinke, R. J. Chem. Phys. 1995, 102, 3593.

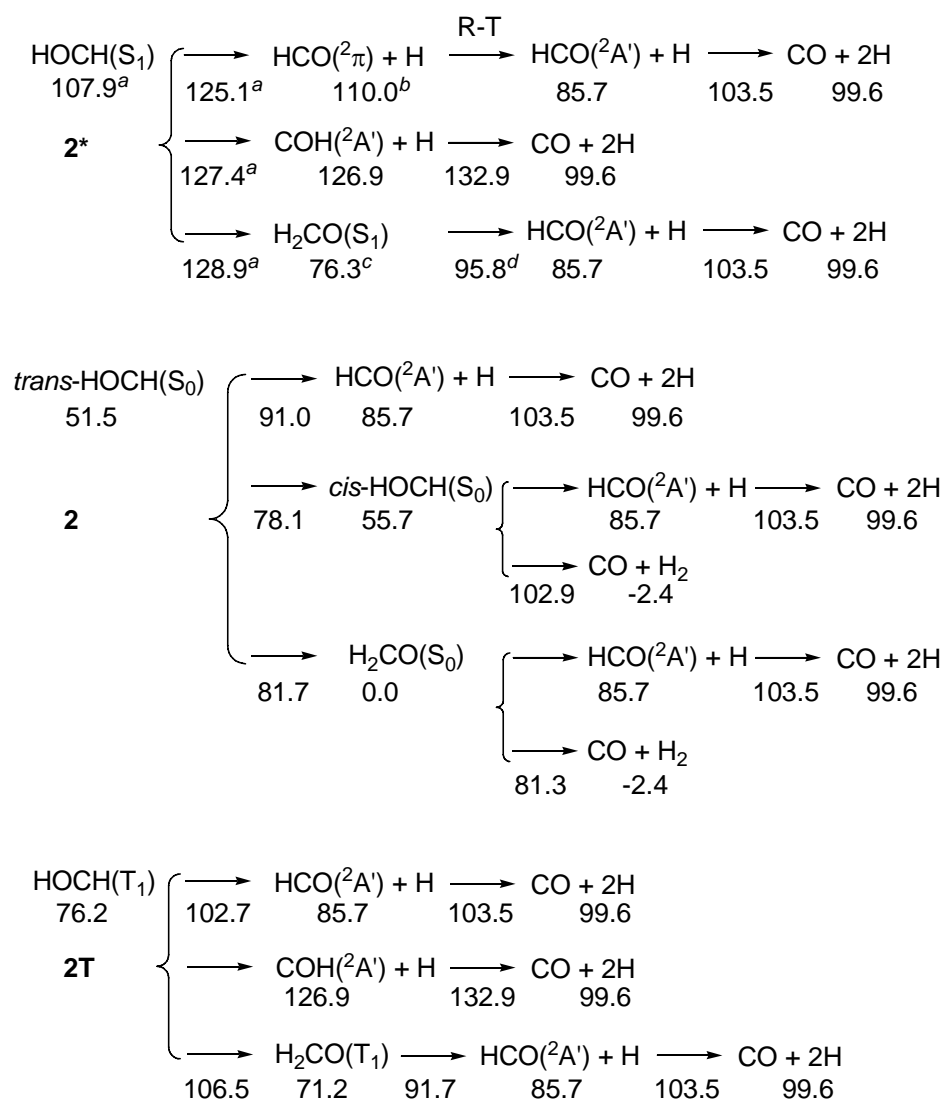


**Figure 3.9.** Unimolecular reaction pathways of hydroxymethylene S<sub>0</sub>, S<sub>1</sub>, and T<sub>1</sub> states. Energies (kcal/mol) relative to the ground state of formaldehyde (inclusive of ZPVEs) are indicated.

Values under reaction arrows refer to the TS energies (relative to formaldehyde); absence of a number means a barrierless reaction. Energies are calculated at CCSD(T)/aug-cc-pVTZ//CCSD/6-311G(d,p) level, except for: <sup>a</sup> CAS(12,12)-avg-MRMP//CAS(12,10)-avg, <sup>b</sup> CAS(11,9)-MRMP//CAS(11,9) energy difference between HCO(<sup>2</sup>π) and HCO(<sup>2</sup>A') added to CCSD(T) value of the latter species, <sup>c</sup> CAS(12,12)-MRMP//CAS(12,10) <sup>d</sup> CAS(12,10)-avg-MRMP//CAS(12,10)-avg, all with 6-311G(d,p) basis set. R-T: Renner-Teller coupling.

### 3.1.8 Effect of Reaction Medium.

In order to get an idea of the magnitude of reaction rates, kinetics of various processes originating from **2** (middle part in Figure 3.9) is investigated using microcanonical RRKM theory.<sup>132</sup> At an initial energy of  $E=169$  kcal/mol (i.e. with 117.5 kcal/mol excess energy in hydroxymethylene), the microcanonical rate constants,  $k(E)$ , are all of the order  $10^{13} \text{ s}^{-1}$ . To compete with such high rates, coupling to the surrounding medium must be strong and requires condensed phases. There is some evidence that not all solids may act as efficient heat sinks. In their study of carbon atom reactions at 10 K in an Ar matrix containing 1% H<sub>2</sub>O, Jeong et al. could detect only CO as the reaction product; no trace of hydroxymethylene or formaldehyde was found.<sup>75c</sup> Apparently coupling to the argon matrix is weak, reactions proceeding as if in the gas phase. Similarly, in reactions of carbon with *cis*- and *trans*-2-butene oxide at 77 K, Skell et al. concluded that excess energies of some intermediates were not easily absorbed by the frozen matrix.<sup>135</sup> On the other hand, in reactions of arc generated carbon with a surplus of H<sub>2</sub>O at 77 K, formaldehyde was observed.<sup>75b</sup> Rate of vibrational energy transfer from the intermediates to the ice medium must have been larger than reaction rates, in this case. It is reasonable to assume that hydroxymethylene, the precursor to formaldehyde, was quickly stabilized by good mechanical coupling to ice, and trapped. Formaldehyde would then be formed during warm-up in the process of analyzing the products. This could occur by a unimolecular H-shift in *trans*-HCOH(S<sub>0</sub>) with a barrier of 30.2 kcal/mol (Figure 3.9). We also examined the possibility of an intermolecular reaction of hydroxymethylene with a nearby water molecule. Processes considered, together with energetics at two theoretical levels, are depicted in Figure 3.10A.

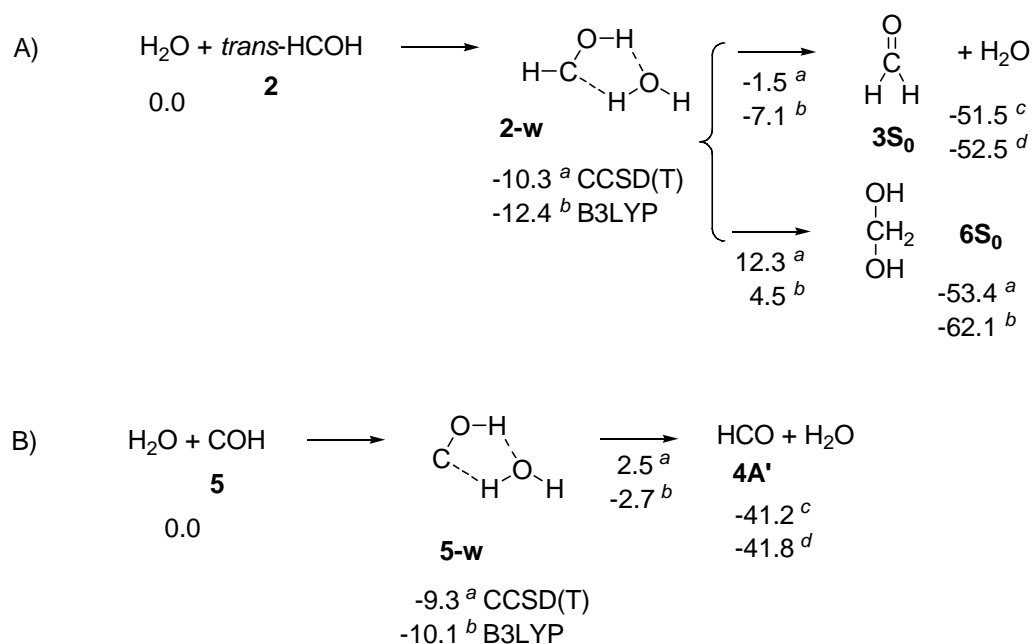


**Figure 3.10.** Reactions between: A) ground-state hydroxymethylene and water, B) ground-state isoformyl and water.

Enthalpies (kcal/mol, 0 K) relative to the reactants are indicated. Values under reaction arrows refer to TS energies (relative to the reactants). Theoretical levels: <sup>a</sup> CCSD(T)//CCSD/6-311G(d,p), <sup>b</sup> B3LYP/6-311G(d,p), <sup>c</sup> CCSD(T)/aug-cc-pVTZ//CCSD/6-311G(d,p), <sup>d</sup> B3LYP/aug-cc-pVTZ, using B3LYP ZPVE corrections in all.

Hydroxymethylene **2** forms a stable H-bonded complex with water (**2-w** in Figure 3.10). This complex can rearrange to methanediol **6S<sub>0</sub>** if 22.6 kcal/mol is available, or produce formaldehyde with a barrier of only 8.8 kcal/mol (CCSD(T) values in Figure 3.10A). The former process is an OH insertion by the carbene while the latter one is a concerted, synchronous H-exchange reaction. Clearly, the latter process will be preferred on energetic grounds. These calculations suggest that if hydroxymethylene is trapped (i.e. excess vibrational energy removed) by the ice medium, formaldehyde should be formed by an intermolecular process, and not by a unimolecular rearrangement (of hydroxymethylene). Note the role of water as a catalyst in this process.

It is reasonable to ascribe the fast vibrational relaxation of **2** in ice to the H-bonding interactions between the two species. Similarity of interaction between

**2** and a water molecule in ice to those in the rest of H-bonded network of ice lattice apparently leads to a rapid transfer of excess energy of **2** to ice. Hydroxymethylene in its excited states, **2T** and **2\***, also form stable H-bonded complexes (**2T-w** and **2\*-w** in Figure 3.11) with complexation energies of -7.1 and -5.3 kcal/mol, respectively.<sup>a</sup> We expect that the vibrational relaxation of these species in ice should also be fast. After reaching its lowest vibrational level, **2T** will undergo intersystem crossing to **2**. Similarly, through internal conversion and/or radiative transition, **2\*** will end up with **2**. The net result is a contribution of **2T** and **2\*** to the production of formaldehyde.

The same factors causing rapid stabilization of hydroxymethylene also account for why CO was not observed in the investigations of ref 75b. Under the conditions of these experiments, the only source that could generate CO is the isoformyl radical produced by O-H fission of singlet complexes **1** and **1\*** (see Figure 3.8). The fact that no CO was detected indicates that excess vibrational energy of COH must have been quickly dissipated by the ice medium. This is in accord with the energetically favorable complexation of COH with water as depicted in Figure 10B.<sup>b</sup> Complex **5A'-w** will eventually produce the more stable formyl radical **4A'**. The optimized structures of **5A'-w** and its TS are included in Figure 3.11.

---

<sup>a</sup> The triplet complex **2T-w** is calculated at CCSD(T)//CCSD with 6-311G(d,p) basis set using B3LYP/6-311G(d,p) ZPVEs. The excited singlet complex **2S<sub>1</sub>-w** is calculated at CAS(8,8)-avg-MRMP/6-311G(d,p) level, with all active orbitals on the hydroxymethylene fragment.

<sup>b</sup> The OH insertion path is not included in Figure 9B because the TS has a considerably high energy: 22.4 and 31.7 kcal/mol above that of COH+H<sub>2</sub>O at B3LYP/6-311G(d,p) and CCSD(T)//CCSD/6-311G(d,p) levels, respectively.

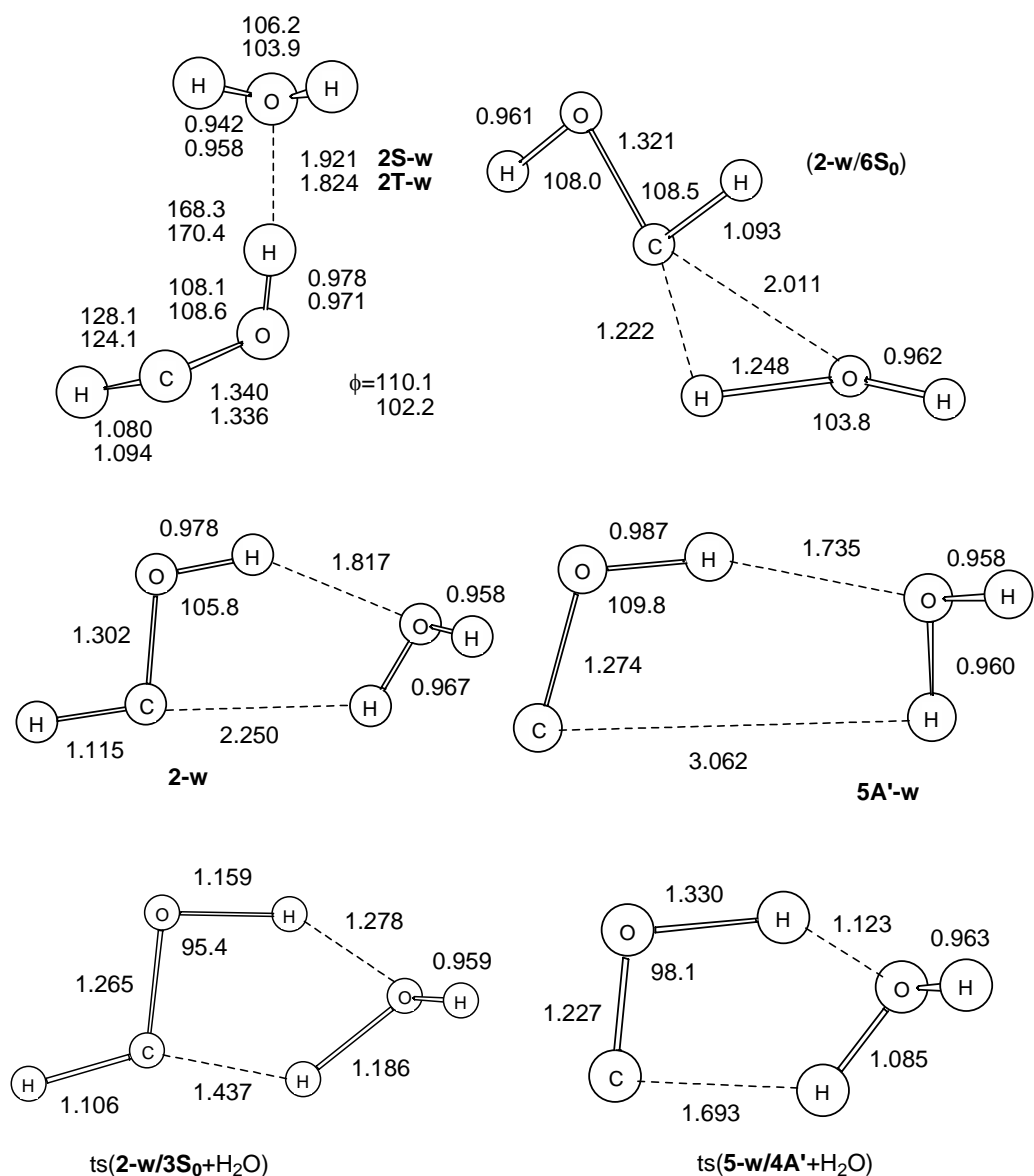


**Figure 3.11.** H-bonded complexes of hydroxymethylene and isoformyl radical with a water molecule.

TSs leading to methanediol (upper right), formaldehyde+H<sub>2</sub>O (lower left), and formyl+H<sub>2</sub>O (lower right) are also shown. Bond lengths are in angstroms and angles are in degrees;  $\phi$  is the dihedral angle of HCOH fragment in **2-w** and **2T-w**. Theoretical level is CCSD/6-311G(d,p) for all, excepting **2\*-w**. The latter structure is optimized at CAS(8,8)-avg/6-311G(d,p) level.

### 3.1.9 Conclusions.

Reactions of singlet ( $^1\text{S}$  and  $^1\text{D}$ ) and triplet ( $^3\text{P}$ ) carbon atoms with water were studied computationally. It will be assumed that the carbon vapor contains a mixture of  $\text{C}(^1\text{S})$ ,  $\text{C}(^1\text{D})$ , and  $\text{C}(^3\text{P})$  atoms. CASSCF calculations indicate that  $\text{C}(^1\text{S})$  is unreactive toward  $\text{H}_2\text{O}$ . This metastable species with a lifetime of 1.6 s appears to have no choice but radiatively decay to  $\text{C}(^1\text{D})$ , and then react. The  $^1\text{D}$  and –probably also-  $^3\text{P}$  carbons first form a loose complex (1) with water, which thereafter dissociates or rearranges. The formation of products from 1T is problematic, since it requires additional kinetic energies to overcome the barriers that are higher in energy than the energy of the reactants. Due to the large excess energies of intermediates involved, subsequent reactions are fast; of the order  $10^{13} \text{ s}^{-1}$  from RRKM calculations. In the absence of efficient transfer of non-fixed energies to the surrounding medium, all of the reaction paths will conclude with irreversible dissociation reactions.

If the triplet carbons are assumed –or in a finely designed experiment, tuned to carry no extra translational energy they should be apparently unreactive. With  $E_{\text{coll}}=8 \text{ kcal/mol}$ , the triplet complex 1T has only the rearrangement path to  $\text{HOCH}(\text{T})$  available to it. The latter species is formed with  $62.9+8\approx 71 \text{ kcal/mol}$  excess energy, and it undergoes further reactions (Figure 3.9). The reaction path from 2T branches into three paths producing 3T, formyl, isoformyl, and atomic hydrogen. Triplet formaldehyde 3T also dissociates into formyl plus atomic hydrogen. Both the formyl and isoformyl radicals should have sufficient energy to further dissociate. Thus, in the reaction of  $\text{C}(^3\text{P})$  with water under conditions where vibrational relaxation rates are smaller than  $10^{13} \text{ s}^{-1}$ , the expected end-products are CO and atomic hydrogen. The behavior of  $\text{C}(^3\text{P})+\text{H}_2\text{O}$  system is somewhat different from that of the analogous  $\text{C}(^3\text{P})+\text{H}_2\text{S}$  system. Under similar conditions, the latter reaction produces mainly HCS plus atomic hydrogen since energy is not available for further dissociation of HCS.<sup>74,133</sup>

Accessible pathways of the singlet  $C(^1D)+H_2O$  system are more complicated due to the presence of two reactive PESs with branchings occurring along each (Figures 3.8 and 3.9). Nevertheless, the final products of the reaction are predicted to be mostly CO plus atomic hydrogen as in the reaction of  $C(^3P)$ , along with a small amount of  $H_2$  originating from fragmentations of *cis*-hydroxymethylene and formaldehyde that occur as intermediates. The products originating from the open shell singlet complex  $1^*$  suffer from the same problem with the triplet PES. Its blockage or accessibility depends on how high an additional kinetic energy can be carried by the incoming carbons.

The conclusions thus far apply to the reactions in the gas phase as well as in condensed phases involving inert matrices.

Experimental observation of formaldehyde as the major product in reactions of arc carbons with pure water at liquid nitrogen temperatures is attributed to H-bonding interactions between hydroxymethylene and water molecules. Similar interactions also prevent dissociation of COH so that carbon monoxide should not be produced, in agreement with experiments. The frozen matrix is reactive, in this case. Presumably, strong coupling to the ice medium leads to the removal of excess vibrational energies of hydroxymethylenes in various electronic states in less than  $10^{-13}$  s. It is proposed that formaldehyde is formed by an intermolecular reaction of hydroxymethylene with a water molecule where water acts as a catalyst. Likewise, the formyl radical HCO is expected as another product, arising from the reaction of isoformyl with water.

We note that since the OH insertion TS,  $1T/2T$ , lies 2.7 kcal/mol above the reactants,  $C(^3P)+H_2O$ , the  $^3P$  carbons may be less reactive than  $^1D$  carbons, or may be unreactive at all depending on the method of generation, as predicted by some studies.<sup>50</sup>

## 3.2 Reactions of <sup>1</sup>D and <sup>3</sup>P Carbon Atoms With Methanol

Our aim in this part of the study was to explore the reaction mechanisms and energy profile of the reactions of the first excited singlet, <sup>1</sup>D and ground state triplet, <sup>3</sup>P carbon atoms with methanol. The previous section was of high importance in order to provide insight to the C + methanol reactions. A detailed investigation of the paths which are probable routes to the formation of major endproducts such as CO, acetaldehyde, and dimethoxymethane were presented. As there are a number of species involved in both PESs the discussion often makes emphasis on the goal of exploring the most feasible routes under known experimental conditions for the formation of the final products.

### 3.2.1 Computational Details

The geometries of stationary points were optimized at B3LYP/6-31G(d,p), B3LYP/6-311G(d,p) and CCSD/6-311G(d,p) levels, and their nature as being a minimum or a first order saddle point, were confirmed by harmonic vibrational frequency calculations at the same levels of theory. Intrinsic reaction coordinate (IRC) calculations were performed to confirm the connectivity of reaction paths, at the level of geometry optimizations, whenever needed. The DFT computations with the double  $\zeta$  basis set, were used to account for the basis set effects and dependencies of stationary structures, when compared to the triple  $\zeta$  basis computations performed with DFT. (See Appendices A to C for Cartesian coordinates, and absolute energies)

The barrierless nature of some reactions were confirmed by rigid scans, increasing the relevant internal coordinate starting from its equilibrium value, at the UB3LYP/6-31G(d,p) level of theory. 1000 single point energy calculations were performed for each bond length scan with 0.01 Å increments. The variations in bond angles were done with 50 steps each being 1.5°. A few CCSD/6-311G(d,p) scans were also performed for some of the structures.

Optimizations performed on the singlet PES were based on spin restricted references. UB3LYP computations on the singlet PES were performed for locating some species that could not be located with the spin restricted functional, and presented here for the purpose of comparison. Single point energy refinements were performed on B3LYP/6-31G(d,p) optimized geometries, employing the 6-311G(d,p) basis set at the coupled cluster singles and doubles level augmented by a perturbative correction for connected triple excitations (CCSD(T)) where inner-shells were excluded (FC) from the correlation calculation(CCSD(T,FC)/6-311G(d,p)//B3LYP/6-31G(d,p)). For some species CCSD(T,FC)/cc-pVTZ//B3LYP/6-31G(d,p) energies were also computed. Single point FC energy calculations on CCSD optimized geometries were performed with two (CCSD(T)) methodologies; first using the standard 6-311G(d,p) basis set(CCSD(T,FC)/6-311G(d,p)//CCSD/6-311G(d,p)), and second employing Dunning's correlation consistent basis set of triple  $\zeta$  quality (CCSD(T,FC)/cc-pVTZ//CCSD/6-311G(d,p)). This level is used in the graphical representations of the relative energies throughout. A set of (CCSD(T)) single point energy calculations with core electrons being correlated was also performed on CCSD optimized geometries using cc-pVTZ basis(CCSD(T,FULL)/cc-pVTZ//CCSD/6-311G(d,p)), in order to analyze the effect of core electron correlation on relative energies. Gaussian 03 (RevD.01) Program suite, with the default criteria for convergences was used for the density functional and coupled cluster methodologies. The species described in the study are labeled as given in Table 3-10. The singlet and triplet species with the same chemical formula, and connectivity in the bonds are represented by the same number, the triplet being shown by an additional "T". For example **6** is singlet acetaldehyde and **6T** is triplet acetaldehyde. Note that the dissociation products -in either PESs- are doublet radicals, and their separated form is represented as a singlet. The transition structures are represented by the names of two consecutive minima separated by a "/"; like **1/4** being the TS from structure singlet **1** to structure singlet **4**. Both the triplet and singlet PESs are discussed by fragmenting a portion of the species due to the large number of

stationary points involved. For this purpose first an equation showing the species in a part of the PES is given and it is followed by the relative 0K enthalpy diagram.

In the following sections first the OH insertion dissociation paths on the singlet PES are discussed. Rearrangements come afterwards. The analogous reactions on the triplet PES (when applicable) are discussed after all the singlet OH insertion and dissociation pathways are finished. Next comes the singlet CH insertion path which is followed by the triplet CH insertion pathway discussions. Intermolecular reactions on the singlet PES are given at the end. Unlike water reactions possible paths on the first excited singlet surface<sup>a</sup> are excluded from our investigations.

---

<sup>a</sup> The path originating from the open shell singlet ( $1A''$ ) state of initial C+methanol complex.

**Table 3-10. Representation of the singlet and triplet species investigated.**

Label	Species
R(S)	$C(^1D)+MeOH$
R(T)	$C(^3P)+MeOH$
1	$C--OHMe$
1'	$C--OHMe$
2	$COH+Me$
3	$COMe+H$
4	$Me-O-C-H$
4'	cis-4
5	$HCO+Me$
6	$MeCHO$
7	$MeCO+H$
8	$H_2C=C=O+H_2$
9	$CO+Me+H$
10	$H_2C=O+CH_2$
11	$CO+CH_4$
12	$CO+H_2+CH_2$
13	$H_2C=CHOH$
14	$H_2O+C_2H_2$
15	$HO-CH_2--H--C$
16	$HO-CH_2-C-H$
17	$H_2C-CH_2-O$
18	$H_2C-O-CH_2$
19	$Me-C-OH$
20	$H_2C-CHO+H$
21	$H_2C-C-OH+H$
22	$HC-CHOH+H$
23	$H_2C-OH+CH$
24	$H_2C-CH+OH$
25	$MeO+CH$
26	$HC-O-CH_2+H$
27	$H_2+HO-C=CH$
28	$Me-C+OH$
29	$c-CH_2CO+H_2$
30	$CHCHO+H_2$
31T	$O(^3P)+C_2H_4$

### 3.2.2 Conditions of Typical Experiments

All the reactions under investigation were studied according to the following assumptions, as obtained from the detailed investigation of the available experimental data; and from the insight that our study of C + water system provided:

Presence, hence interference of higher order carbon clusters such as  $C_2$ ,  $C_3$ ,  $C_4$  were not taken into account. Only the atomic carbon reactions were investigated, as C is the main constituent of carbon vapor used in the experiments, and we investigate the formation of products containing one carbon more than the substrate.

Contribution of  $^1S$  state of atomic carbon was assumed not to be to a significant extent. This assumption was previously presented (See Figure 3.3) to be valid with a detailed investigation of approach of carbon atoms to water. The reactions of  $^3P$ , and  $^1D$  states of C are investigated here.

The intermolecular reactions of two or more intermediates were not taken into account as the probability of them meeting in a sea of substrate will obviously be negligible, but the intermolecular reactions with the surrounding methanol molecules are investigated, for simulating the reactions taking place in a frozen matrix.

The criterion for the possibility of formation of a species is its energy relative to the energies of the reactants. In the gas phase the reactive intermediates lack a medium to interact with and dissipate heat, thus this assumption can explain the conversion of every intermediate to the end products (*vide infra*). On the other hand, the condensed phase reactions have an effective, excess vibrational energy extinguisher, and when an intermediate loses its excess energy and gets trapped by the medium, only a reaction path with a relatively low barrier may be accessible.

### 3.2.3 Energetics of the Singlet PES

The calculated 0K enthalpies at various levels, together with the available experimental data, for the species are listed in Table 3-11 for the singlet minima and in Table 3-12 for the singlet TSs.

**Table 3-11. Relative 0K enthalpies of the singlet minima at the levels as specified. <sup>a</sup>**

Label	Species	B3LYP 6-311G (d,p)	CCSD(T) 6-311G (d,p)	CCSD(T) cc-pVTZ	EXP. <sup>b</sup>
R(S)	C( <sup>1</sup> D)+MeOH	-	191.1	191.0	192.0
1	C--OHMe	-	173.5	171.3	
1'	C--OHMe	-	177.9	176.4	
2	COH+Me	119.9	119.6	121.6	
3	COMe+H	142.2	139.3	141.8	
4	Me-O-C-H	68.1	67.4	67.1	
4'	cis-4	71.8	71.5	70.6	
5	HCO+Me	77.7	78.0	80.3	84.0
6	MeCHO	0.0	0.0	0.0	0.0
7	MeCO+H	86.5	83.5	86.5	
8	H <sub>2</sub> C=C=O+H <sub>2</sub>	22.6	25.2	26.0	
9	CO+Me+H	98.1	87.1	93.2	98.5
10	H <sub>2</sub> C=O+CH <sub>2</sub> ( <sup>1</sup> A <sub>1</sub> )	115.4	111.5	112.1	115.5
11	CO+CH <sub>4</sub>	-5.5	-12.2	-8.3	-4.8
12	CO+H <sub>2</sub> +CH <sub>2</sub> ( <sup>1</sup> A <sub>1</sub> )	114.9	103.6	108.4	104.3
13	H <sub>2</sub> C=CHOH	13.4	12.9	10.5	10.2 <sup>c</sup>
14	H <sub>2</sub> O+C <sub>2</sub> H <sub>2</sub>	42.5	39.1	36.9	35.7
15	HO-CH <sub>2</sub> --H--C	-	187.5	186.3	
16a	HO-CH <sub>2</sub> -C-H	91.1	92.7	90.2	
16b	HO-CH <sub>2</sub> -C-H	96.2	95.5	93.3	
17	H <sub>2</sub> C-CH <sub>2</sub> -O	30.5	30.2	28.1	
19	Me-C-OH	51.6	50.8	50.7	
20	H <sub>2</sub> C-CHO+H	92.3	91.3	93.1	
21	H <sub>2</sub> C-C-OH+H	117.6	116.7	117.5	
22	HC-CHOH+H	122.5	120.9	121.4	
23	H <sub>2</sub> C-OH+CH	174.3	172.2	173.4	
24	H <sub>2</sub> C-CH+OH	116.0	115.4	116.5	
25	MeO+CH	179.5	178.8	181.2	
26	HC-O-CH <sub>2</sub> +H	165.1	163.1	164.8	
27	H <sub>2</sub> +HO-C=CH	60.5	60.6	60.3	

<sup>a</sup> All the values are relative to singlet acetaldehyde and in kcal/mol.

<sup>b</sup> Data taken from Computational Chemistry Comparison and Benchmark Database (CCCBDB) at <http://srdata.nist.gov/cccbdb/default.htm>.

<sup>c</sup>  $\Delta H_{298}$

**Table 3-12. Relative 0K enthalpies of the singlet TSs at the levels as specified.<sup>a</sup>**

Label	Point group	B3LYP 6-311G (d,p)	CCSD(T) 6-311G (d,p)	CCSD(T) cc-pVTZ
1/19		-	193.6	190.7
1/2		-	171.4	169.8
1/3		164.9	170.2	169.2
1/4		-	179.2	177.0
2/9		122.3	124.6	127.6
3/9	$C_s$	141.3	139.1	142.1
4/5	$C_s$	90.3	85.8	88.7
4/4'	$C_I$	97.2	97.9	96.6
4/6	$C_I$	114.7	115.9	114.0
4/10	$C_s$	112.5	114.3	113.7
4'/11	$C_s$	99.6	85.6	87.6
4'/5		85.4		
5/9		97.7	93.0	97.5
6/8	$C_I$	78.2	83.2	81.2
6/11	$C_s$	79.9	82.8	82.8
6/13	$C_I$	66.3	69.3	67.1
6/19	$C_s$	80.0	80.4	79.1
13/14		89.4	92.2	89.7
7/9		102.4	97.0	101.5
15/16a		-	190.0	189.3
16a/16b		100.8	99.3	97.7
16a/27		124.1	129.7	126.4
16b/17		99.3	98.1	96.1

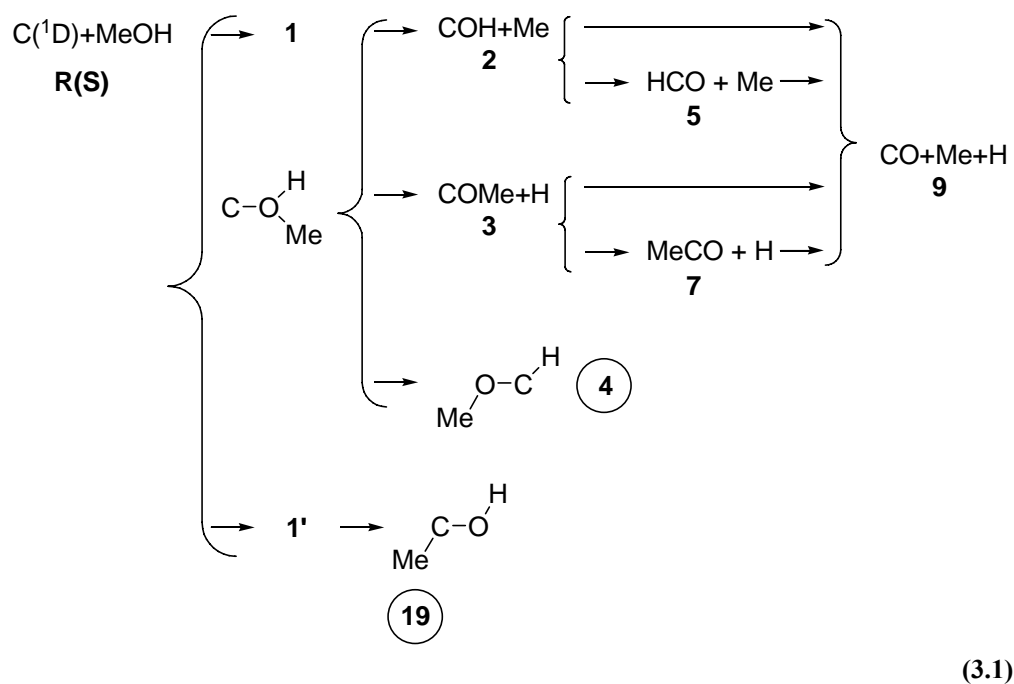
<sup>a</sup> All the values are relative to singlet acetaldehyde and in kcal/mol.

### 3.2.4 Primary CO Formation Paths On the Singlet PES

In analogy with the carbon-water system first the attack of carbon to the oxygen was studied. The loose<sup>a</sup> C + methanol complex is found to exist both in the singlet and triplet PESs. Equation 3.1 illustrates the early stages in the reaction of singlet carbon atoms with methanol, and the selected species from this part

<sup>a</sup> **1** has C-O bond length between the attacking C and the methanol oxygen of 1.727 Å at CCSD/6-311G(d,p) optimized geometry. The corresponding bond length for T1 is 1.862 Å.

of the PES are given with geometrical parameters in Figure 3.12. Enthalpy surface of this part of the reaction is shown in Figure 3.13.



The attack of carbon to the oxygen and the formation of complexes **1** and **1'** are energetically downhill processes on the singlet PES. The three exit channels from the  $C_s$  symmetric complex **1** are; the departure of the methyl group; the loss of the hydroxyl hydrogen; and the migration of hydrogen from hydroxyl function to the carbon, which yields trans methoxymethylene, namely OH insertion. Migration of methyl group to the carbon to yield methylhydroxycarbene, **19** is a result of the rearrangement of the higher energy conformer of initial complex **1'**. Selected geometric parameters of **1**, **1'**, and **4** are given in Figure 3.12.

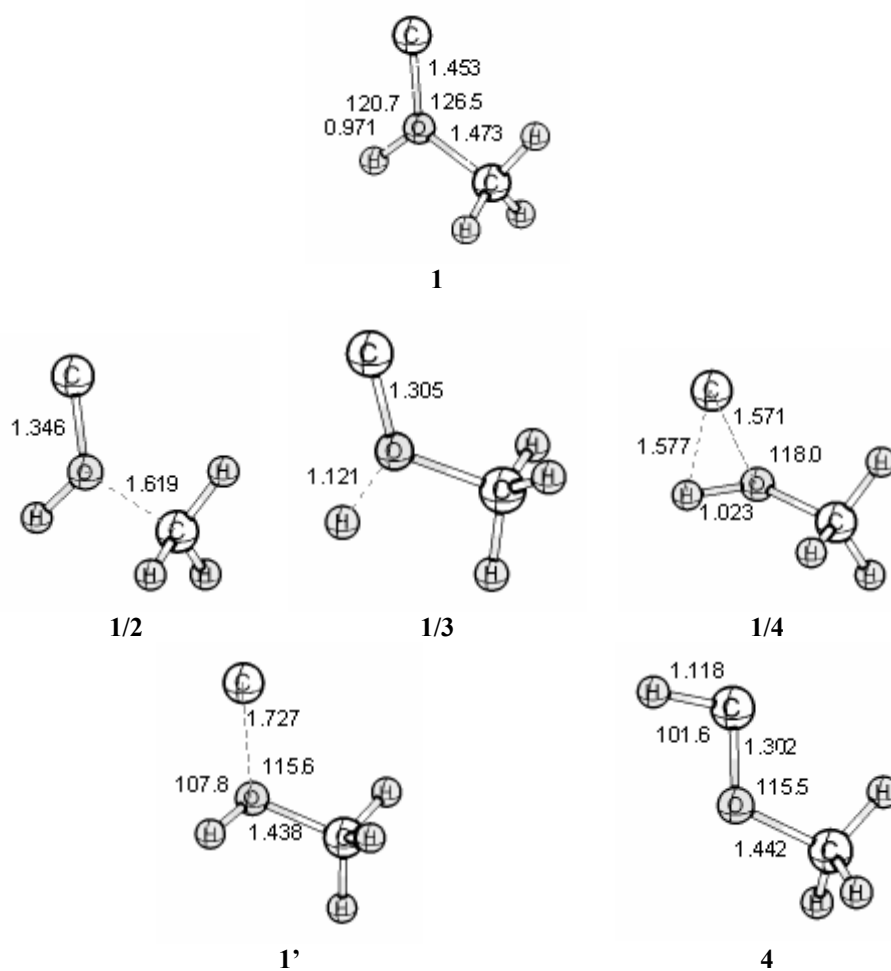


**Figure 3.12.** Selected geometric parameters of CCSD/6-311G(d,p) geometries of some key species on the singlet PES. Bond lengths are given in angstroms with 3, bond angles are given in degrees with 1 significant figures.

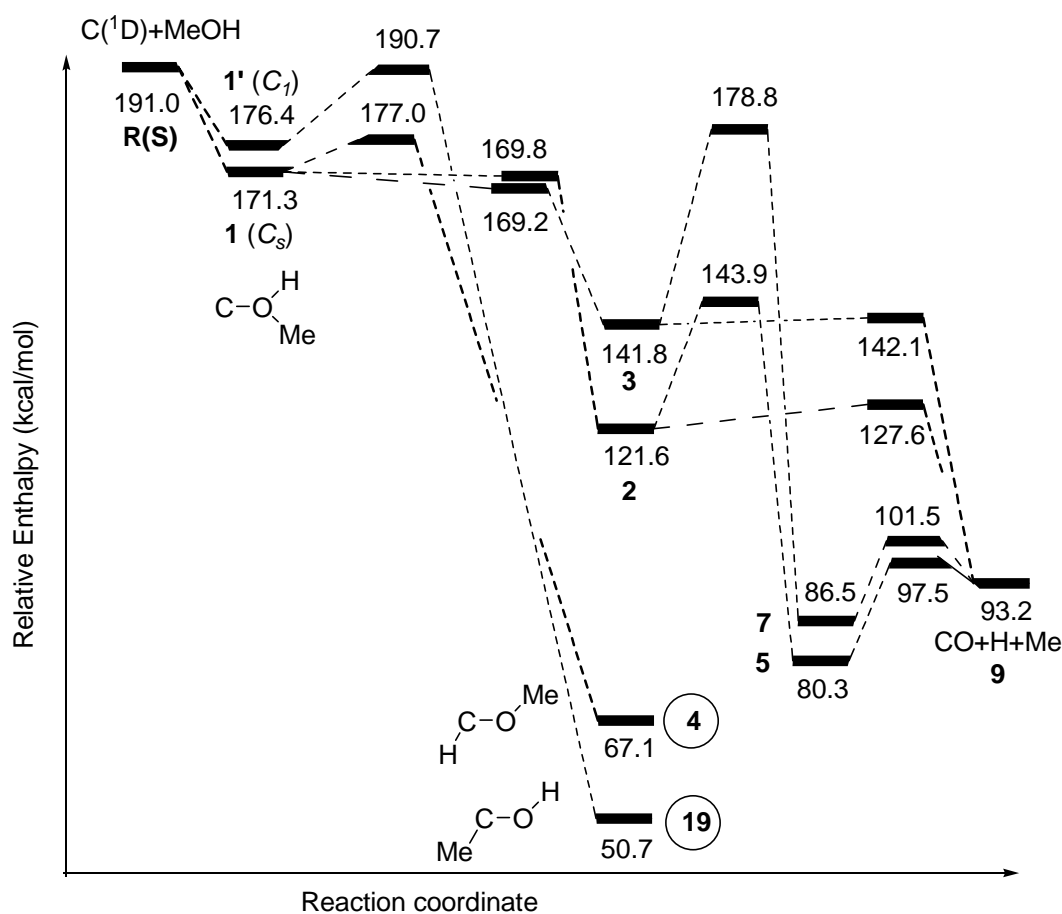


**Figure 3.13.** Relative 0K enthalpy ( $\Delta H_0$ ) surface corresponding to the processes in Equation 3.1.

Enthalpy values are given relative to that of acetaldehyde (species **6**) calculated at CCSD(T)/cc-pVTZ//CCSD/6-311g(d,p) level using ZPVE obtained at CCSD/6-311g(d,p) level.

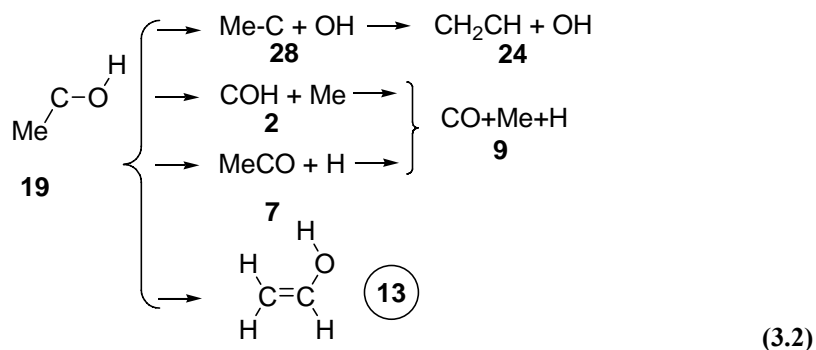
Structure **1'** with C<sub>1</sub> symmetry can not be taken as responsible from formation of **19** with the methodology presented here. The barrier it has for the rearrangement to **19** is only 0.3 kcal/mol less than the initially available energy, and this is within the error margin of our calculations. Moreover singlet carbon atoms inserting into O-C bonds of acyclic systems<sup>a</sup> are never reported in the literature. Higher level calculations can be utilized in the future to compare the energy of **1'**/**19** with that of the reactants. Although we predict the routes

<sup>a</sup> On the other hand our group has found theoretical evidence about singlet carbon atoms inserting into O-C bonds of cyclic systems.

originating from **1'** to be not operative, we studied the probable exit channels from **19**. (See Equation. 3.2 and Figure 3.14)

Apparently, the first two dissociation paths of **1** readily produce the products under investigation, and deoxygenation is mainly due to these two. Energy of **1/2**, and **1/3** lying below **1** after inclusion of ZPVE, strongly supports this phenomenon. It is worthwhile to note that the energetics of the two paths (2 routes to CO formation, and one to OH insertion) are very different. The ~100 kcal/mol stabilization on formation of the carbene is a huge amount compared to the energy loss of products from the first two paths. Moreover the dissociations of **2** and **3** to final products do not have high barriers. All the methods used in this study predict barriers less than 10 kcal/mol for these two paths. Keeping in mind the barrierless dissociation of **1** to **2**, and **3**; we can conclude that the production of CO, methyl, and atomic hydrogen from attack of <sup>1</sup>D carbon atoms to methanol is a very fast and favorable process, and accounts for much, if not all of the CO observed in the experiments. This is a very important result, as the deoxygenation of alcohols by carbon atoms lacked a plausible mechanism up to date.

The possible exit channels from carbene **19** are schematized in Equation 3.2 and the relative enthalpy diagram is given in Figure 3.14.



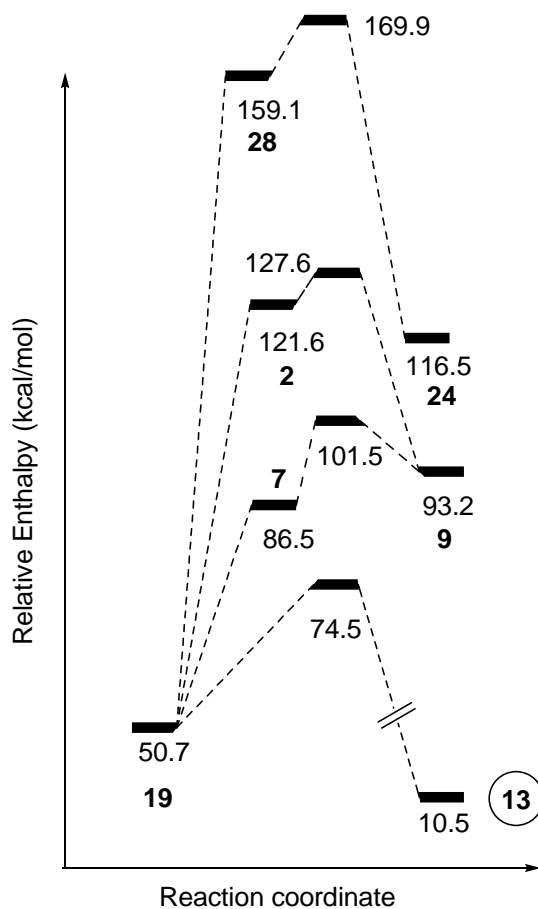
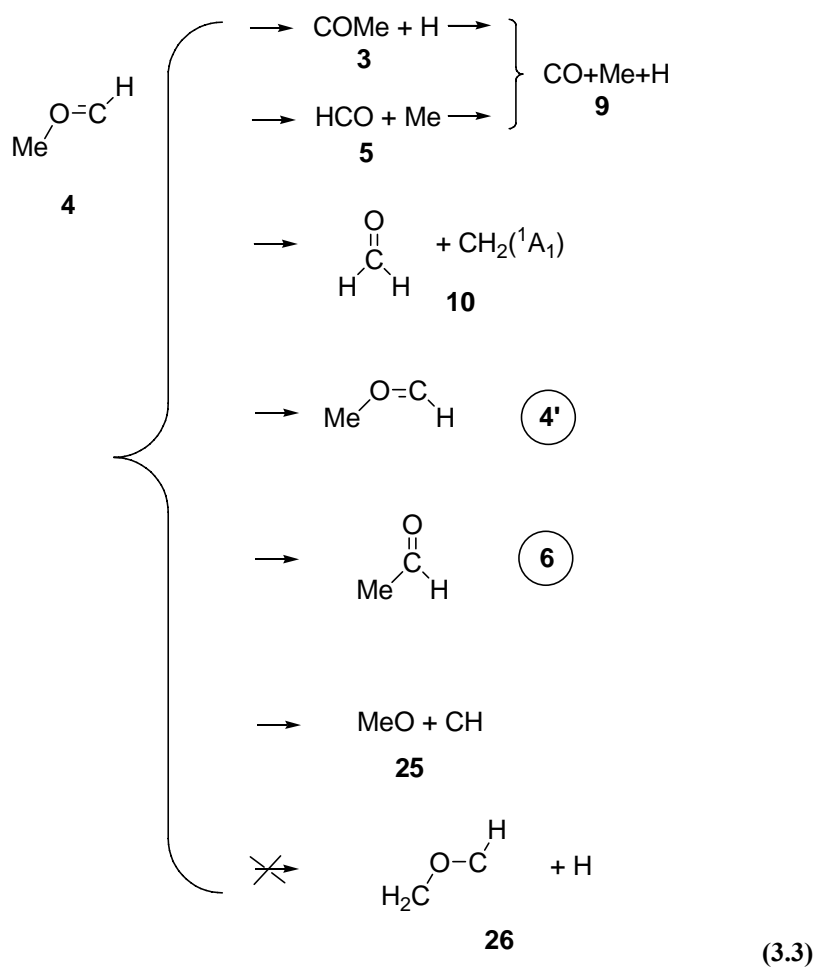


**Figure 3.14.** Relative 0K enthalpy ( $\Delta H_0$ ) profile corresponding to the processes in Equation 3.2 of singlet carbene **19**.

Enthalpy values are given relative to that of acetaldehyde (species **6**) calculated at CCSD(T)/cc-pVTZ//CCSD/6-311g(d,p) level using ZPVE obtained at CCSD/6-311g(d,p) level.

As described in the discussion about the exit channels from **1** and **1'**, formation of carbene **19**, can not be boldly defended on the basis of the results here. On the other hand the diagram given in Figure 3.14 enables us to comment that if **19** had a chance to be generated, the likely product originating from it in the gas phase will be mainly CO as seen from the least endothermic barrierless path from **19** to **7** and the subsequent dissociation to the final products.

Further reactions of singlet trans-methoxycarbene is given in Equation 3.3, and the corresponding enthalpy diagram is shown in Figure 3.15. Carbene **4** can be termed as one of the most important intermediates on the singlet PES. This is because it is the species that does not quickly generate CO; opens up paths to species other than CO, CH<sub>3</sub>, and H; and exhibits a high stabilization in energy, thus the probability to be captured in an energy well.



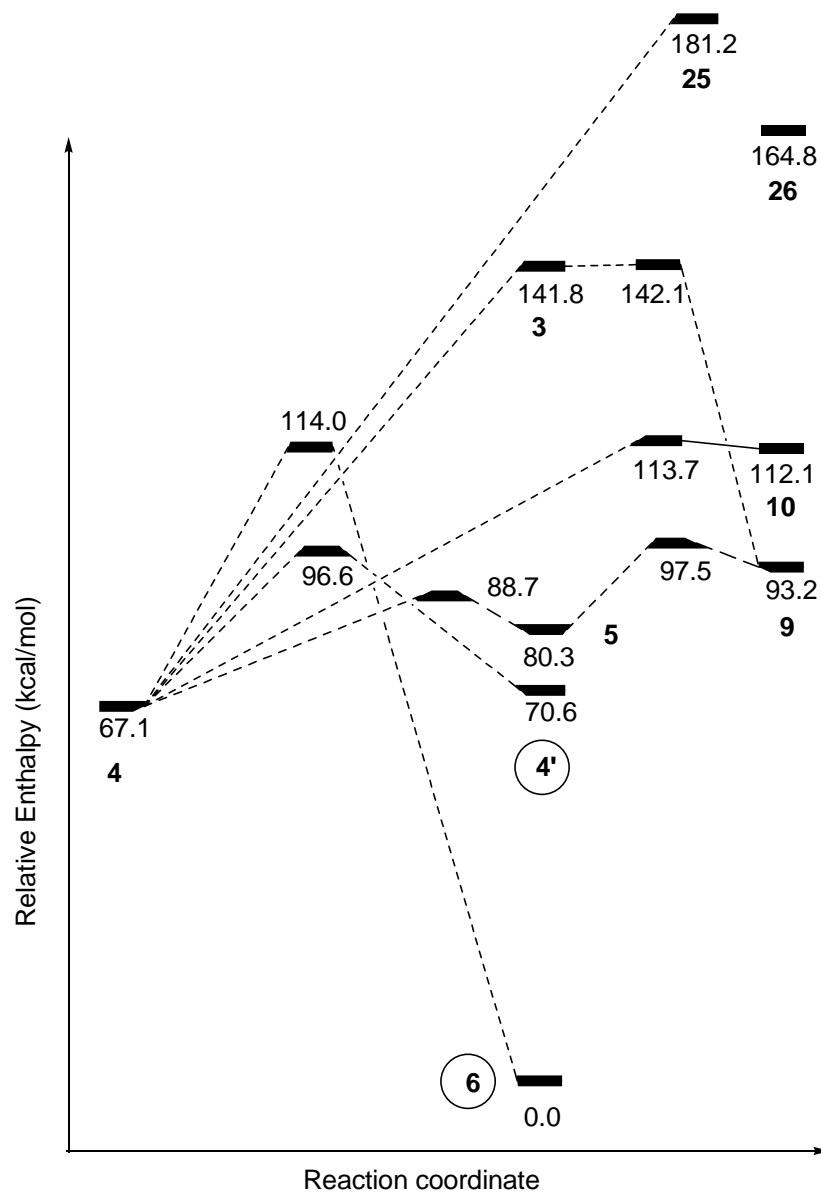


**Figure 3.15.** Relative 0K enthalpy ( $\Delta H_0$ ) profile corresponding to the processes in eon 3.3 of trans-methoxycarbene **4**. Enthalpy values are given relative to that of acetaldehyde (species **6**) calculated at CCSD(T)/cc-pVTZ//CCSD/6-311g(d,p) level using ZPVE obtained at CCSD/6-311g(d,p) level.

If the reactions take place in the gas phase, without loss of the excess vibrational energy the exit channels from **4** suggests that in addition to CO,



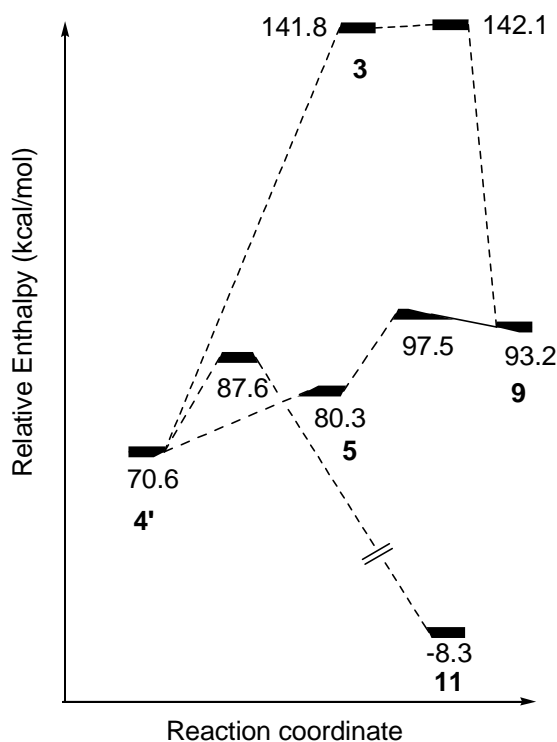
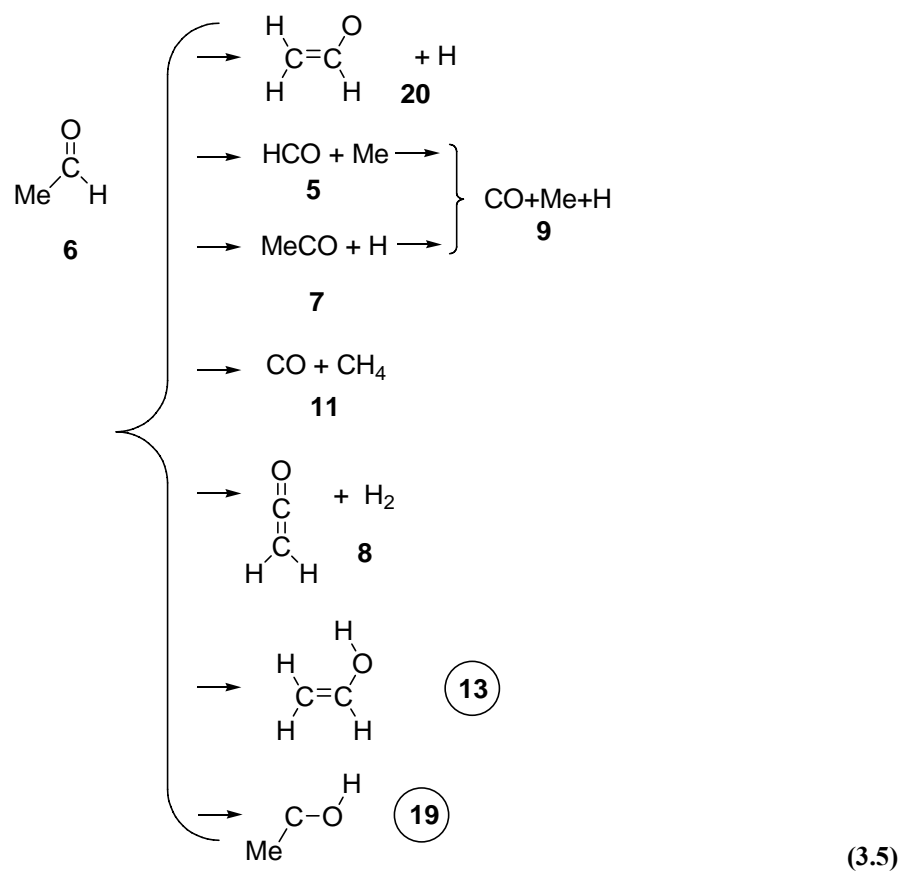


**Figure 3.16.** Relative 0K enthalpy ( $\Delta H_0$ ) profile corresponding to the processes in Equation 3.4 of cis-methoxycarbene **4'**. Enthalpy values are given relative to that of acetaldehyde (species **6**) calculated at CCSD(T)/cc-pVTZ//CCSD/6-311g(d,p) level using ZPVE obtained at CCSD/6-311g(d,p) level.

It is interesting to observe the two barrierless paths from **4'** are the ones, to **3**, and **5**; just as what we saw in the exit channels from **4**. So if the energetics and the medium of the reaction permit the existence of **4'**, the most favorable products from it would again be CO, methyl, and atomic hydrogen; a remarkable finding in C + methanol system, yielding this “trio” whenever possible. Also note the possible CO + methane production as the global energy minimum of the  $C_2H_4O$  PES, which is identical to the global minimum of C +  $H_2O$  PES in the sense that the methyl group of methanol when replaced by hydrogen yields water. Generalizing this, the global minimum of C +  $R_1OR_2$  system can be expected to be CO +  $R_1-R_2$ .

After finishing the possible routes originating from **4'** we turn into another important species, acetaldehyde produced by a 1-2 hydrogen shift from **4**.

Acetaldehyde is one of the three major products observed in carbon arc studies with frozen methanol. The possible exit channels from acetaldehyde are depicted in Equation 3.5, and the relevant energy diagram is illustrated in Figure 3.17.



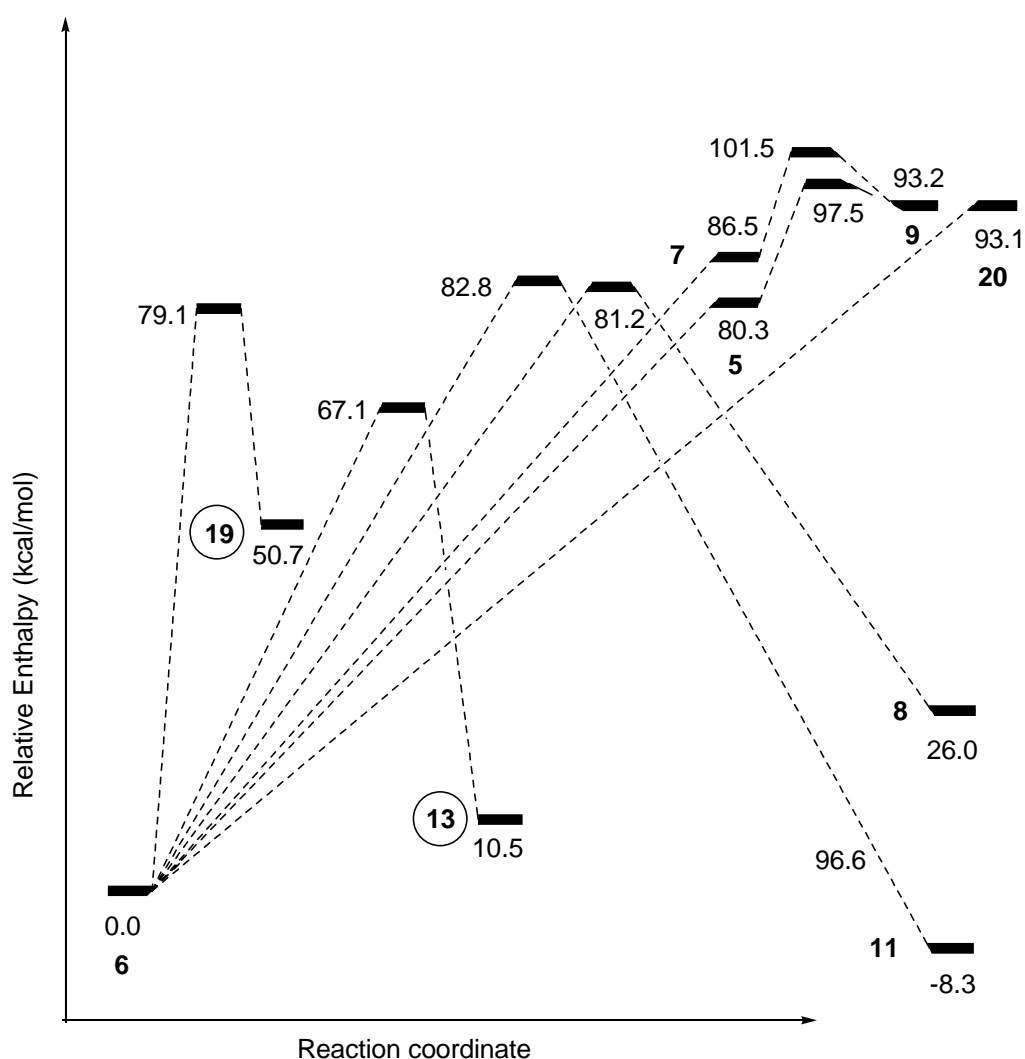
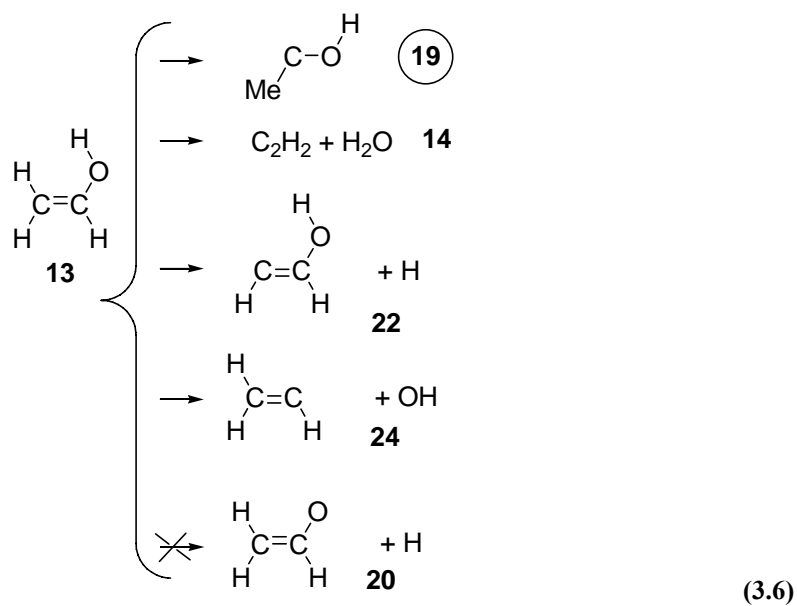


**Figure 3.17.** Relative 0K enthalpy ( $\Delta H_0$ ) profile of processes in Equation 3.5. Enthalpy values are given relative to that of acetaldehyde (species **6**) calculated at CCSD(T)/cc-pVTZ//CCSD/6-311g(d,p) level using ZPVE obtained at CCSD/6-311g(d,p) level.

The complexity of Figure 3.17 can be reduced by stating the presence of two lowest energy barrierless paths, which represent the dissociations of **6** to **5** and **7**, both further dissociate to give our final products with barriers around 15kcal/mol. At this stage the ostensible disappearance of acetaldehyde as stated above conflicts with acetaldehyde being a major product in the experiments. This fact is reminiscent of another path operative for acetaldehyde production, and it will be discussed in the following sections.

One of the important rearrangement products of **6**, as seen from Figure 3.17, is vinyl alcohol, for which the probable paths are given in Equation 3.6.<sup>a</sup> Corresponding enthalpy profile for the species in Equation 3.6 is shown in Figure 3.18.



<sup>a</sup> Dissociation of **13** into **20** is forbidden by symmetry. The  $\text{CH}_2\text{CHO}$  radical in **20** has a planar structure with a  $^2\text{A}''$  ground electronic state. Taking the H on the same plane the overall system **20** has a  $^1\text{A}''$  electronic state whereas **6** has a closed shell  $^1\text{A}'$  state.

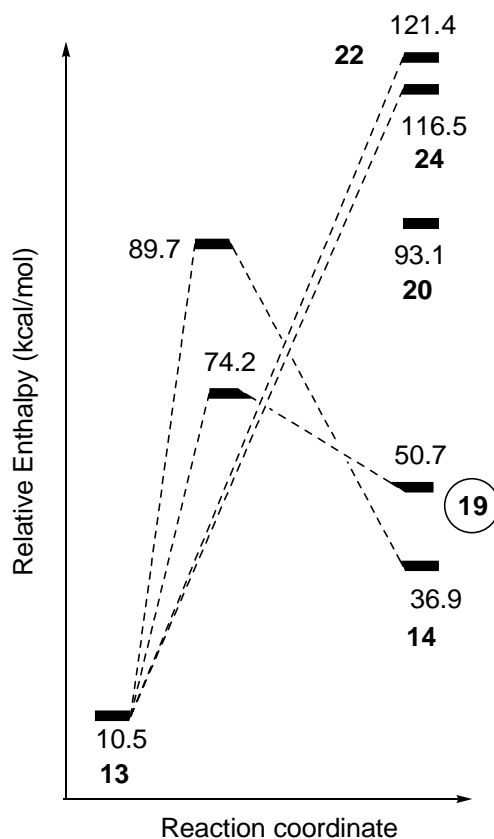


**Figure 3.18.** Relative 0K enthalpy ( $\Delta H_0$ ) profile corresponding to the processes in Equation 3.6. Enthalpy values are given relative to that of acetaldehyde (species **6**) calculated at CCSD(T)/cc-pVTZ//CCSD/6-311g(d,p) level using ZPVE obtained at CCSD/6-311g(d,p) level.

The barrierless dissociation of **13** to **22** and **24** are the most important exit channels, and there is also chance for a vibrationally excited vinyl alcohol molecule (carrying  $191.0 - 10.5 = 180.5$  kcal excess energy) to yield water and acetylene which are not reported in experiments, either due to the characteristics of the reaction medium or their amount being below the detection limit of the setup.

### 3.2.5 OH Insertion and Dissociation Paths on the Triplet PES

The calculated enthalpies on the triplet PES relative to singlet acetaldehyde are given in Table 3-13 for the minima, and in Table 3-14, for the TSs respectively.

**Table 3-13. Relative 0K enthalpies of the triplet minima the levels as specified. <sup>a</sup>**

Label	Species	B3LYP	CCSD(T)	CCSD(T)	EXP. <sup>b</sup>
		6-311G (d,p)	6-311G (d,p)	cc-pVTZ	
R(T)	C( <sup>3</sup> P)+MeOH	162.8	154.4	157.4	162.8
1T	C--OHMe	147.0	144.2	146.1	
4T	Me-O-C-H	92.2	93.8	94.1	
6T	MeCHO	71.7	75.8	76.9	
10T	H <sub>2</sub> C=O+CH <sub>2</sub> ( <sup>3</sup> B <sub>1</sub> )	110.2	99.4	102.2	
13T	H <sub>2</sub> C=CHOH	74.1	77.3	76.6	
15T	HO-CH <sub>2</sub> --H--C	156.7	154.8	158.9	
16T	HO-CH <sub>2</sub> -C-H	92.0	88.7	89.0	
17T	H <sub>2</sub> C-CH <sub>2</sub> -O	81.2	84.6	85.2	
18T	H <sub>2</sub> C-O-CH <sub>2</sub>	84.2	88.0	87.1	
19T	Me-C-OH	78.7	79.8	80.4	

<sup>a</sup> All the values are relative to singlet acetaldehyde and in kcal/mol.

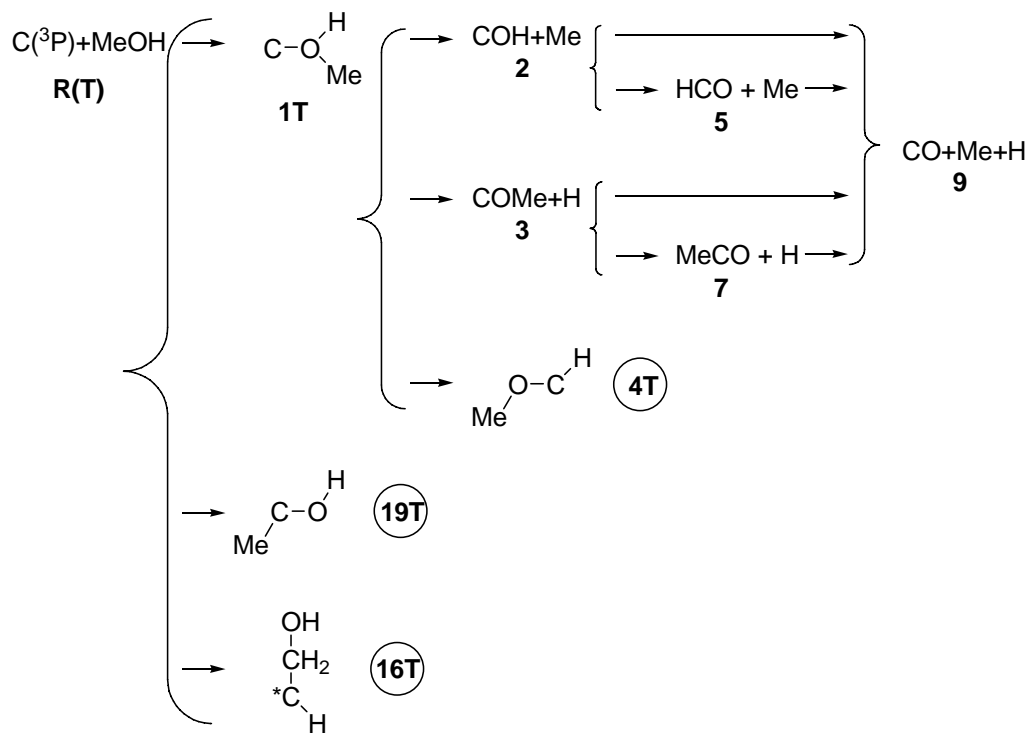
<sup>b</sup> Data taken from Computational Chemistry Comparison and Benchmark Database (CCCBDB) at <http://srdata.nist.gov/cccbdb/default.htm>.

**Table 3-14. Relative 0K enthalpies of the triplet TSs at the levels as specified. <sup>a</sup>**

Label	B3LYP	CCSD(T)	CCSD(T)
	6-311G (d,p)	6-311G (d,p)	cc-pVTZ
15T/16T	158.5	159.7	159.2
1T/19T	175.5	179.1	177.7
1T/2	157.2	162.2	162.6
1T/3	165.1	171.1	171.5
1T/4T	157.9	158.7	158.5
4T/5	100.9	107.3	108.1
4T/6T	132.7	136.8	135.6
4T/18T	126.4	129.6	128.9
6T/5	84.8	89.9	90.6
6T/7	91.8	95.0	96.3
6T/13T	105.2	110.5	109.6
6T/17T	111.0	118.5	117.7
6T/20	109.7		
13T/19T	123.7	128.5	127.2
13T/16T	128.1	132.1	130.7
18T/10T	114.3	119.1	120.0
17T/10T	106.4	107.9	108.8

<sup>a</sup> All the values are relative to singlet acetaldehyde and in kcal/mol.

The initial stage of the reaction of <sup>3</sup>P carbon atoms is schematized in Equation 3.7 and the corresponding enthalpy profile is given in Figure 3.20.



(3.7)

In Figure 3.19, the selected geometric parameters for some of the triplet species, calculated at CCSD/6-311G(d,p) level of theory is given. The initial complex **1T** is the most loose structure among **1**, **1'**, and **1T**.

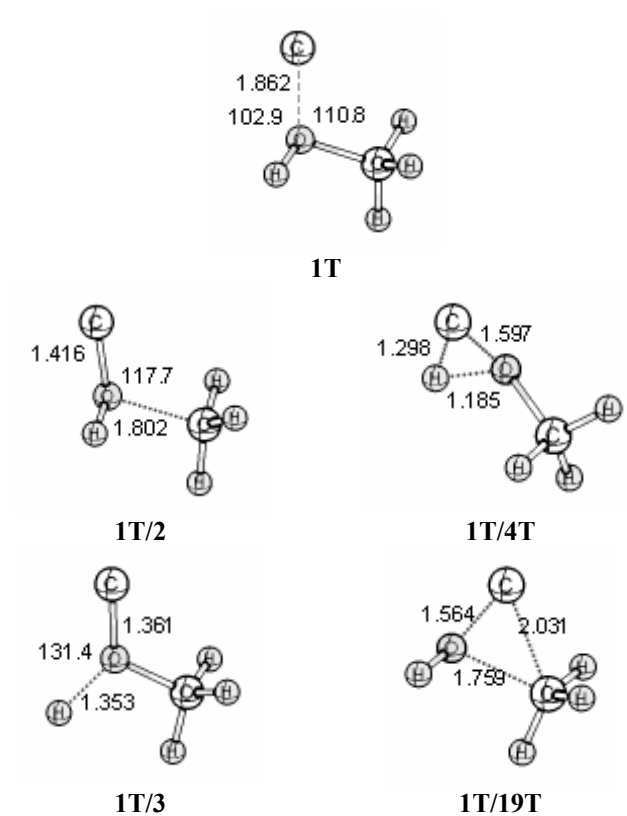


**Figure 3.19.** Selected geometric parameters of some key stationary points on the triplet PES calculated at CCSD/6-311G(d,p) level of theory. Bond lengths are given in angstroms with 3, bond angles are given in degrees with 1 significant figures.

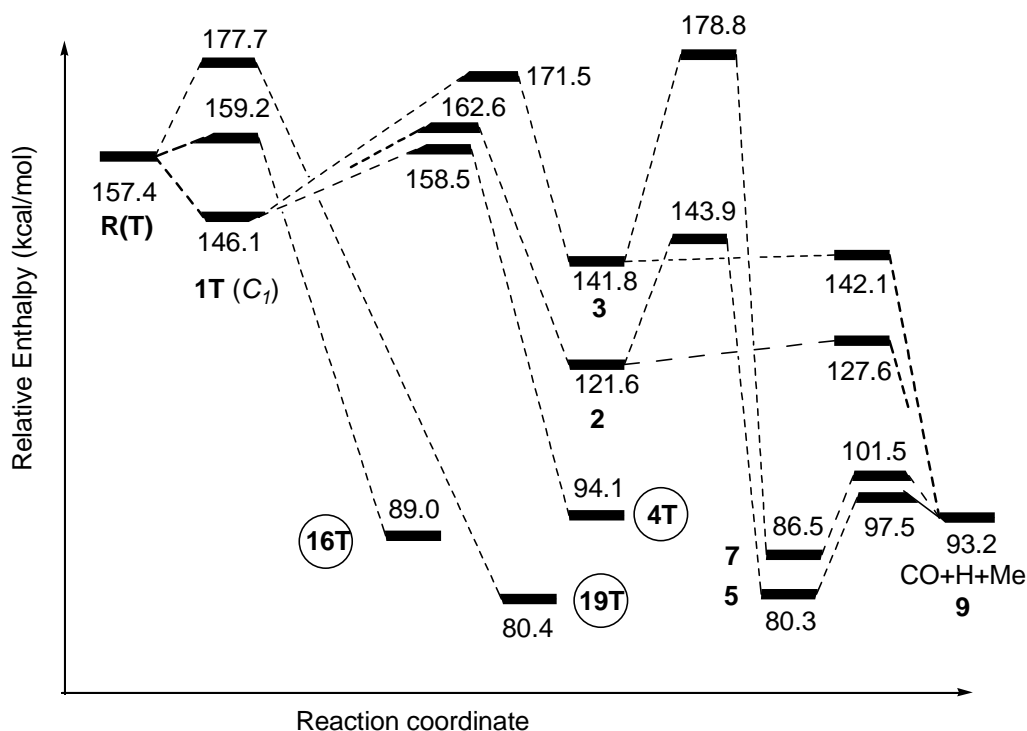


**Figure 3.20.** Relative 0K enthalpy ( $\Delta H_0$ ) profile of processes Relative 0K enthalpy ( $\Delta H_0$ ) profile corresponding to the processes on the triplet PES, originating from **1T** as schematized via Equation 3.7.

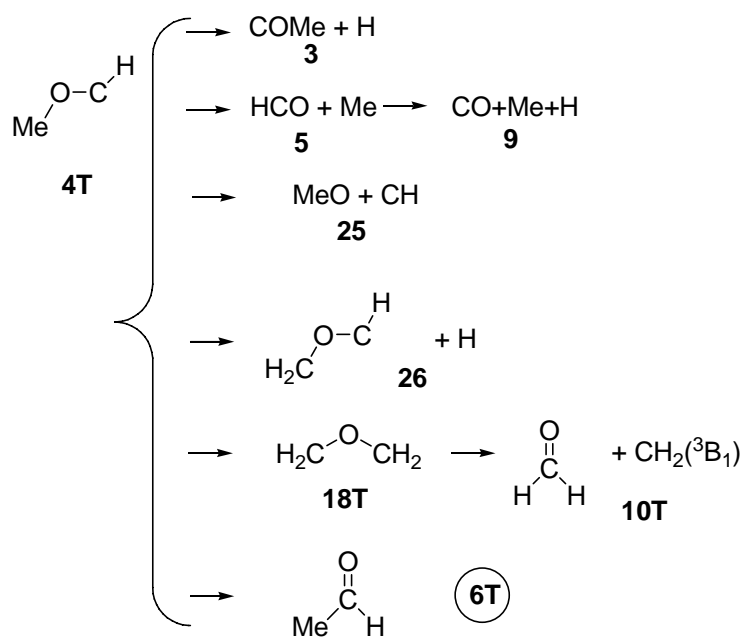
Enthalpy values are given relative to that of acetaldehyde (species **6**) calculated at CCSD(T)/cc-pVTZ//CCSD/6-311g(d,p) level using ZPVE obtained at CCSD/6-311g(d,p) level.

As immediately seen from Figure 3.20 all the barriers on the path for the rearrangement or dissociation of complex **1T** lie higher in energy than the initially available energy. This means if the carbon atoms do not carry extra translational energies due to the method of generation they should not react and prefer to back-dissociate into reactants. This sort of extra translational energy can be available in carbon arc experiments but we are not aware of any strong-evidence supporting this fact, and consequently we can not term  $^3\text{P}$  carbons to be reactive towards the oxygen of methanol.

Although we consider the further reactions of **1T** as skeptic, we have analyzed all the possible products from **1T**. This is due to two main reasons. First of all not for the OH fission, methyl dissociation, and OC insertion paths from **1T** but

for the OH insertion path yielding **4T**, the 1.1 kcal/mol difference between the reactants and **1T/4T** is such a small amount of energy for which our theoretical predictions may fail. So with some -futuristic- higher level of theory we may see a slight change for these two energies, and conclude that path **1T** to **4T** is viable; or we may be confident that it is blocked. Second if the incoming carbon atoms are shown to carry extra energies of a few kcal/mol, the path will not be termed as closed. So we continued the investigation of the species on the triplet PES. Further reactions of **4T**, and **6T** were given in the following diagrams. However by making use of the current experience and the available experimental data we believe the ground state triplet carbon atoms generated by arcing to be unreactive towards frozen methanol substrate.

Equation 3.8 illustrates the exit channels from **4T**, and the corresponding energy diagram is given in Figure 3.21.



(3.8)

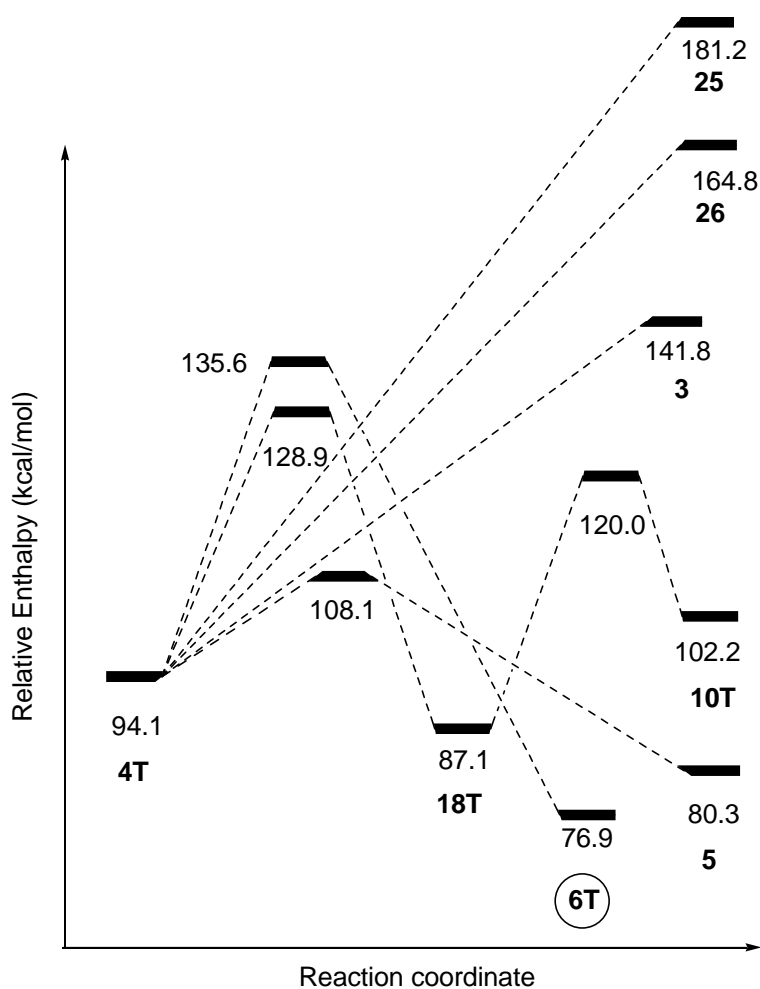
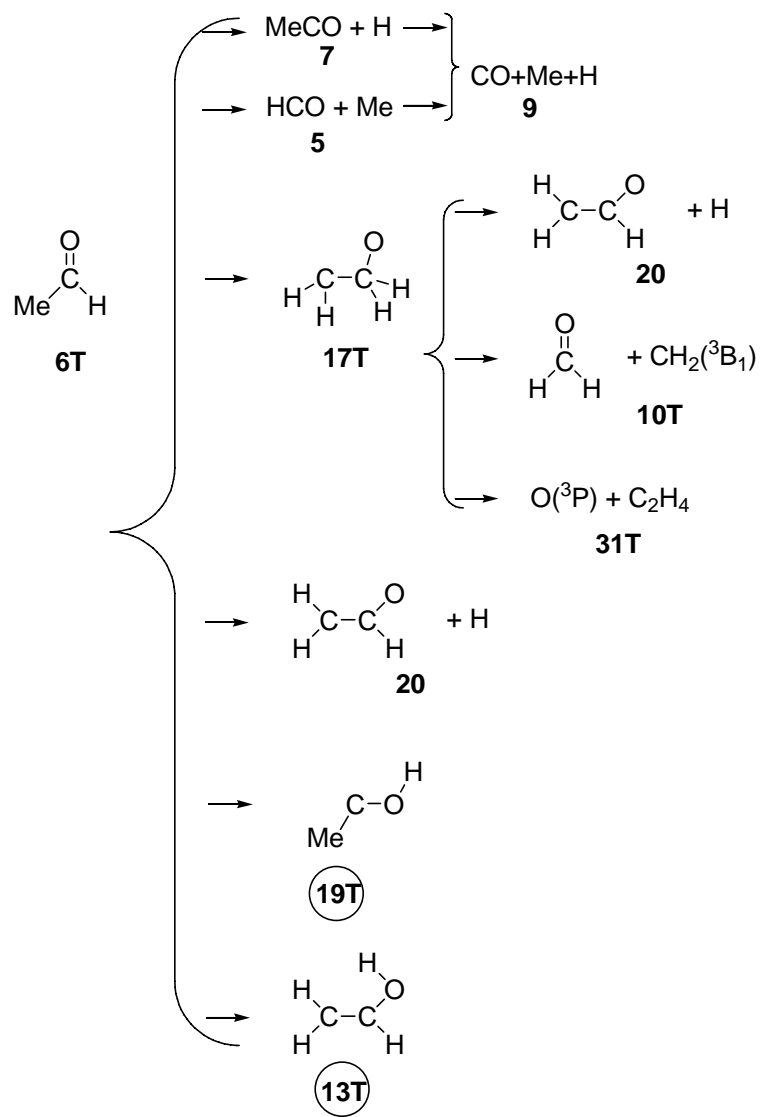


**Figure 3.21.** Relative 0K enthalpy ( $\Delta H_0$ ) profile of processes on the triplet PES, originating from 4T as schematized via Equation 3.8. Enthalpy values are given relative to that of acetaldehyde (species 6) calculated at CCSD(T)/cc-pVTZ//CCSD/6-311g(d,p) level using ZPVE obtained at CCSD/6-311g(d,p) level.

Here it is important to note that the most favorable path as an exit channel from 4T is the barrierless dissociation of the methyl group leaving formyl. Formyl is known to further dissociate, thus 4T yields the final products 9, i.e. CO, CH<sub>3</sub>, H.

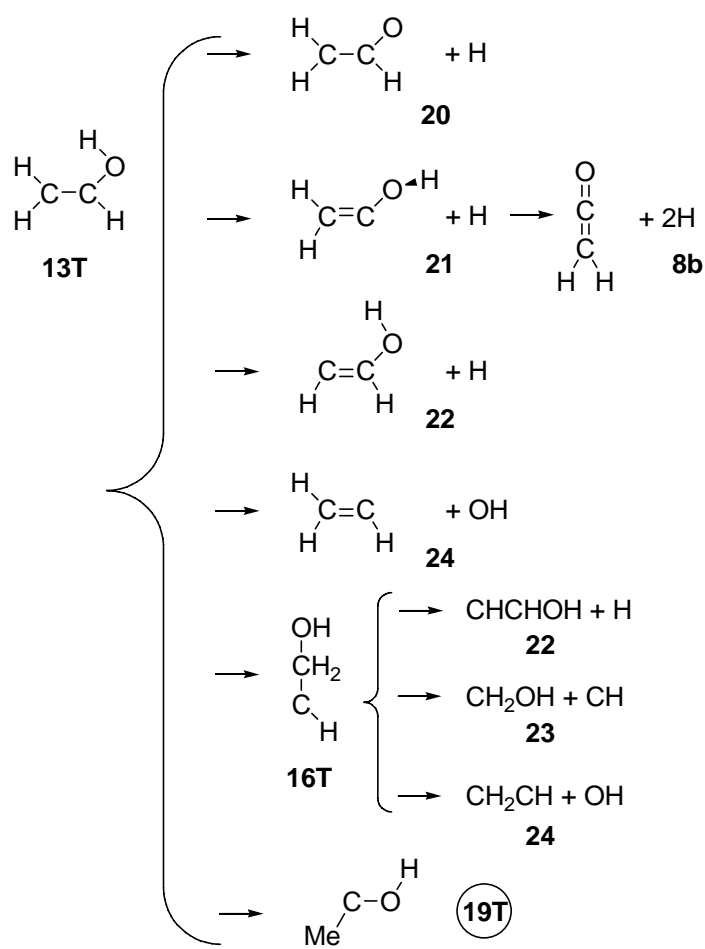
Continuing with the exit channels from 6T, the available paths are schematized with Equation 3.9, and the relevant energy diagram is depicted in Figure 3.22.

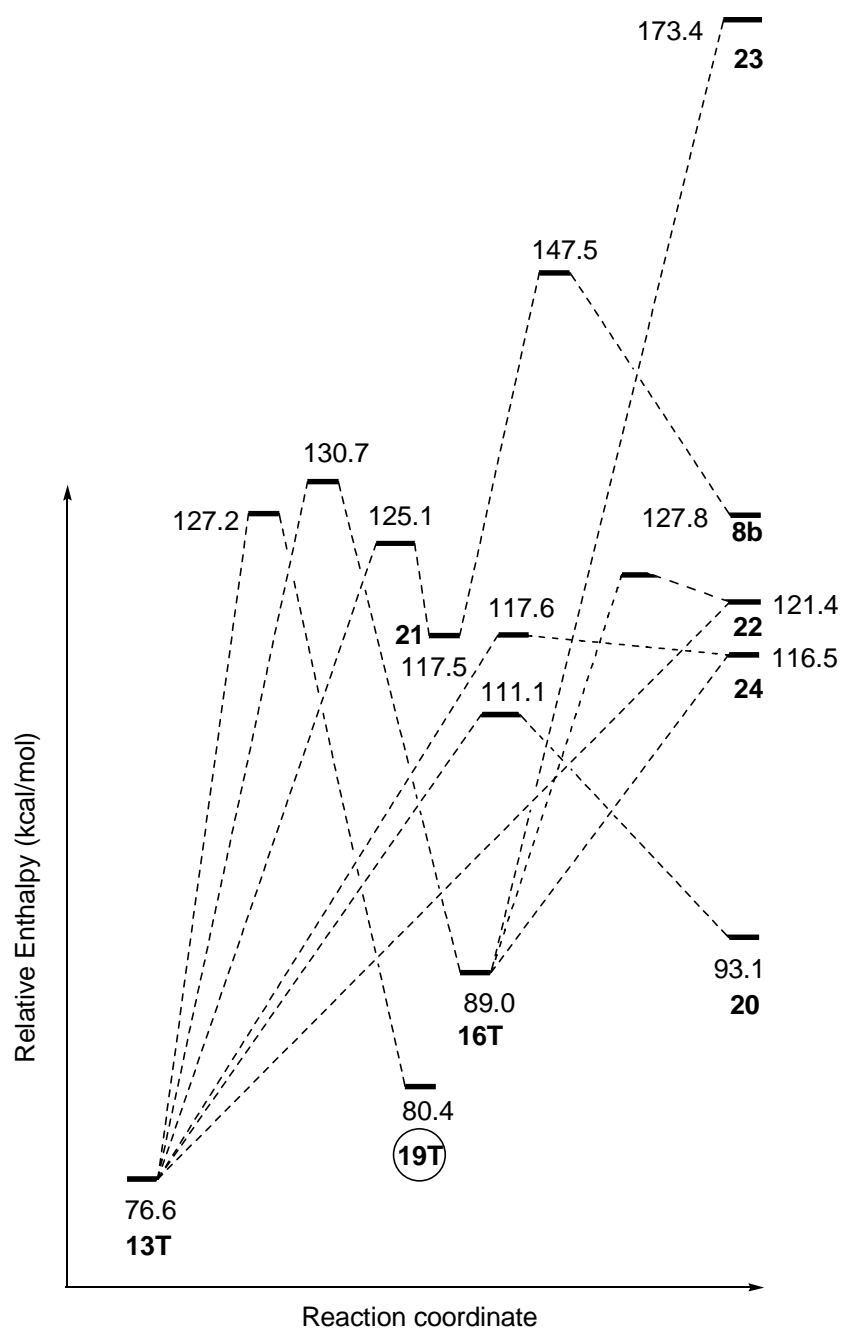


(3.9)



rearrangement to **6T**. We again note that the extra energy of attacking carbon atoms and energetics of the experimental medium is very important to judge the generation of these species, actually all the species on the triplet surface.

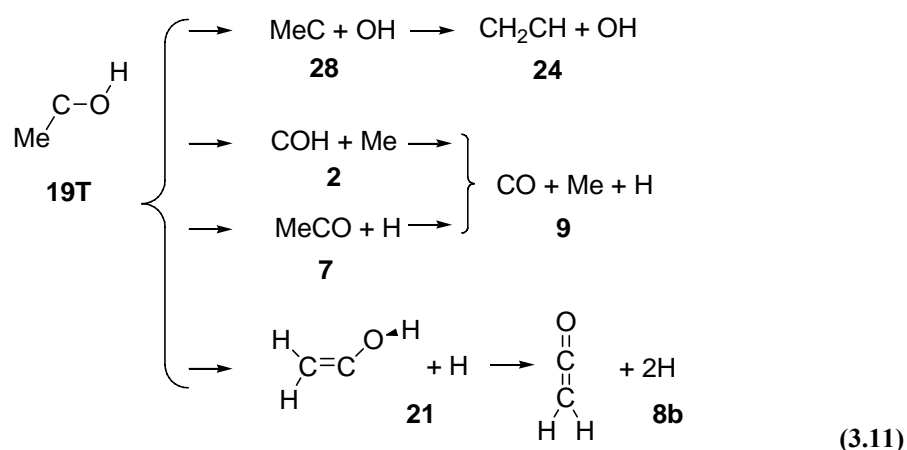




**Figure 3.23.** Relative 0K enthalpy ( $\Delta H_0$ ) profile of processes on the triplet PES, originating from **13T** as schematized via Equation 3.10. Enthalpy values are given relative to that of acetaldehyde (species **6**) calculated at CCSD(T)/cc-pVTZ//CCSD/6-311g(d,p) level using ZPVE obtained at CCSD/6-311g(d,p) level.

The high activation energies needed to rearrange **13T** seem as the characteristics of this part of the PES. From this scheme further conversion probabilities of **13T** may appear. If **13T** is proven to be feasible to occur in some specific experimental condition, the crossing to the singlet PES, and the probability to be trapped by the medium can be investigated.

The least feasible of the exit channels from **1T**, the formation of **19T**, if somehow **1T/19T** traversed, will have the following probabilities all being dissociative pathways, ( See Equation 3.11) and the enthalpy profile of the species in Equation 3.10 are given in Figure 3.24.



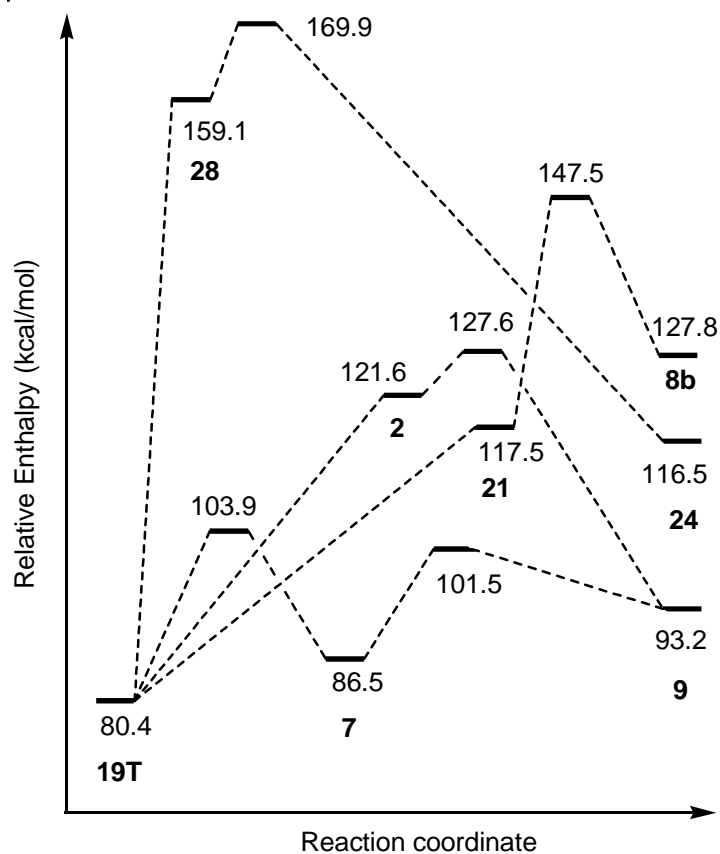


**Figure 3.24.** Relative 0K enthalpy ( $\Delta H_0$ ) profile corresponding to the processes on the triplet PES, originating from **19T** as schematized via Equation 3.10. Enthalpy values are given relative to that of acetaldehyde (species **6**) calculated at CCSD(T)/cc-pVTZ//CCSD/6-311g(d,p) level using ZPVE obtained at CCSD/6-311g(d,p) level.

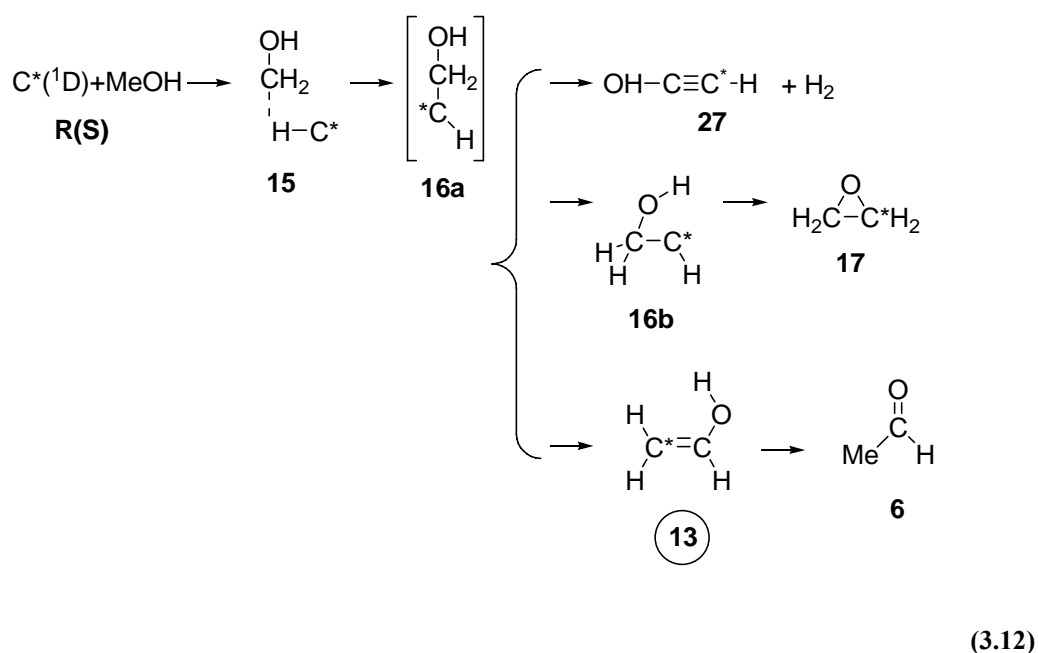
The most favorable of the paths in Figure 3.24 is the barrierless dissociation to methyl and isoformyl, and the subsequent dissociation to the final products. The subsequent barriers to other two barrierless paths (i.e. to **21** and **28** are higher in energy than the 6.0 kcal/mol **2/9** to **2** difference)

Our computations on the triplet PES concerning the complete exit channels from **1T**, provide us with the picture of, blockage of OC insertion via **1T/19T**, and H fragmentation via **1T/3** due to the TS energies being more than the initially available energy. Similarly anticipating methyl fragmentation via **1T/2**, and OH insertion via **1T/4T** as viable, will be a very bold prediction as the methodological error in computed enthalpies may, work both in favor or disfavor of their accessibility. But even if **1T/2**, and **1T/4T** are traversed, the

intermediates from the former will yield the final products as in the singlet PES via **2**, and **2/9**. Considering the intermediates from the latter, it is much more favorable to obtain methyl and formyl, than to end up with triplet acetaldehyde, but if triplet acetaldehyde does not decay to singlet acetaldehyde ( $T_1$  to  $S_0$  crossing), it is possible to dissipate the methyl, or the hydrogen via **6T/5**<sup>a</sup> and **6T/7**; and then yield the final products with activation energies not more than 20 kcal/mol for each of the two transition states on each route.

### 3.2.6 CH Insertion Path on the Singlet PES.

Products arising from insertion of singlet carbon atoms into CH bonds of methanol are illustrated in Equation 3.12. The incoming carbon atom is distinguished by an asterisk. The corresponding enthalpy profile is shown in Figure 3.26. The selected geometric parameters of some key stationary points on the singlet CH insertion path is given in Figure 3.25.



<sup>a</sup> This is a well studied reaction. See for example: (a) O. Setokuchi, S. Matsuzawa and Y. Shimizu. Chem. Phys. Lett. 284 (1998), p. 19. (b) R.A. King, W.D. Allen and H.F. Schaefer III. J. Chem. Phys. 112 (2000), p. 5585.

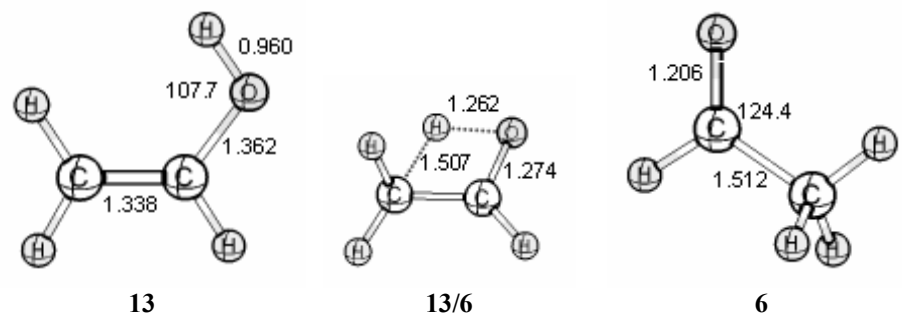


**Figure 3.25.** Selected geometric parameters of some key stationary points on the singlet CH insertion path calculated at CCSD/6-311G(d,p) level of theory. Bond lengths are given in angstroms with 3, bond angles are given in degrees with 1 significant figures.

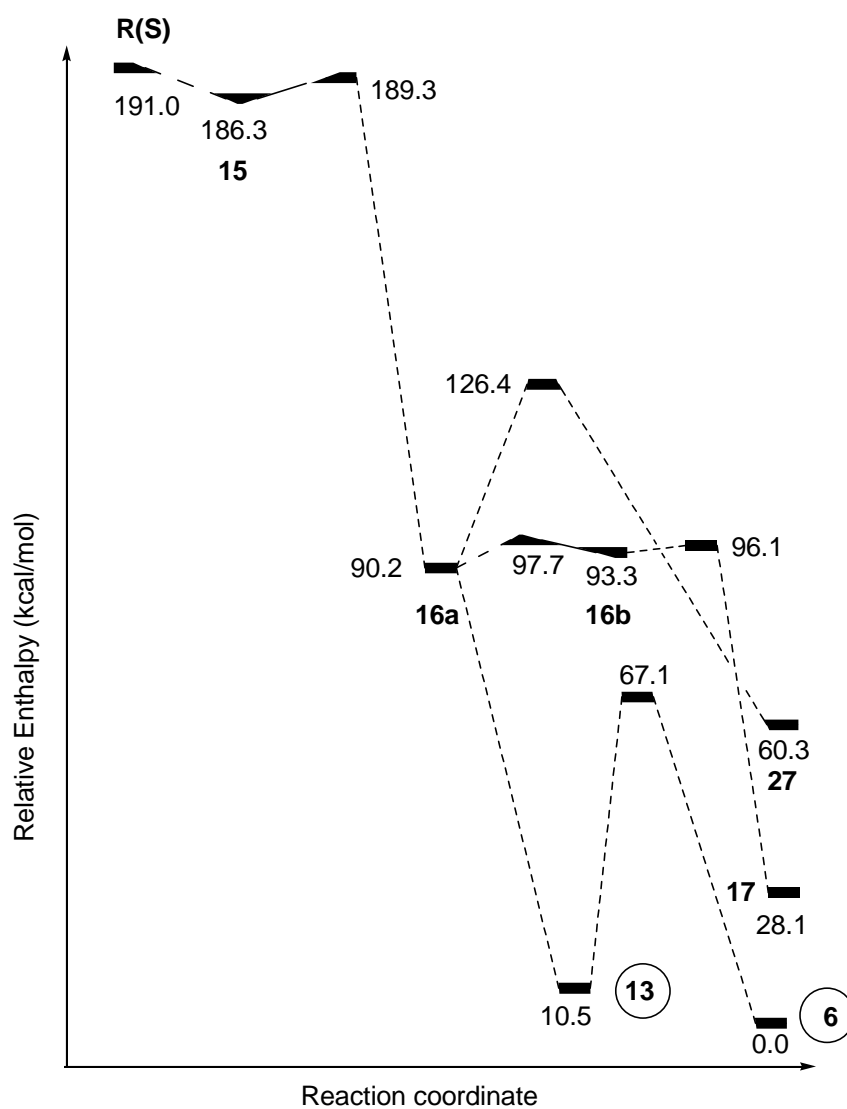
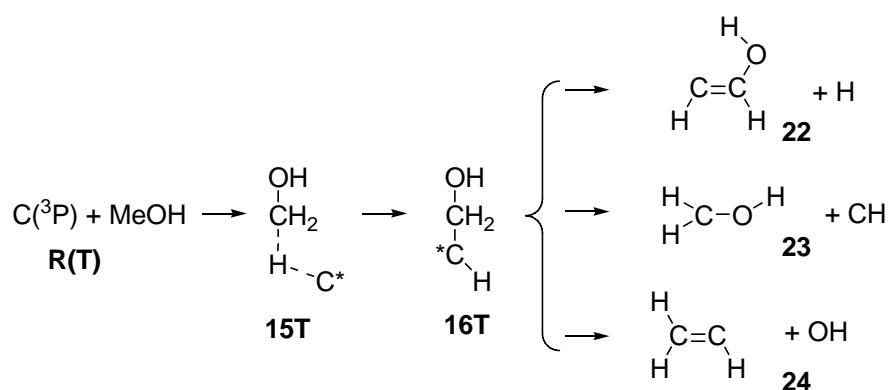


**Figure 3.26.** Relative 0K enthalpy ( $\Delta H_0$ ) profile of processes on the singlet CH insertion path, schematized via Equation 3.10. Enthalpy values are given relative to that of acetaldehyde (species 6) calculated at CCSD(T)/cc-pVTZ//CCSD/6-311g(d,p) level using ZPVE obtained at CCSD/6-311g(d,p) level.

We propose the enol form of acetaldehyde, i.e. vinyl alcohol (**13**) being the immediate CH insertion product on the singlet PES. This picture is well supported by the very low barrier of 3 kcal/mol from **15** to **16a**, and the barrierless hydrogen migration from **16a** to enol. This interesting phenomenon was confirmed by isotope labeling studies<sup>71</sup> with the failure to observe any products, whose precursor may be singlet hydroxymethyl-carbene (**16**); and this fact was attributed to the very rapid rearrangement of the carbene to enol. We predict one possible channel from **13** in the gas phase as conversion to acetaldehyde. It is also possible for enol **13** to get trapped in the condensed phase and yield acetaldehyde upon warming as the equilibrium<sup>136</sup> between the keto and enol form is in favor of **6**. Isotope labeling studies due to Skell confirm the production of acetaldehyde from CH insertion; and the OH insertion path is proven to be blocked for acetaldehyde generation in the condensed medium. This is in excellent agreement with our predictions, and this fact will be summarized in the following sections.

### 3.2.7 CH Insertion Path on the Triplet PES.

The CH insertion path was also studied for the triplet carbon atoms. The relative energy diagram for the scheme given in Equation 3.13 is shown in Figure 3.27.



(3.13)

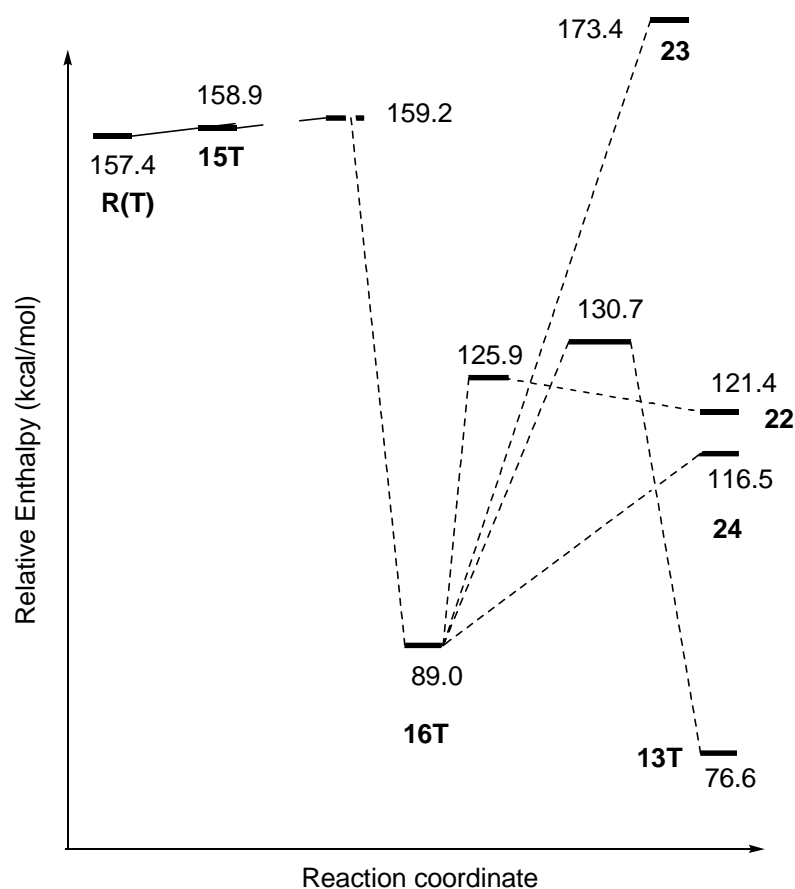


**Figure 3.27.** Relative 0K enthalpy ( $\Delta H_0$ ) profile of processes on the triplet CH insertion path, schematized via Equation 3.13. Enthalpy values are given relative to that of acetaldehyde (species **6**) calculated at CCSD(T)/cc-pVTZ//CCSD/6-311g(d,p) level using ZPVE obtained at CCSD/6-311g(d,p) level.

For the triplet PES, the complex **15T** is questionable to yield the triplet carbene **16T**, because of the activation barrier lying 1.8 kcal/mol above the initially available energy, and this is surprisingly similar to the uncertainty in OH insertion and methyl fragmentation paths from **1T**. Moreover the formation of the initial complex –although the increase in energy is very low- is an endothermic process. As a result, our calculations show the  $^3\text{P}$  carbon atoms being unreactive towards CH bonds, which is in excellent agreement with the rate data reported<sup>72</sup> about the reactions of  $^3\text{P}$  and  $^1\text{D}$  carbons with methane;

singlet carbons reacting 10 thousand times faster.(Refer to the section 1.5.1 CH Insertion)

### **3.2.8 Intermolecular Dimethoxymethane Formation Path**

In our search for the products containing one more carbon atom compared to methanol the discussion up to here works fine, however for investigating a possible route for the formation of dimethoxymethane, it is necessary to consider the reaction of one of the intermediates having C<sub>2</sub>H<sub>4</sub>O stoichiometry with the methanol available from the medium of the reaction. Such an intermediate is either **4**, **4'**, or **6**. If **4'** or **6** were expected to react with the medium, there is no logic in discarding the possibility of reaction of **4**. If **4** were expected to react with a methanol molecule from the matrix this should mean the trapping of carbene **4** in a potential well and such a mechanism as we illustrate in Figure 3.28 will work for the blockage of unimolecular rearrangement, and dissociation paths from **4**, i.e. the diminished probability of reactions of **4'**, and/or **6** with methanol. Note that the generation of acetaldehyde (**6**) is via **4'** which is formed from rearrangement of **1** to **4** on the singlet OH insertion path.

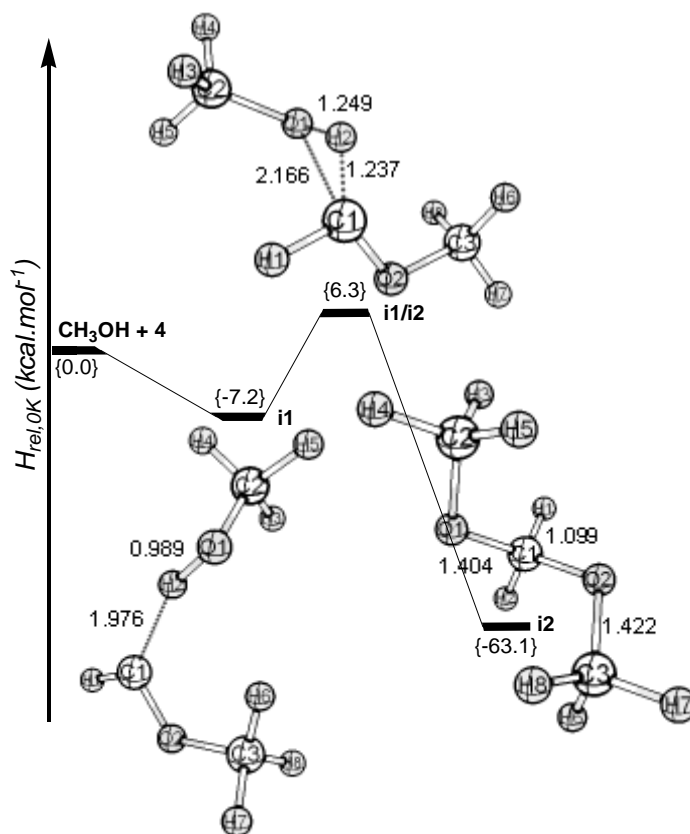


**Figure 3.28.** Relative 0K enthalpy ( $\Delta H_0$ ) diagram for the intermolecular dimethoxymethane formation path on the singlet PES computed at {CCSD(T)/cc-pVTZ//B3LYP/6-31G(d,p)} level of theory.

The schematization is roughly to scale. This mechanism is assumed to dominate in the condensed phase. Selected bond lengths shown on the species are in angstroms optimized at B3LYP/6-31G(d,p) level of theory.

The route to the formation of **i1** with  $\sim 7$  kcal/mol stabilization is the most favorable of the non-dissociative routes from **4** (both unimolecular and intermolecular channels considered). The feasibility of traversing a nearly 14 kcal/mol barrier, which lies about 6 kcal/mol above the energy of the reactants, in order to form **i2** may be argued. First the non-fixed energy of about 110 kcal/mol upon formation of **4** may not get lost completely via coupling to the medium. Adding the possibility of incomplete dissipation of 7 kcal exothermicity it may be possible to obtain dimethoxymethane from **4** as the most favorable product. In another view **4** seems almost certain to get trapped by the medium in frozen matrix conditions. Warming up the products for

analysis may result in the formation of dimethoxymethane. Thus it is plausible to correlate the yield of dimethoxymethane with the ability of the medium to trap carbene **4**. Thus we propose that dimethoxymethane will not be observed in gas phase experiments.

This reasoning has very important effects on the routes we discussed about the OH, OC, CH insertions, and the dissociations on the triplet and singlet PESs of the system under investigation. In a condensed medium only the reactions as fast as the rapid dissociations of **1** to **2**, and **3** will have chance to compete with the stabilization of **4**. All the routes originating from **4** –as stated above- will be plugged, as a result of trapping of carbene **4**. So double OH insertion should be the operative mechanism for dimethoxymethane production. In the case of CH insertion the very fast production of enol (**13**) will be the only allowed route. Whereas gas phase reactions have the potential to yield various stable and radicalic species (with primary generation of CO), the products from a condensed phase reaction will be limited. This picture very well fits the available experimental data about C + methanol system.

The net effect of attacking carbon on production of CO arises as; entering the system by being loosely bound, shooting out one R group –either H, or methyl-, followed by dissociation of the other and yielding CO. So we here can introduce the term “abstraction” for the production mechanism of CO in carbon atom reactions with methanol. The literature of atomic carbon reactions does not provide us with information of abstraction as a CO generation mechanism, in reactions with neither water nor alcohols. We want to add that our unpublished work which is not included here about bigger alcohols such as ethanol, and ethers such as dimethylether support the applicability of the abstraction mechanism to them also.

### 3.2.9 Conclusions

Theoretical investigation of the reactions of first excited singlet ( $^1D$ ) and ground state triplet ( $^3P$ ) carbon atoms with methanol were presented. Comments on the feasible pathways are based on the enthalpies at CCSD(T)/cc-pVTZ//CCSD, and CCSD(T)/cc-pVTZ//RB3LYP/6-31G(d,p) levels. The most important entrance channel of C ( $^1D$ ) to methanol was proposed to be the attack to the most electronegative atom i.e. oxygen. Considering the reactions of free carbon atoms with frozen methanol substrate; a detailed inspection of unimolecular dissociation pathways leading to CO formation shows the most probable CO generation paths as the rapid dissociations of the initial  $C_s$  symmetric closed shell complex  $^1A'$  to 2, and 3, then the subsequent dissociations of isoformyl and methoxymethyne on the singlet PES. OC insertion is shown to be unlikely. Dimethoxymethane generation is due to the intermolecular reactions of methanol with methoxymethylene. Acetaldehyde forms as a result of a rapid CH insertion (followed by a 1-2 hydrogen shift) on the singlet PES. Triplet carbon atoms do not seem to be responsible from -at least- majority of the products. The experimental isolation of the species is highly dependent on the ability of the medium to trap the intermediates via effective transfer of excess energy. The viable paths yielding the experimentally observed products are given in Figure 3.29.

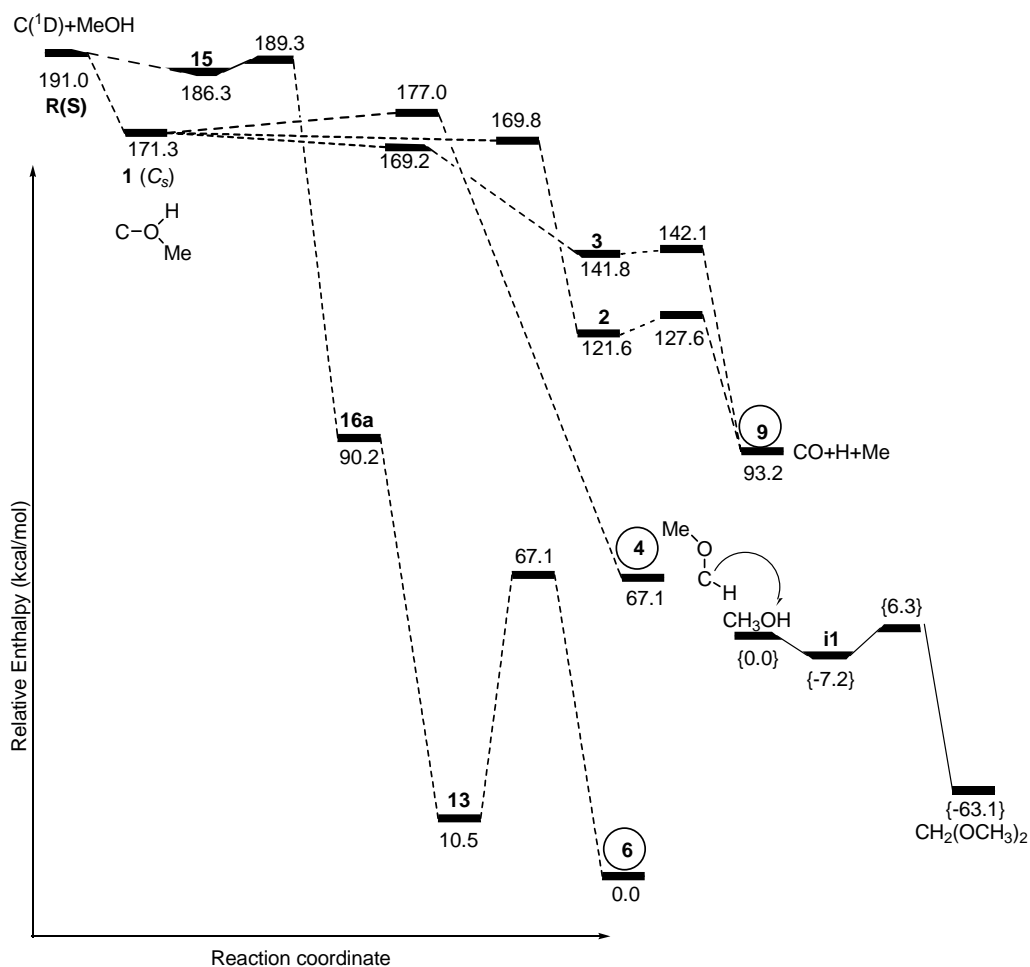


**Figure 3.29.** Relative 0K enthalpy ( $\Delta H_0$ ) diagram for the overall operative paths in the condensed phase.

Unimolecular paths are reported at  $\{\text{CCSD(T)/cc-pVTZ//CCSD/6-311G(d,p)}\}$  level of theory, whereas the intermolecular dimethoxymethane formation path at  $\{\text{CCSD(T)/cc-pVTZ//B3LYP/6-31G(d,p)}\}$  level; using ZPVE obtained at  $\{\text{CCSD/6-311G(d,p)}$ , and  $\{\text{B3LYP/6-31G(d,p)}\}$  levels respectively. The schematization is roughly to scale.

In the gas phase nearly all the products are CO, CH<sub>3</sub>, and H as a result of the reactions on the singlet PES. Small amounts of CH<sub>3</sub>CHO, CH<sub>4</sub>, CH<sub>2</sub>, CH<sub>2</sub>CO, C<sub>2</sub>H<sub>2</sub>, H<sub>2</sub>O and H<sub>2</sub> are also expected. In the condensed phase the very early and rapid reactions seem to have chance, the subsequent rearrangements are hard to occur. Radicalic species predicted to occur by our theoretical results would be hard to observe. Their isolation will be strictly dependent on the possibility of their side reactions and the ingenuity of the experimental setup.

The triplet surface –if reactive- will have low yields of products. The quality of the answers, to the accessibility of routes for the rearrangements of the initial complexes **1T**, and **15T**, are spoiled by the uncertainty in the state of the art computational chemistry techniques.

When dealing with closed shell singlet species B3LYP/6-311G(d,p) performs nearly identical with CCSD/6-311G(d,p) on geometry optimizations. On the other hand energy calculations at the CCSD(T)/cc-pVTZ level are necessary for a reliable description of the PES. Using the CCSD(T,FULL)/cc-pVTZ energy calculations seem to improve the quality of the results only slightly; so thanks to the cancellation of errors, the computationally costly inclusion of core electron correlation, is not crucial for the relative energy scheme, and FC calculations may be preferred over full core-correlation calculations when a large, correlation consistent basis set is used.

The methanol reactions presented here do not contain investigations of the first excited singlet state, i.e. the open shell singlet state of the initial loose complex **1**. The accessibility of the paths forming the open shell complex, and the feasibility of the routes from it, together with the product spectrum due to the rearrangements, dissociations, and surface crossings is left as a future work for our research group. These findings show that, the CO formation mechanism, an obscure problem, is resolved, and results in agreement with available experimental data are achieved.

Summarizing the triplet PES mechanisms, it is questionable to expect products generated from <sup>3</sup>P carbon atoms attacking methanol. We failed to locate any channel that clearly shows a reaction of <sup>3</sup>P carbon atoms with methanol, and it will be interesting to find high levels of theory that will significantly and systematically converge to energy differences, and alleviate the problem of predicting the blockage or accessibility of routes via **1T/2**, **1T/4T**, and **15T/16T**.

## CHAPTER IV

### CONCLUSION

*Science at its best provides us with better questions, not absolute answers.*

*Norman Cousins, 1976*

*Truth, in science, can be defined as the working hypothesis best fitted to open the way to the next better one.*

*Konrad Lorenz*

*Were I to await perfection, my book would never be finished.*

*History of Chinese Writing  
Tai T'ung, 13th Century*

The conclusions for the separate systems of C + water, and C + methanol were given previously at the end of the relevant discussions. We here restate some important findings about these systems; and compare and contrast the most notable features of them with main emphasis of combining the two systems of reactions in one general view.

Reactions of singlet ( $^1\text{S}$  and  $^1\text{D}$ ) and triplet ( $^3\text{P}$ ) carbon atoms with water, and  $^1\text{D}$  and  $^3\text{P}$  carbon atoms with methanol were studied computationally. The carbon vapor containing a mixture of  $\text{C}(^1\text{S})$ ,  $\text{C}(^1\text{D})$ , and  $\text{C}(^3\text{P})$  atoms, is predicted to react with the oxygen, OH bond and CH bond of the substrate

mainly with the  $^1\text{D}$  state. While  $\text{C}(^1\text{S})$  was proven to be unreactive  $\text{C}(^3\text{P})$  can hardly be defended to be reactive, and can safely be defined as unreactive. Much higher levels of theory that will significantly and systematically converge to energy differences, and alleviate the problem of predicting the blockage or accessibility of the initial routes on the triplet PESs may be employed in the future.

The major product, CO forms as a result of oxygen abstraction, which is observed as a fast, energetically quite favorable process. The scheme of this oxygen abstraction is promising to be applicable to substrates with the general formula  $\text{R}_1\text{-O-R}_2$ . Thus the deoxygenation scheme applies to reactions of carbon atoms with water, alcohols, and ethers.<sup>a</sup>

The global energy minimum of  $\text{C} + \text{R}_1\text{OR}_2$  system can be expected to be  $\text{CO} + \text{R}_1\text{-R}_2$ ; which is the case for water with  $\text{C} + \text{H}_2\text{O}$ , and for methanol with  $\text{CO} + \text{CH}_4$ .

OH insertion, both for water and methanol, yields trappable carbenes; the carbene being a key species on the spectrum of the end products. Water matrix trapping the carbene opens the path to the formation of formaldehyde; and exhibits a prototype reaction for the formation of dialkoxymethanes. This mechanism operative for methanol reactions and dimethoxymethane formation as a result of the reaction of singlet trans carbene (**4**) with the methanol matrix is in principle the “same” topology of reaction.

Formation of acetaldehyde in methanol reactions is unique in the sense that there can be no comparison for the reaction scheme in the water system. But surprisingly, the same energetic requirements hold, i.e. acetaldehyde generation is possible because it is a fast, and energetically downhill process.

---

<sup>a</sup> Although not discussed here our unpublished results supports this fact both for acyclic, and cyclic ethers (oxiranes).

Gas phase product spectrum from the reactions are broader, due to the accessibility of the routes originating from the otherwise trapped intermediates; and the excess energy of the reactions being carried by them. In the condensed phase the very early and rapid reactions seem to have chance, the subsequent rearrangements are hard to occur. The conclusions thus far apply to the reactions in the gas phase as well as in condensed phases involving inert matrices; and the experimental isolation of the species is highly dependent on the ability of the medium to trap the intermediates via effective transfer of excess energy.

As a result, by employing the state of art *ab initio* quantum chemistry techniques, the CO formation mechanism, an obscure problem in C + water, and C + alcohols, systems is resolved; prototypical mechanisms in water are utilized for methanol; predictions for higher alcohols and ethers are obtained; and results in excellent agreement with available experimental data are achieved. In addition to these by analyzing the ostensibly inaccessible pathways, valuable data for some (high energy) experiments which may be studied in the future is collected.

## REFERENCES

- [1] Kaiser R. I. *Chem. Rev.* 2002, 102, 1309.
- [2] Shevlin, P.B. *Reactive Intermediates*; Abramovich, R.A., Ed.; Plenum Press: New York, 1980; Vol. I, pp 1-36. and the references therein.
- [3] Mackay, C. *Carbenes*; Moss, R. A., Jones, M., Jr., Eds.; Wiley-Interscience: New York, 1975; Vol. II, pp 1-42. and the references therein.
- [4] Himmel, H. J.; Downs, A. J.; Greene, T. M. *Chem. Rev.* 2002, 102, 4191. the references therein.
- [5] Casavecchia, P. *Rep. Prog. Phys.* 2000, 63, 355. and the references therein.
- [6] Kaiser, R. I. *Chem. Rev.* 2002, 102, 1309, and the references therein.
- [7] Flanagan G.; Ahmed S. N.; Shevlin P. B. *J. Am. Chem. Soc.* 1992, 114, 3892.
- [8] (a) Nicoll, G.; Francisco, J. S. *Environ. Sci. Technol.* 1998, 32, 3200. (b) Frenklach, M.; Ebert, L. B. *J. Phys. Chem.* 1988, 92, 561. (c) Iijima, S.; Wakabayashi, T. T.; Achiba, Y. *J. Phys. Chem.* 1996, 100, 5839. (d) Richter, H.; Granata, S.; Green, W. H.; Howard, J.B. *Proc. Combust. Inst.* 2005, 30, 1397. (e) Frenklach, M.; Schuetz, C. A.; Ping, J. *Proc. Combust. Inst.* 2005, 30, 1389. (f) D'Anna, A.; Violi, A. *Energy Fuels* 2005, 19, 79.
- [9] Perry, M. D.; Raff, L. M. *J. Phys. Chem.* 1994, 98, 4375.
- [10] Vacca, J. R. *The World's 20 Greatest Unsolved Problems*; Prentice Hall: New Jersey, 2005; pp 509-537.
- [11] Weltner, W.; Van Zee, R. J. *Chem. Rev.* 1989, 89, 8, 1713.
- [12] Wolf, A. P.; Redvanly, C. S. *Int. J. Appl. Radiat. Isotopes* 1977, 28, 29.
- [13] (a) Bettinger, H. F.; Schleyer, P. v. R.; Schaefer, H. F.; Schreiner, P. R.; Kaiser, R. I.; Lee, Y. T. *J. Chem. Phys.* 2000, 113, 4250. (b) Geise, M. C.; Hadad, C. M.; Zheng, F.; Shevlin, P. B. *J. Am. Chem. Soc.* 2002, 124, 355. (c) McKee, M. L.; Shevlin, P. B.; Zottola, M. J. *J. Am. Chem. Soc.* 2001, 123, 9418. (d) Scholefield, M. R.; Goyal, S.; Choi, J. H.; Reisler, H. J. *Phys. Chem.* 1995, 99, 14605.

- [14] Jeong G. H.; Klabunde K. J.; Pan O. G.; Paul G. C.; Shevlin P. B.; *J. Am. Chem. Soc.* 1989, 111, 8784.
- [15] Kim G. S.; Nguyen T. L.; Mebel A. M.; Lin S. H.; Nguyen M. T. J. *Phys. Chem. A* 2003, 107, 1788.
- [16] M. J. S. Dewar et al. *J. Am. Chem. Soc.*, 103, 10, 2802, 1981.
- [17] Mackay, C. In "Carbenes"; Moss, R. A., Jones, M., Jr., Eds.; Wiley-Interscience: New York, 1975; Vol. 11, pp 1-42.
- [18] H. W. Kroto, J. R. Heath, S. C. O'Brien, R. F. Curl & R. E. Smalley, *Nature* 318, 162 – 163.
- [19] Mallard, W.G., Linstrom, P. J., Eds. NIST Chemistry WebBook, NIST Standard Reference Database Number 69; National Institute of Standards and Technology, Gaithersburg MD, 20899, June 2005 (<http://webbook.nist.gov>).
- [20] Ahmed S. N.; McKee M. L.; Shevlin P. B.; *J. Am. Chem. Soc.* 1983, 105, 3942.
- [21] Foltin, M.; et al. *J. Chem. Phys.* 1997, 107, 6246-6256.
- [22] Lin, Y. T.; Mishra, R. K.; Lee, S. L. *J. Phys. Chem. B* 1999, 103,3151-3155.
- [23] Shevlin, P. B.; McPherson, D. W.; Melius, P. J. *Am. Chem. Soc.*, 105, 3, 488 - 491, 1983.
- [24] Shevlin, P. B.; McPherson, D. W.; Melius, P. J. *Am. Chem. Soc.*, 103, 23, 7006 - 7007, 1981.
- [25] Andrews, R.; Jacques, D.; Qian, D.; Rantell, T. *Acc. Chem. Res.* 2002; 35(12); 1008-1017.
- [26] Goroff, N.S. *Acc. Chem. Res.* 1996; 29(2); 77-83.
- [27] Irle, G. Zheng, Z. Wang and K. Morokuma, *J. Phys. Chem. B*, 110, 14531-14545 (2006).
- [28] Diethard K. Bohme *Chem. Rev.*; 1992; 92(7); 1487-1508.
- [29] S. Iijima, T. Wakabayashi, Y. Achiba, *J. Phys. Chem.* 1996, 100, 5839-5843.
- [30] M. J. S. Dewar et al. *J. Am. Chem. Soc.*, 103, 10, 2802, 1981.
- [31] Hideo Tomioka, *Acc. Chem. Res.* 1997, 30, 315-321.
- [32] Dötz, K. H.; Tomuschatt, P., *Chem. Soc. Rev.*, 1999, 28 187.
- [33] Wulff, W. D., *Organometallics*, 1998, 17, 3116.
- [34] Hegedus, L. S., *Tetrahedron*, 1997, 53, 4105.
- [35] de Meijer, A.; Schirmer, H.; Duetsch, M., *Angew. Chem. Int. Ed. Engl.*, 2000, 39, 3964.

- [36] Bernasconi, C. F., *Chem. Soc. Rev.*, 1997, 26, 299.
- [37] Harvey, D. F.; Sigano, D. M., *Chem. Rev.*, 1996, 96, 271.
- [38] Herndon, J. W., *Coord. Chem. Rev.*, 1999, 181, 177.
- [39] Dieter Enders and Tim Balensiefer, *Acc. Chem. Res.* 2004, 37, 534-541.
- [40] Wolfgang Kirmse, *Eur. Jour. Org. Chem.* 2005, 2, 2005, 237-260.
- [41] A.P. Wolf, *Adv. Phys. Org. Chem.* 2, 201, 1964.
- [42] R. F. Peterson and R. Wolfgang, *Adv. High. Temp. Chem.* 4, 43, 1971.
- [43] P. B. Shevlin, *J. Am. Chem. Soc.* 94, 1379, 1972.
- [44] Bergeat, A.; Loison, J-C. *Phys. Chem. Chem. Phys.*, 2001, 3, 2038 - 2042.
- [45] D. G. Williamson, and K. D. Bayes, *J. Am. Chem. Soc.* 90, 1957, 1967.
- [46] N. G. Moll and W. E. Thompson, *J. Chem. Phys.* 44, 2684, 1966.
- [47] D. E. Milligan and M. E. Jacox, *J. Chem. Phys.* 45, 1387, 1966.
- [48] D. E. Milligan and M. E. Jacox, *J. Chem. Phys.* 44, 2850, 1966.
- [49] D. Husain, A. X: Ioannou, *J. Photochem. Photobiol. A*, 129, 1-7, 1999.
- [50] Schreiner, P. R.; Reisenauer, H. P.; *ChemPhysChem* 2006, 7, 880.
- [51] Kaiser, R. I.; Lee, Y. T.; Suits, A. G. *J. Chem. Phys.* 1996, 105, 19, 8705.
- [52] Kaiser, R. I.; Stranges, D. ; Lee, Y. T.; Suits, A. G. *J. Chem. Phys.* 1996, 105, 19, 8721.
- [53] Kaiser, R. I.; Ochsenfeld, C. ; Head-Gordon, M.; Lee, Y. T.; Suits, A. G. *J. Chem. Phys.* 1997, 106, 5, 1729.
- [54] Kaiser, R. I.; Stranges, D. ; Lee, Y. T.; Bevsek, H. M. ; Suits, A. G. *J. Chem. Phys.* 1997, 106, 5, 4945.
- [55] Taylor, K. K.; Ache, H. J.; Wolf, A. P.; *J. Am. Chem. Soc.* 1975, 97, 5970.
- [56] Wolf, A. P.; *Adv. Phys. Org. Chem.* 1964, 2, 201.
- [57] Wolf, A. P. *Adv. Phys. Org. Chem.* 1964, 2, 201.
- [58] MacKay, C.; Polak, P.; Rosenberg, H. E.; Wolfgang, R. *J. Am. Chem. Soc.* 1962, 84, 308.
- [59] (a) Gaspar, P. P.; Berowitz, D. M.; Strongin, D. R.; Svoboda, D. L.; Tuchler, M. B.; Ferrieri, R. A; Wolf, A. P. *J. Phys. Chem.* 1986, 90, 4691.

- (b) Armstrong, B. M.; Zheng, F.; Shevlin, P. B. *J. Am. Chem. Soc.* 1998, 120, 6007.
- [60] Skell, P. S.; Havel, J. J.; McGlinchey, M. J. *Acc. Chem. Res.* 1973, 6, 97.
- [61] Kaiser, R. I.; Mebel, A. M.; *Int. Rev. Phys. Chem.* 2002, 21, 2, 307.
- [62] Dede, Y.; Özkan, İ. 2007 unpublished.
- [63] (a) Palino, G. F.; Voigt, A. F., Reactions of recoil carbon atoms in methanol and ethanol. *J. Amer. Chem. Society* 1969, 91, (2), 242-250.
- [64] Voigt, A. F.; Palino, G. F.; Williams, R. L., Reactions of Recoil Carbon Atoms with Oxygen-Containing Molecules.II. Structural Dependence of Carbon Monoxide Yields. *The Journal of Physical Chemistry* 1971, 75, (15).
- [65] Voigt, A. F.; Williams, R. L., Reactions of recoil carbon atoms with oxygen-containing molecules. III. Reaction mechanisms in methanol. 1971, 75, (15), 2253-2258.
- [66] Pan, W.; Shevlin, P. B.; 118, 10004, 1996.
- [67] Kaiser, R. I.; Nguyen T. L.; Lee, Y. T. *J. Chem. Phys.* 2002, 116, 4, 1318.
- [68] Skell, P. S.; Klabunde, K. J.; Plonka, J. H.; Roberts, J. S.; Williams-Smith, D. L.; *J. Am. Chem. Soc.* 1973, 95, 5, 1547.
- [69] Figuera, J. M.; Shevlin, P. B.; Worley, S. D.; *J. Am. Chem. Soc.* 1976, 98, 13, 3820.
- [70] Skell, P. S.; Plonka, J. H. *J. Am. Chem. Soc.* 1970, 92, 836.
- [71] Skell, P. S.; Harris, R. F. *J. Am. Chem. Soc.* 1969, 91, 4440.
- [72] Husain, D.; Kirsch, L. J. *Trans. Faraday Soc.* 1971, 67, 3166.
- [73]  $\Delta E_a = RT \ln(47)$  with  $T=300$  K, using simple collision theory result modified by a Boltzmann factor. See, e.g. Atkins, P.; Paula J. *Physical Chemistry, Seventh Edition*; Oxford University Press Inc., New York, 2002, pp 945.
- [74] Galland, N.; Caralp, F.; Rayes, M-T.; Hannachi, Y.; Loison, J-C.; Dorthe, G.; Bergeat, A. *J. Phys. Chem. A* 2001, 105, 9893.
- [75] (a) Ahmed S. N.; McKee M. L.; Shevlin P. B. *J. Am. Chem. Soc.* 1983, 105, 3942. b) Ahmed, S. N.; McKee, M. L.; Shevlin, P. B. *J. Am. Chem. Soc.* 1985, 107, 1320. (c) Jeong G. H.; Klabunde K. J.; Pan O. G.; Paul G. C.; Shevlin P. B. *J. Am. Chem. Soc.* 1989, 111, 8784.
- [76] Hwang, D-Y.; Mebel, A. M.; Wang, B. C. *Chem. Phys.* 1999, 244, 143.

- [77] Lowe, J. P., Quantum Chemistry, Academic Press Inc., 1978, New York, pp 1.
- [78] G98 Source Code 19999.exe Gaussian 98 (Rev. A.9), Gaussian, Inc., Pittsburgh PA, 1998.
- [79] Hinchliffe, Alan, Computational Quantum Chemistry, John Wiley & Sons Ltd., 1988, New York, pp x.
- [80] Richards, G. W.; Cooper, D. L. Ab Initio Molecular Orbital Calculations for Chemists, Oxford University Press: New York, 1983; pp 94 -101.
- [81] Hehre, W. J.; Random, L.; Scheleyer, P. v. R.; Pople, J. A. Ab Initio Molecular Orbital Theory; John Wiley & Sons: New York, 1986
- [82] J. Phys. Chem. A 2006, 110, 1031-1040 J. Daniel Figueroa-Villar et al.
- [83] Richards, G. W.; Cooper, D. L. Ab Initio Molecular Orbital Calculations for Chemists, Oxford University Press: New York, 1983; pp 94 -101.
- [84] Heitler, W.; London, F. Z Phys 1927, 44, 455.
- [85] Slater, J. C. Phys Rev 1930, 35, 509; Phys Rev 1931, 35, 1109;
- [86] Phys Rev 1932, 33, 255.
- [87] Clementi E, Corongiu G. 728. 105, 6, 2005, Comments on Computational Chemistry: From Diatomic Molecules to lArge Biochemical Systems.
- [88] Hartree, D. R. Proc Roy Soc A 1933, 141, 282.
- [89] Fock, V. Z Phys 1930, 62, 795.
- [90] Hund, F. R. Z Phys 1927, 40, 742; Z Phys 1927, 42, 93; Z Phys 1928, 51, 759.
- [91] See references in Herzberg, G. Spectra of Diatomic Molecules; D. Van Nostrand: Princeton, NJ, 1951.
- [92] Mulliken, R. S. Phys Rev 1928, 32, 186; Phys Rev 1928, 32,
- [93] Roothaan, C. C. J. Rev Mod Phys 1951, 23, 69.
- [94] Roothaan, C. C. J. Rev Mod Phys 1960, 32, 179.
- [95] Boys, S. F. Proc Roy Soc A 1950, 200, 542; see, in addition, McWeeny, R. F. Proc Roy Soc A 1946, 196, 215.
- [96] E. Schrödinger, Ann. Physik. 79 (1926) 361.
- [97] W. Pauli, Phys. Rev. 1940, 58. 716.
- [98] J. C. Slater, Phys. Rev. 35, 210 (1930).

- [99] Hartree, D. R. Proc. Camb. Phil. Soc. 1928, 24, 89.
- [100] Fock, V. Z. Phys. 1930, 61, 161.
- [101] Pople, J. A.; Nesbet, R. K. J. Chem. Phys., 22, 1954, 571.
- [102] D. E. Woon and T. H. Dunning Jr., J. Chem. Phys. 98, 1358 (1993).
- [103] R. A. Kendall, T. H. Dunning Jr. and R. J. Harrison, J. Chem. Phys. 96, 6796 (1992).
- [104] T. H. Dunning Jr., J. Chem. Phys. 90, 1007 (1989).
- [105] F Jensen, Introduction to Computational Chemistry. pp 169
- [106] S. F. Boys, Proc. Roy. Soc. (London) A201 (1950) 125.
- [107] J. A. Pople, J. S. Binkley, R. Seeger, Int. J. Quant. Chem. Symp. 10 (1976) 1.
- [108] Roos, B. O.; Taylor, P.; Siegbahn, P. E. Chem. Phys. 1980, 48, 157.
- [109] Ruedenberg, K.; Schmit, M. W.; Gilbert, M. M.; Elbert, S. T. Chem. Phys. 1982, 71, 1, 41.
- [110] Møller, C.; Plesset, M. S. Phys. Rev. 1934, 46, 618.
- [111] Roos, B. O.; Andersson, K.; Fulscher, P.; MAlmqvist, A.; Serrano-Andres, L.; Pierloot, K.; Merchan, M. Adv. Chem. Phys. 1996, 93, 219.
- [112] Hirao, K. Chem.Phys.Lett. 1993, 201, 59.
- [113] Nakano, H. J. Chem. Phys. 1993, 99, 7983.
- [114] Kozlowski, P. M.; Davidson, R. E. J. Chem. Phys. 1994, 100, 3672.
- [115] Cizek, J. J. Chem. Phys. 1966, 45, 4256.
- [116] Cizek, J. Adv. Chem. Phys. 1969, 14, 35.
- [117] Bartlett, R. J. J. Phys. Chem. 1989, 93, 1697.
- [118] J. A. Pople, R. Krishnan, H. B. Schlegel and J. S. Binkley, Int. J. Quant. Chem. 14, 545 (1978).
- [119] J. A. Pople, M. Head-Gordon and K. Raghavachari, J. Chem. Phys. 87, 5968 (1987).
- [120] Hohenberg, P. ; Kohn, W. Phys. Rev. B. 1964, 136, 864.
- [121] W. Kohn, L. J. Sham, Phys. Rev., 140, (1965), A1133.
- [122] A. D. Becke, J. Chem. Phys., 98, 5648, (1993)
- [123] C. Lee, W. Yang and R. G. Parr, Physical Review B, 37, 785, (1988)
- [124] Gaussian 03, Revision D.01, M. J. Frisch, G. W. Trucks, H. B. Schlegel, G. E. Scuseria, M. A. Robb, J. R. Cheeseman, J. A. Montgomery, Jr., T. Vreven, K. N. Kudin, J. C. Burant, J. M. Millam, S. S. Iyengar, J.

Tomasi, V. Barone, B. Mennucci, M. Cossi, G. Scalmani, N. Rega, G. A. Petersson, H. Nakatsuji, M. Hada, M. Ehara, K. Toyota, R. Fukuda, J. Hasegawa, M. Ishida, T. Nakajima, Y. Honda, O. Kitao, H. Nakai, M. Klene, X. Li, J. E. Knox, H. P. Hratchian, J. B. Cross, V. Bakken, C. Adamo, J. Jaramillo, R. Gomperts, R. E. Stratmann, O. Yazyev, A. J. Austin, R. Cammi, C. Pomelli, J. W. Ochterski, P. Y. Ayala, K. Morokuma, G. A. Voth, P. Salvador, J. J. Dannenberg, V. G. Zakrzewski, S. Dapprich, A. D. Daniels, M. C. Strain, O. Farkas, D. K. Malick, A. D. Rabuck, K. Raghavachari, J. B. Foresman, J. V. Ortiz, Q. Cui, A. G. Baboul, S. Clifford, J. Cioslowski, B. B. Stefanov, G. Liu, A. Liashenko, P. Piskorz, I. Komaromi, R. L. Martin, D. J. Fox, T. Keith, M. A. Al-Laham, C. Y. Peng, A. Nanayakkara, M. Challacombe, P. M. W. Gill, B. Johnson, W. Chen, M. W. Wong, C. Gonzalez, and J. A. Pople, Gaussian, Inc., Wallingford CT, 2004.

[125] (a) GAMESS: Schmidt, M. W.; Baldrige, K. K.; Boatz, J. A.; Elbert, S. T.; Gordon, M. S.; Jensen, J. J.; Koseki, S.; Matsunaga, N.; Nguyen, K. A.; Su, S.; Windus, T. L.; Dupuis, M.; Montgomery, J. A. *J. Comput. Chem.* 1993, 14, 1347.

[126] Özkan, İ., Unpublished.

[127] Schmidt, M. W.; Gordon, M. S. *Annu. Rev. Phys. Chem.* 1998, 49, 233.

[128] (a) Nakano, H. *J. Chem. Phys.* 1993, 99, 7983. (b) Nakano, H. *Chem. Phys. Lett.* 1993, 207, 372. (c) Hirao, K. *Chem. Phys. Lett.* 1992, 190, 374. (d) Hirao, K. *Chem. Phys. Lett.* 1992, 196, 397. (e) Hirao, K. *Chem. Phys. Lett.* 1993, 201, 59.

[129] GAMESS: Schmidt, M. W.; Baldrige, K. K.; Boatz, J. A.; Elbert, S. T.; Gordon, M. S.; Jensen, J. J.; Koseki, S.; Matsunaga, N.; Nguyen, K. A.; Su, S.; Windus, T. L.; Dupuis, M.; Montgomery, J. A. *J. Comput. Chem.* 1993, 14, 1347.

[130] Frisch, M. J.; Trucks, G. W.; Schlegel, H. B.; Scuseria, G. E.; Robb, M. A.; Cheeseman, J. R.; Zakrzewski, V. G.; Montgomery, J. A., Jr.; Stratmann, R. E.; Burant, J. C.; Dapprich, S.; Millam, J. M.; Daniels, A. D.; Kudin, K. N.; Strain, M. C.; Farkas, O.; Tomasi, J.; Barone, V.; Cossi, M.; Cammi, R.; Mennucci, B.; Pomelli, C.; Adamo, C.; Clifford, S.; Ochterski, J.; Petersson, G. A.; Ayala, P. Y.; Cui, Q.; Morokuma, K.; Malick, D. K.; Rabuck, A. D.; Raghavachari, K.; Foresman, J. B.; Cioslowski, J.; Ortiz, J. V.; Baboul, A. G.; Stefanov, B. B.; Liu, G.; Liashenko, A.; Piskorz, P.; Komaromi, I.; Gomperts, R.; Martin, R. L.; Fox, D. J.; Keith, T.; Al-Laham, M. A.; Peng, C. Y.; Nanayakkara, A.; Challacombe, M.; Gill, P. M. W.; Johnson, B.; Chen, W.; Wong, M. W.; Andres, J. L.; Gonzalez, C.; Head-Gordon, M.; Replogle, E. S.; Pople, J. A., Gaussian 98 (Rev. A.9), Gaussian, Inc., Pittsburgh PA, 1998.

[131] (a) Ishida, K.; Morokuma, K.; Komornicki, A. *J. Chem. Phys.* 1977, 66, 2153. (b) Fukui, K. *Acc. Chem. Res.* 1981, 14, 363.

- [132] Abrams, M. L.; Sherrill, C. D. *J. Phys. Chem. A*, 2003, 107 (29), 5611-5616.
- [133] Robinson, P. J.; Holbrook, K. A. *Unimolecular Reactions*; Wiley-Interscience, 1972.
- [134] Kaiser, R. I.; Ochsenfeld, C.; Head-Gordon, M.; Lee, Y. T. *J. Chem. Phys.* 1999, 110, 2391.
- [135] Numerous studies of the ground PESs of CH<sub>2</sub>O and HCO have been reported. See e.g., (a) Zhang, X.; Zou, S.; Harding, L. B.; Bowman, J. M. *J. Phys. Chem. A* 2004, 108, 8980. (b) Marenich, A. V.; Boggs, J. E. *J. Phys. Chem. A* 2003, 107, 2343; and the references therein.
- [136] Skell, P. S.; Klabunde, K. J.; Plonka, J. H.; Roberts, J. S.; Williams-Smith, D. L. *J. Am. Chem. Soc.* 1973, 95, 1547.
- [137] *Organic Chemistry*, 6th ed pp 755 New York Solomons, T. W. Graham. 1996 John Wiley & Sons.

## APPENDIX A

### ELECTRONIC AND ZERO POINT ENERGIES OF STATIONARY STRUCTURES AT VARIOUS LEVELS IN REACTIONS OF ATOMIC CARBON WITH METHANOL

Table A 1. Electronic and Zero Point Energies of Singlet Minima at B3LYP/6-311G(d,p) Level.

Label	Species	Energies	
		E <sub>SCF</sub> (AU) B3LYP/6-311G(d,p)	E <sub>ZPV</sub> (kcal/mol) B3LYP/6-311 G(d,p)
2	COH+Me	-153.673366	26.834260
3	COMe+H	-153.637311	26.490030
4	Me-O-C-H	-153.767885	34.346840
4'	cis-4	-153.761188	33.881340
5	HCO+Me	-153.740352	26.670370
6	MeCHO	-153.876861	34.647660
7	MeCO+H	-153.726772	26.960700
8	H <sub>2</sub> C=C=O+H <sub>2</sub>	-153.827324	26.136970
9	CO+Me+H	-153.699993	21.732310
10	H <sub>2</sub> C=O+CH <sub>2</sub> ( <sup>1</sup> A <sub>1</sub> )	-153.680699	26.965400
11	CO+CH <sub>4</sub>	-153.879983	31.153250
12	CO+H <sub>2</sub> +CH <sub>2</sub>	-153.670164	19.836030
13	H <sub>2</sub> C=CHOH	-153.856733	35.455200
14	H <sub>2</sub> O+C <sub>2</sub> H <sub>2</sub>	-153.802146	30.306910
16a	HO-CH <sub>2</sub> -C-H	-153.727844	32.284880
16b	HO-CH <sub>2</sub> -C-H	-153.722981	34.320490
17	H <sub>2</sub> C-CH <sub>2</sub> -O	-153.830129	35.808940
19	Me-C-OH	-153.794391	34.459150
20	H <sub>2</sub> C-CHO+H	-153.716865	26.533680
21	H <sub>2</sub> C-C-OH+H	-153.676990	26.871720
22	HC-CHOH+H	-153.669026	26.776770
23	H <sub>2</sub> C-OH+CH	-153.587579	27.382860
24	H <sub>2</sub> C-CH+OH	-153.681560	28.091930
25	MeO+CH	-153.578098	26.708680
26	HC-O-CH <sub>2</sub> +H	-153.598193	24.883840
27	H <sub>2</sub> +HO-C=CH	-153.767053	26.289860
28	Me-C+OH	-153.604104	27.266000
29	c-CH <sub>2</sub> CO+H <sub>2</sub>	-153.721261	26.450070
30	CHCHO+H <sub>2</sub>	-153.698791	24.981420
8b	H <sub>2</sub> C=C=O+2H	-153.647753	19.816330

**Table A 2. Electronic and Zero Point Energies of Singlet Minima Calculated at Various Coupled Cluster Levels as Specified.**

Label	Species	$E_{\text{SCF}}$ (AU)	$E_{\text{ZPV}}$ (kcal/mol)	$E_{\text{SCF}}$ (AU)	$E_{\text{SCF}}$ (AU)	$E_{\text{SCF}}$ (AU)
		CCSD/ 6-311G(d,p)	CCSD/ 6-311G(d,p)	CCSD(T)/ 6-311G(d,p)	CCSD/ cc-pVTZ	CCSD(T)/ cc-pVTZ
R(S)	C( <sup>1</sup> D)+MeOH	-153.162928	32.749480	-153.176785	-153.258141	-153.277931
1	C--OHMe	-153.189471	33.709220	-153.206336	-153.287649	-153.310801
1'	C--OHMe	-153.184040	34.860630	-153.201213	-153.281350	-153.304596
2	COH+Me	-153.268597	27.486350	-153.282366	-153.360853	-153.380105
3	COMe+H	-153.234004	27.395810	-153.250843	-153.325227	-153.347814
4	Me-O-C-H	-153.359950	35.012520	-153.377530	-153.455299	-153.478869
4'	cis-4	-153.352421	34.627857	-153.370355	-153.448732	-153.472724
5	HCO+Me	-153.331586	26.950100	-153.347813	-153.423268	-153.445003
6	MeCHO	-153.467139	35.239970	-153.485322	-153.562130	-153.586240
7	MeCO+H	-153.321090	27.375102	-153.339645	-153.411554	-153.435863
8	H <sub>2</sub> C=C=O+H <sub>2</sub>	-153.410368	26.339084	-153.431040	-153.504262	-153.530642
8b	H <sub>2</sub> C=C=O+2H	-153.242027	20.017553	-153.262699	-153.331926	-153.358305
9	CO+Me+H	-153.308630	21.856430	-153.325155	-153.394748	-153.416449
10	H <sub>2</sub> C=O+CH <sub>2</sub> ( <sup>1</sup> A <sub>1</sub> )	-153.279330	27.427185	-153.295212	-153.373754	-153.395169
11	CO+CH <sub>4</sub>	-153.481011	31.506624	-153.498766	-153.570296	-153.593565
12	CO+H <sub>2</sub> +CH <sub>2</sub>	-153.279214	19.976137	-153.295969	-153.367390	-153.389190
13	H <sub>2</sub> C=CHOH	-153.447671	35.804437	-153.465611	-153.545924	-153.570393
14	H <sub>2</sub> O+C <sub>2</sub> H <sub>2</sub>	-153.397495	30.484412	-153.415438	-153.495632	-153.519822
15	HO-CH <sub>2</sub> --H--C	-153.165107	33.563830	-153.183815	-153.262046	-153.286603
16a	HO-CH <sub>2</sub> -C-H	-153.317954	32.787700	-153.333706	-153.416645	-153.438568
16b	HO-CH <sub>2</sub> -C-H	-153.314440	34.909470	-153.332671	-153.412354	-153.436965
17	H <sub>2</sub> C-CH <sub>2</sub> -O	-153.421373	36.581290	-153.439349	-153.519415	-153.543605
19	Me-C-OH	-153.386869	35.134810	-153.404156	-153.481973	-153.505277
20	H <sub>2</sub> C-CHO+H	-153.309830	26.791000	-153.326330	-153.402175	-153.424473
21	H <sub>2</sub> C-C-OH+H	-153.269297	27.357700	-153.286827	-153.362910	-153.386480
22	HC-CHOH+H	-153.263007	27.305520	-153.280067	-153.357110	-153.380193
23	H <sub>2</sub> C-OH+CH	-153.187433	28.013640	-153.199371	-153.280958	-153.298381
24	H <sub>2</sub> C-CH+OH	-153.277508	28.565170	-153.290839	-153.371038	-153.389889
25	MeO+CH	-153.177362	27.550300	-153.188134	-153.269156	-153.285154
26	HC-O-CH <sub>2</sub> +H	-153.192970	25.394220	-153.209769	-153.285348	-153.307935
27	H <sub>2</sub> +HO-C=CH	-153.355284	26.494451	-153.374845	-153.450670	-153.476263
28	Me-C+OH	-153.203568	22.552570	-153.214862	-153.295880	-153.312547
29	c-CH <sub>2</sub> CO+H <sub>2</sub>	-153.315249	26.883591	-153.335542	-153.408770	-153.434873
30	CHCHO+H <sub>2</sub>	-153.280305	24.917931	-153.303282	-153.375428	-153.404009

**Table A 3. Electronic and Zero Point Energies of Triplet Minima at B3LYP/6-311G(d,p) Level.**

Label	Species	$E_{\text{SCF}}$ (AU)	
		B3LYP/6-311G(d,p)	B3LYP/6-311 G(d,p)
R(T)	C( $^3\text{P}$ )+MeOH	-153.613383	32.077090
1T	C--OHMe	-153.640923	33.612050
4T	Me-O-C-H	-153.727712	33.263690
6T	MeCHO	-153.759860	32.894790
10T	H <sub>2</sub> C=O+CH <sub>2</sub> ( $^3\text{B}_1$ )	-153.689827	27.521830
13T	H <sub>2</sub> C=CHOH	-153.755497	32.600780
15T	HO-CH <sub>2</sub> --H--C	-153.622721	31.881570
16T	HO-CH <sub>2</sub> -C-H	-153.727444	32.930560
17T	H <sub>2</sub> C-CH <sub>2</sub> -O	-153.742958	31.790470
18T	H <sub>2</sub> C-O-CH <sub>2</sub>	-153.738603	32.115400
19T	Me-C-OH	-153.749467	33.383150
31T	O( $^3\text{P}$ )+C <sub>2</sub> H <sub>4</sub>	-153.699364	31.882410

**Table A 4. Electronic and Zero Point Energies of Triplet Minima Calculated at Various Coupled Cluster Levels as Specified.**

Label	Species	$E_{\text{SCF}}$ (AU)		$E_{\text{ZPV}}$ (kcal/mol)	$E_{\text{SCF}}$ (AU)	
		CCSD/ 6-311G(d,p)	CCSD(T)/ 6-311G(d,p)		CCSD(T)/ 6-311G(d,p)	CCSD/ cc-pVTZ
R(T)	C( $^3\text{P}$ )+MeOH	-153.224023	32.749480	-153.235298	-153.314659	-153.331487
1T	C--OHMe	-153.239589	34.101376	-153.253691	-153.331323	-153.351546
4T	Me-O-C-H	-153.318921	33.983404	-153.333763	-153.413515	-153.434265
6T	MeCHO	-153.347683	33.721733	-153.362150	-153.441096	-153.461314
10T	H <sub>2</sub> C=O+CH <sub>2</sub> ( $^3\text{B}_1$ )	-153.300575	27.910504	-153.315189	-153.391669	-153.411648
13T	H <sub>2</sub> C=CHOH	-153.344593	33.304730	-153.359042	-153.440684	-153.461056
15T	HO-CH <sub>2</sub> --H--C	-153.224825	33.770000	-153.236280	-153.313601	-153.330679
16T	HO-CH <sub>2</sub> -C-H	-153.328488	34.204810	-153.342356	-153.422960	-153.442735
17T	H <sub>2</sub> C-CH <sub>2</sub> -O	-153.333025	32.535380	-153.346180	-153.427335	-153.446158
18T	H <sub>2</sub> C-O-CH <sub>2</sub>	-153.326692	32.894050	-153.341417	-153.423023	-153.443644
19T	Me-C-OH	-153.341992	34.188930	-153.356547	-153.436018	-153.456492
31T	O( $^3\text{P}$ )+C <sub>2</sub> H <sub>4</sub>	-153.305131	32.033530	-153.318008	-153.394853	-153.412720

**Table A 5. Electronic and Zero Point Energies of Singlet Transition Structures at B3LYP/6-311G(d,p) Level.**

<b>Label</b>	<b>E<sub>SCF</sub> (AU) B3LYP/6-311G(d,p)</b>	<b>E<sub>ZPV</sub> (kcal/mol) B3LYP/6-311 G(d,p)</b>
1/3	-153.604981	28.974050
2/9	-153.662728	22.601810
3/9	-153.636823	25.337890
4/5	-153.725230	29.805280
4/4'	-153.718445	32.451990
4/6	-153.689872	32.024690
4/10	-153.690943	30.463090
4'/11	-153.712126	30.837920
4'/5	-153.733179	29.929160
5/9	-153.701058	22.057300
6/8	-153.743420	29.107700
6/11	-153.743272	30.698210
6/13	-153.765948	31.328730
6/19	-153.743328	30.874780
13/14	-153.727943	30.618790
7/9	-153.696238	23.736700
16a/16b	-153.713697	33.016840
16a/27	-153.669980	28.890020
16b/17	-153.714694	32.206130
28/24	-153.591389	24.911710
21/8b	-153.630064	20.684070

**Table A 6. Electronic and Zero Point Energies of Singlet Transition Structures Calculated at Various Coupled Cluster Levels as Specified.**

Label	E <sub>SCF</sub> (AU) CCSD/ 6-311G(d,p)	E <sub>ZPV</sub> (kcal/mol) CCSD/ 6-311G(d,p)	E <sub>SCF</sub> (AU) CCSD(T)/ 6-311G(d,p)	E <sub>SCF</sub> (AU) CCSD/ cc-pVTZ	E <sub>SCF</sub> (AU) CCSD(T)/ cc-pVTZ
1/19	-153.149100	31.670390	-153.171115	-153.248250	-153.276596
1/2	-153.187191	32.253361	-153.207362	-153.284468	-153.310811
1/3	-153.184294	30.141791	-153.205893	-153.280817	-153.308450
1/4	-153.174556	31.538627	-153.193911	-153.272562	-153.298257
2/9	-153.250589	22.745930	-153.266881	-153.341111	-153.363014
3/9	-153.229268	25.371464	-153.247999	-153.319445	-153.344065
4/5	-153.288299	30.047665	-153.340353	-153.379143	-153.436629
4/4'	-153.309348	33.060966	-153.325844	-153.406340	-153.428888
4/6	-153.275720	32.783606	-153.296762	-153.373122	-153.400628
4/10	-153.275156	31.338330	-153.296989	-153.370624	-153.398764
4'/11	-153.296384	30.485720	-153.341345	-153.388250	-153.438991
5/9	-153.299437	22.383660	-153.316575	-153.387809	-153.410303
6/8	-153.318660	29.566365	-153.343666	-153.416407	-153.447757
6/11	-153.322641	31.163377	-153.346911	-153.417226	-153.447844
6/13	-153.347005	31.974747	-153.369737	-153.445019	-153.474165
6/19	-153.329154	31.420310	-153.351128	-153.425947	-153.454115
13/14	-153.310857	31.624596	-153.332699	-153.409078	-153.437612
7/9	-153.294687	24.396314	-153.313424	-153.382796	-153.407179
15/16a	-153.161801	32.506160	-153.178227	-153.257541	-153.280175
16a/16b	-153.308648	33.715400	-153.324589	-153.406067	-153.428159
16a/27	-153.249392	29.681350	-153.269826	-153.348876	-153.375949
16b/17	-153.303203	32.903340	-153.325188	-153.400847	-153.429315
28/24	-153.186468	25.537780	-153.200640	-153.280205	-153.299948
21/8b	-153.208353	20.990150	-153.229336	-153.301404	-153.328551

**Table A 7. Electronic and Zero Point Energies of Triplet Transition Structures at B3LYP/6-311G(d,p) Level.**

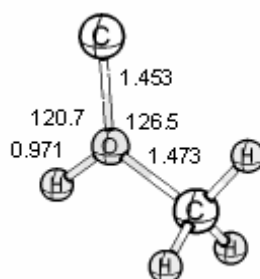
Label	$E_{\text{SCF}}$ (AU)		$E_{\text{ZPV}}$ (kcal/mol)	
	B3LYP/6-311G(d,p)		B3LYP/6-311 G(d,p)	
15T/16T	-153.617471		30.372310	
1T/19T	-153.592482		31.681160	
1T/2	-153.621172		31.445750	
1T/3	-153.604213		28.615090	
1T/4T	-153.617975		30.137370	
4T/5	-153.709839		30.734960	
4T/6T	-153.660243		31.447610	
4T/18T	-153.667597		29.704360	
6T/5	-153.734674		30.185240	
6T/7	-153.720394		28.241780	
6T/13T	-153.701778		30.025280	
6T/17T	-153.692126		29.692060	
6T/20	-153.691058		27.723020	
6T/19T	-153.698396		30.381410	
13T/19T	-153.672513		30.079390	
13T/16T	-153.664698		29.652820	
18T/10T	-153.685823		29.028760	
17T/10T	-153.698519		29.089340	
17T/20	-153.711699		27.845260	
13T/20	-153.699055		27.714140	
13T/21	-153.671869		27.612450	
13T/24	-153.689901		30.157000	
19T/7	-153.712445		28.272500	
16T/22	-153.669376		27.895320	

**Table A 8. Electronic and Zero Point Energies of Triplet Transition Structures Calculated at Various Coupled Cluster Levels as Specified.**

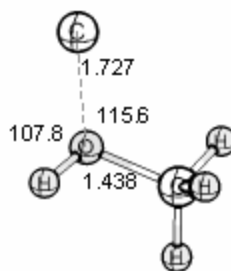
Label	E <sub>SCF</sub> (AU) CCSD/ 6-311G(d,p)	E <sub>ZPV</sub> (kcal/mol) CCSD/ 6-311G(d,p)	E <sub>SCF</sub> (AU) CCSD(T)/ 6-311G(d,p)	E <sub>SCF</sub> (AU) CCSD/ cc-pVTZ	E <sub>SCF</sub> (AU) CCSD(T)/ cc-pVTZ
15T/16T	-153.207121	31.151490	-153.224372	-153.302428	-153.326036
1T/19T	-153.176344	32.424671	-153.195441	-153.273000	-153.298649
1T/2	-153.203223	31.821634	-153.221418	-153.297103	-153.321709
1T/3	-153.185039	29.705672	-153.203851	-153.278935	-153.304046
1T/4T	-153.207163	30.950024	-153.225628	-153.301974	-153.326828
4T/5	-153.289502	30.968221	-153.307455	-153.382996	-153.407208
4T/6T	-153.243711	32.129114	-153.262304	-153.340249	-153.365196
4T/18T	-153.253789	30.360820	-153.271094	-153.349524	-153.373052
6T/5	-153.316959	30.802559	-153.334962	-153.410691	-153.434765
6T/7	-153.305027	28.887400	-153.323870	-153.397752	-153.422633
6T/13T	-153.283845	30.698520	-153.301938	-153.379933	-153.404357
6T/17T	-153.270632	30.342470	-153.288623	-153.366510	-153.390801
6T/19T	-153.284097	31.066200	-153.301696	-153.379491	-153.403296
13T/19T	-153.256460	30.802330	-153.273435	-153.353256	-153.376521
13T/16T	-153.250680	30.368220	-153.267026	-153.347583	-153.370168
18T/10T	-153.269993	29.501760	-153.286391	-153.363366	-153.385864
17T/10T	-153.289732	30.038120	-153.305107	-153.383279	-153.404526
17T/20	-153.296631	28.293340	-153.312434	-153.391151	-153.412885
13T/20	-153.277311	28.022720	-153.295997	-153.372794	-153.397679
13T/21	-153.255719	28.225990	-153.274165	-153.351110	-153.375636
13T/24	-153.272981	30.710530	-153.289837	-153.368586	-153.391614
19T/7	-153.292933	28.787140	-153.311208	-153.385964	-153.410428
16T/22	-153.256238	28.443620	-153.273207	-153.351698	-153.374774

## APPENDIX B

### SINGLET PES, CCSD/6-311G(d,p) OPTIMIZED GEOMETRIES AND CARTESIAN COORDINATES OF MINIMA IN REACTIONS OF ATOMIC CARBON WITH METHANOL

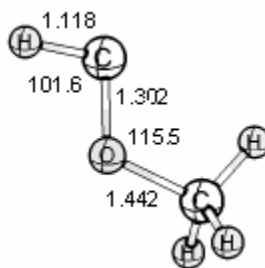


Atomic Number	Coordinates (Angstroms)		
	X	Y	Z
6	1.452648000	0.466130000	0.000000000
8	0.000000000	0.441546000	0.000000000
6	-0.856651000	-0.756650000	0.000000000
1	-0.510004000	1.267348000	0.000000000
1	-0.129260000	-1.566016000	0.000000000
1	-1.468359000	-0.745291000	0.905384000
1	-1.468359000	-0.745291000	-0.905384000



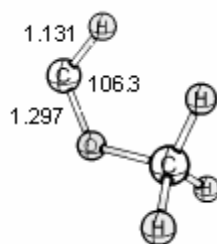
1'

Atomic Number	X	Y	Z
6	0.00000000	0.00000000	0.00000000
8	0.00000000	0.00000000	1.72747400
6	1.29695100	0.00000000	2.34941700
1	1.18001200	0.00000000	3.43495200
1	1.84765700	0.89146400	2.04269700
1	1.88140000	-0.74402900	1.80453000
1	-0.56615100	0.64099500	2.16686700



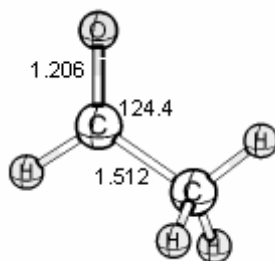
4

Atomic Number	X	Y	Z
6	1.109984000	0.135101000	-0.000010000
8	-0.206588000	-0.454016000	0.000010000
1	1.628054000	-0.218170000	-0.894281000
1	1.009701000	1.221978000	-0.000575000
1	1.627683000	-0.217232000	0.894848000
6	-1.198858000	0.389206000	0.000007000
1	-2.079492000	-0.300291000	-0.000056000



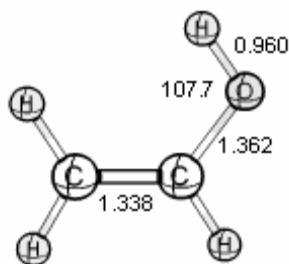
4'

Atomic Number	Coordinates (Angstroms)		
	X	Y	Z
6	-1.081431000	0.160108000	-0.000001000
8	0.205446000	-0.503569000	-0.000003000
1	-1.619284000	-0.160739000	-0.894321000
1	-1.618900000	-0.159964000	0.894830000
1	-0.931044000	1.244236000	-0.000493000
6	1.326560000	0.149475000	0.000004000
1	1.054885000	1.247521000	-0.000010000



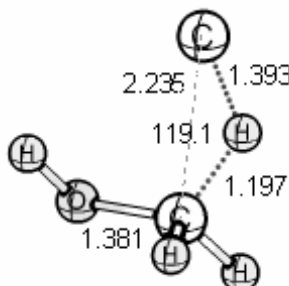
6

Atomic Number	Coordinates (Angstroms)		
	X	Y	Z
6	1.172178000	-0.147392000	-0.000009000
6	-0.236976000	0.401097000	-0.000049000
8	-1.233305000	-0.278861000	0.000011000
1	1.707620000	0.218437000	0.884575000
1	1.149447000	-1.239306000	-0.000741000
1	1.708292000	0.219697000	-0.883652000
1	-0.310130000	1.509830000	0.000084000



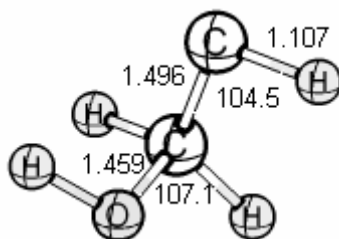
13

Atomic Number	X	Y	Z
6	-0.032563000	0.442810000	-0.000003000
8	1.209048000	-0.118121000	-0.000018000
6	-1.203096000	-0.205148000	-0.000010000
1	0.034449000	1.526709000	0.000039000
1	-1.261852000	-1.291055000	-0.000058000
1	1.099061000	-1.071525000	0.000170000
1	-2.130088000	0.354863000	0.000074000



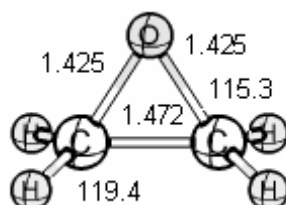
15

Atomic Number	X	Y	Z
6	-1.757004000	-0.297513000	-0.021149000
8	1.037499000	-0.492394000	-0.084283000
6	0.267447000	0.645905000	0.052830000
1	0.625197000	-1.168683000	0.458928000
1	-0.796192000	0.594304000	-0.493510000
1	0.100402000	0.983694000	1.078567000
1	0.707946000	1.439488000	-0.559810000



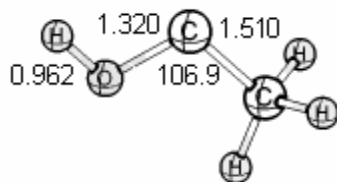
16a

Atomic Number	X	Y	Z
1	-1.308421000	-0.712149000	0.841511000
6	-0.089599000	0.730970000	-0.008546000
8	0.849530000	-0.377140000	0.131428000
6	-1.008969000	-0.435325000	-0.187904000
1	0.129022000	1.354319000	-0.877879000
1	1.024686000	-0.703088000	-0.756259000
1	-0.050116000	1.304166000	0.919907000



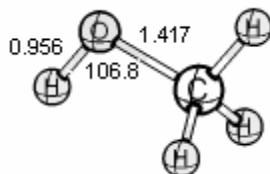
17

Atomic Number	X	Y	Z
1	-1.269826457	-0.645070409	-0.921945809
6	0.735735227	-0.423079439	0.000000334
8	0.000036877	0.797388286	-0.000000693
6	-0.735778773	-0.423036987	-0.000000643
1	1.269785570	-0.645202017	0.921932150
1	-1.269830427	-0.645070862	0.921948191
1	1.269804540	-0.645220564	-0.921919850



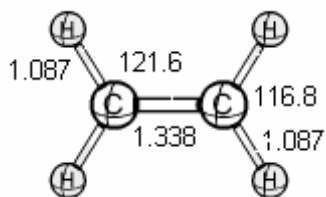
19

Atomic Number	Coordinates (Angstroms)		
	X	Y	Z
8	1.100922000	0.282119000	0.000000000
6	0.137395000	-0.619553000	-0.000001000
6	-1.170171000	0.136226000	-0.000001000
1	1.933305000	-0.199837000	-0.000001000
1	-1.741742000	-0.192876000	-0.877131000
1	-1.060587000	1.228533000	-0.000037000
1	-1.741693000	-0.192818000	0.877183000



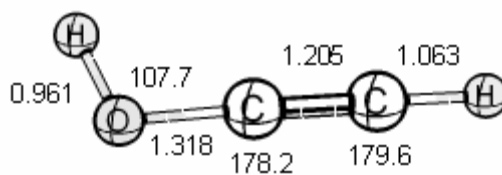
**Methanol**

Atomic Number	Coordinates (Angstroms)		
	X	Y	Z
6	-0.046899000	0.659601000	0.000000000
8	-0.046899000	-0.757167000	0.000000000
1	-1.091639000	0.979761000	0.000000000
1	0.439751000	1.076887000	0.893225000
1	0.439751000	1.076887000	-0.893225000
1	0.868719000	-1.033799000	0.000000000



**Ethylene**

Atomic Number	Coordinates (Angstroms)		
	X	Y	Z
6	0.000000000	0.000000000	0.668919000
6	0.000000000	0.000000000	-0.668919000
1	0.000000000	0.925721000	-1.238825000
1	0.000000000	-0.925721000	-1.238825000
1	0.000000000	-0.925721000	1.238825000
1	0.000000000	0.925721000	1.238825000

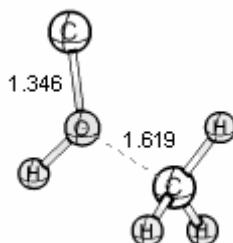


**CHCOH**

Atomic Number	Coordinates (Angstroms)		
	X	Y	Z
6	0.000000000	0.123891000	0.000000000
6	0.233711000	1.306485000	0.000000000
8	-0.295718000	-1.160438000	0.000000000
1	0.432340000	2.351178000	0.000000000
1	0.531139000	-1.649929000	0.000000000

## APPENDIX C

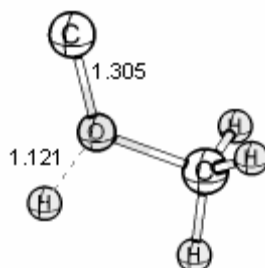
### SINGLET PES, CCSD/6-311G(d,p) OPTIMIZED GEOMETRIES AND CARTESIAN COORDINATES OF TRANSITION STRUCTURES IN REACTIONS OF ATOMIC CARBON WITH METHANOL



1/2

Im. Freq. (cm<sup>-1</sup>) = -706.2950

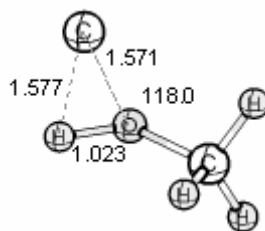
Atomic Number	Coordinates (Angstroms)		
	X	Y	Z
6	-1.209192000	-0.177900000	-0.000027000
8	0.320559000	0.351430000	0.000095000
1	-1.030751000	-1.250579000	-0.001777000
1	-1.669711000	0.199263000	0.914535000
1	0.319620000	1.324450000	-0.000284000
1	-1.671124000	0.202134000	-0.912740000
6	1.457107000	-0.369885000	-0.000054000



1/3

Im. Freq. (cm<sup>-1</sup>) = -1549.0497

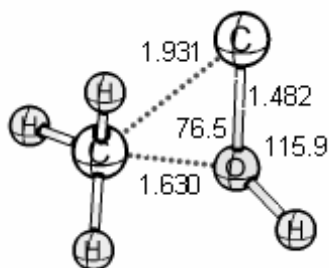
Atomic Number	Coordinates (Angstroms)		
	X	Y	Z
6	-1.092242000	-0.196829000	-0.000249000
1	-1.737268000	0.691776000	-0.039946000
1	-1.208274000	-0.762263000	0.922091000
1	-1.179094000	-0.828543000	-0.881442000
8	0.283489000	0.349774000	-0.000580000
6	1.376312000	-0.363550000	0.000585000
1	0.152301000	1.463108000	0.001916000



1/4

Im. Freq. (cm<sup>-1</sup>) = -1348.6686

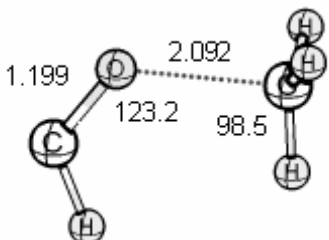
Atomic Number	Coordinates (Angstroms)		
	X	Y	Z
6	-1.470162000	0.392576000	0.006740000
6	1.115714000	0.201207000	0.029190000
8	-0.163853000	-0.470997000	-0.122943000
1	1.021076000	1.113621000	-0.562868000
1	1.281986000	0.444733000	1.079887000
1	-0.760359000	-0.887008000	0.595920000
1	1.894807000	-0.466067000	-0.344976000



1'/19

Im. Freq. (cm<sup>-1</sup>) = -1182.1452

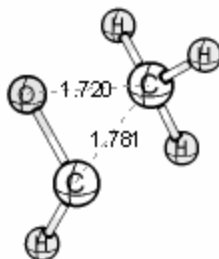
Atomic Number	X	Y	Z
6	-0.806920000	0.838411000	-0.022965000
8	-0.498552000	-0.602721000	0.128608000
6	0.971916000	0.088235000	-0.001858000
1	-0.791254000	-1.191541000	-0.619190000
1	1.405599000	0.232321000	0.979159000
1	0.963653000	0.969140000	-0.673271000
1	1.420439000	-0.748030000	-0.566624000



4/5

Im. Freq. (cm<sup>-1</sup>) = -397.4412

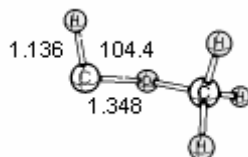
Atomic Number	X	Y	Z
6	-1.193358000	0.831901000	0.000000000
8	0.000000000	0.717485000	0.000000000
6	0.974206000	-1.133297000	0.000000000
1	-1.840971000	-0.082630000	0.000000000
1	1.527645000	-1.037699000	0.924109000
1	1.527645000	-1.037699000	-0.924109000
1	0.100593000	-1.773471000	0.000000000



4/6

Im. Freq. (cm<sup>-1</sup>) = -1006.0802

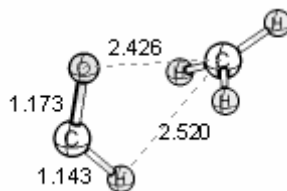
Atomic Number	Coordinates (Angstroms)		
	X	Y	Z
8	0.556828000	-0.681817000	-0.025495000
6	0.704457000	0.596858000	0.192589000
1	1.128328000	1.088159000	-0.734563000
6	-0.987644000	0.075247000	-0.002845000
1	-1.333576000	-0.729394000	-0.658954000
1	-1.393283000	0.042746000	0.999492000
1	-1.156972000	1.020391000	-0.540486000



4/4'

Im. Freq. (cm<sup>-1</sup>) = -1063.3687

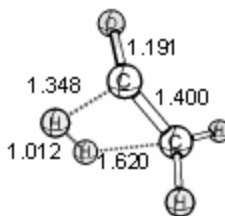
Atomic Number	Coordinates (Angstroms)		
	X	Y	Z
6	-1.076736000	0.180633000	-0.008817000
8	0.171310000	-0.503703000	0.057997000
1	-1.197055000	0.665002000	-0.984763000
1	-1.846442000	-0.577995000	0.128343000
1	-1.154369000	0.932574000	0.788288000
6	1.279928000	0.220943000	-0.194547000
1	1.608239000	0.600580000	0.824335000



4'/11

Im. Freq. (cm<sup>-1</sup>) = -307.3105

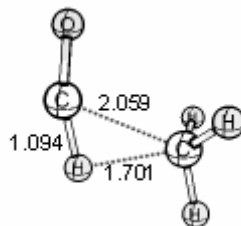
Atomic Number	Coordinates (Angstroms)		
	X	Y	Z
8	0.781705000	-0.612450000	0.000000000
6	-1.555342000	0.038786000	0.000000000
6	1.226763000	0.472829000	0.000000000
1	-1.124118000	0.348756000	-0.938979000
1	-2.597165000	-0.271478000	0.000000000
1	-1.124118000	0.348756000	0.938979000
1	0.563234000	1.403880000	0.000000000



6/8

Im. Freq. (cm<sup>-1</sup>) = -1822.7559

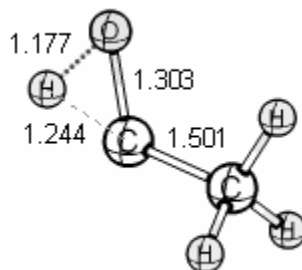
Atomic Number	Coordinates (Angstroms)		
	X	Y	Z
6	1.182893000	-0.224648000	0.031844000
6	-0.150423000	0.179575000	-0.108977000
8	-1.273258000	-0.195867000	0.019084000
1	0.600811000	1.157602000	0.643810000
1	1.432857000	-1.275738000	0.168538000
1	1.927880000	0.440284000	-0.391615000
1	0.029705000	1.515222000	-0.110611000



6/11

Im. Freq. (cm<sup>-1</sup>) = -1845.7965

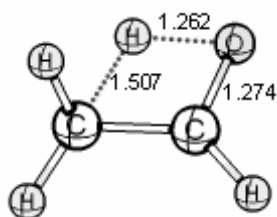
Atomic Number	Coordinates (Angstroms)		
	X	Y	Z
6	1.379019000	-0.144095000	0.000000000
6	-0.551785000	0.571461000	0.000000000
8	-1.278940000	-0.345796000	0.000000000
1	2.261875000	0.506625000	-0.000003000
1	1.332688000	-0.754151000	0.906054000
1	1.332684000	-0.754155000	-0.906051000
1	0.340874000	1.203851000	0.000000000



6/19

Im. Freq. (cm<sup>-1</sup>) = -2202.2363

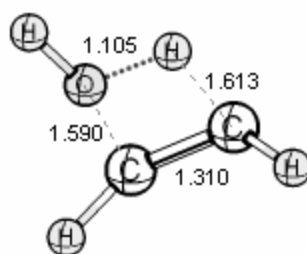
Atomic Number	Coordinates (Angstroms)		
	X	Y	Z
1	1.028583000	1.234793000	0.000000000
6	-1.105472000	-0.480373000	0.000000000
6	0.000000000	0.534330000	0.000000000
8	1.218823000	0.072887000	0.000000000
1	-1.735145000	-0.325394000	0.883624000
1	-0.676049000	-1.490845000	0.000000000
1	-1.735145000	-0.325394000	-0.883624000



13/6

Im. Freq. (cm<sup>-1</sup>) = -2409.2859

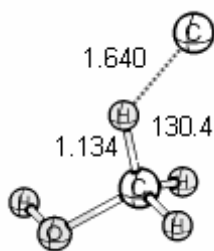
Atomic Number	Coordinates (Angstroms)		
	X	Y	Z
6	-0.117842000	0.534969000	0.045047000
8	-1.098873000	-0.275484000	-0.021490000
6	1.108227000	-0.184850000	-0.052051000
1	-0.320751000	1.606050000	0.131930000
1	1.284419000	-0.772917000	0.852338000
1	-0.120755000	-1.014644000	-0.320557000
1	2.005762000	0.284671000	-0.449760000



13/14

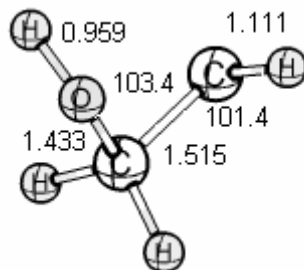
Im. Freq. (cm<sup>-1</sup>) = -1241.0954

Atomic Number	Coordinates (Angstroms)		
	X	Y	Z
1	-2.209049000	-0.239636000	0.044057000
6	-0.280776000	0.589382000	0.001465000
8	1.110477000	-0.173172000	-0.102187000
6	-1.134081000	-0.403884000	0.020616000
1	-0.090331000	1.653629000	-0.034579000
1	1.539526000	-0.153275000	0.764738000
1	0.365179000	-0.988330000	-0.089205000



15/16

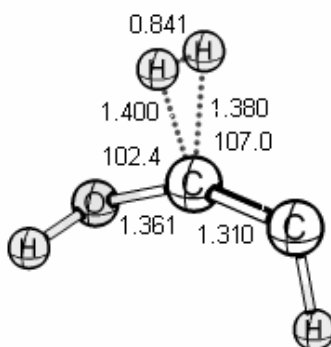
Atomic Number	Coordinates (Angstroms)		
	X	Y	Z
1	0.628938000	-0.382510000	-0.048163000
6	-0.184652000	0.401106000	0.055951000
8	-1.425284000	-0.230648000	-0.127843000
6	2.261319000	-0.228667000	-0.028537000
1	-0.076226000	0.884385000	1.034045000
1	-1.552318000	-0.831854000	0.606911000
1	-0.058130000	1.140529000	-0.734534000



16a/16b

Im. Freq. (cm<sup>-1</sup>) = -468.0055

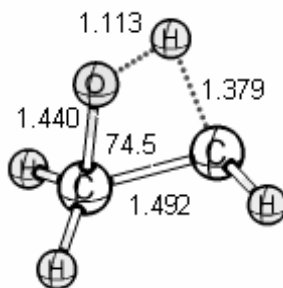
Atomic Number	Coordinates (Angstroms)		
	X	Y	Z
1	-1.211903000	-0.942554000	0.763133000
6	-0.082443000	0.594626000	0.016039000
8	1.029985000	-0.306121000	0.093843000
6	-1.269564000	-0.329530000	-0.161683000
1	0.050858000	1.303160000	-0.809727000
1	1.156164000	-0.657462000	-0.789622000
1	-0.122960000	1.155245000	0.959338000



16a/27

Im. Freq. (cm<sup>-1</sup>) = -1356.1659

Atomic Number	Coordinates (Angstroms)		
	X	Y	Z
1	1.569249000	-1.202272000	-0.064999000
6	0.128497000	0.182793000	-0.006834000
8	-1.172108000	-0.204022000	-0.109829000
6	1.402661000	-0.121420000	0.019100000
1	0.016174000	1.490898000	0.479478000
1	-1.433849000	-0.538655000	0.751303000
1	0.038342000	1.513965000	-0.360746000



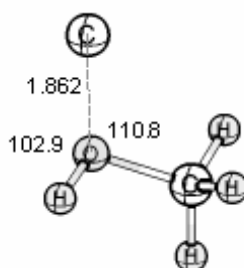
16b/17

Im. Freq. (cm<sup>-1</sup>) = -1354.6286

Atomic Number	Coordinates (Angstroms)		
	X	Y	Z
1	-1.447869000	-0.284502000	0.848815000
6	0.206520000	0.738927000	-0.017076000
8	0.674469000	-0.619078000	0.087505000
6	-1.010504000	-0.114274000	-0.144894000
1	0.577580000	1.266282000	-0.895405000
1	-0.092827000	-1.035740000	-0.603355000
1	0.391270000	1.258669000	0.921725000

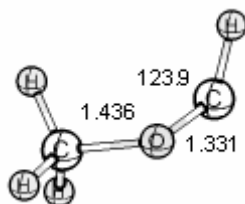
## APPENDIX D

### TRIPLET PES, UCCSD/6-311G(d,p) OPTIMIZED GEOMETRIES AND CARTESIAN COORDINATES OF MINIMA IN REACTIONS OF ATOMIC CARBON WITH METHANOL



**1T**

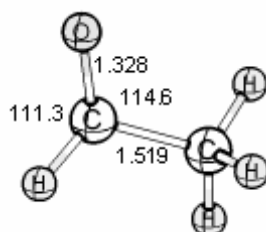
Atomic Number	X	Coordinates (Angstroms) Y	Z
6	1.654601000	-0.373444000	0.025844000
6	-1.070588000	-0.310523000	0.024277000
8	0.055201000	0.567616000	-0.131735000
1	-1.032932000	-1.001982000	-0.816979000
1	-0.999205000	-0.871528000	0.960741000
1	0.083434000	1.165492000	0.620357000
1	-1.996984000	0.270892000	-0.010960000



4T

---

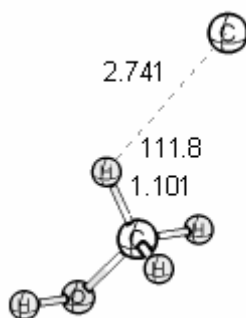
Atomic Number	Coordinates (Angstroms)		
	X	Y	Z
6	1.079803000	0.195166000	-0.000692000
8	-0.162603000	-0.523077000	-0.047221000
1	1.224690000	0.641628000	0.988022000
1	1.864980000	-0.536357000	-0.198877000
1	1.095458000	0.978786000	-0.766649000
6	-1.249098000	0.216017000	0.165571000
1	-1.868532000	0.633459000	-0.634005000



6T

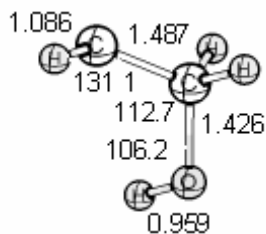
---

Atomic Number	Coordinates (Angstroms)		
	X	Y	Z
6	-1.157294000	-0.162061000	0.019123000
6	0.199890000	0.498873000	-0.145393000
8	1.235455000	-0.313624000	0.029265000
1	-1.937354000	0.563562000	-0.226149000
1	-1.247571000	-1.015626000	-0.659782000
1	-1.310443000	-0.519633000	1.047232000
1	0.356153000	1.459817000	0.362202000



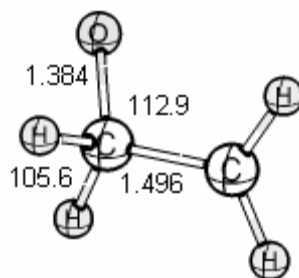
15T

Atomic Number	X	Y	Z
1	0.549712000	1.465528000	0.109265000
6	0.383922000	0.386076000	-0.015466000
8	1.595465000	-0.342783000	-0.089456000
6	-2.877570000	-0.182586000	0.019061000
1	-0.260920000	0.035544000	0.804578000
1	2.049976000	-0.210028000	0.742039000
1	-0.140595000	0.230279000	-0.961807000



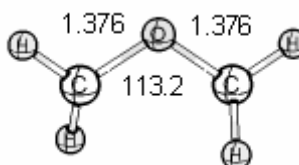
16T

Atomic Number	X	Y	Z
1	-1.761864000	-0.974432000	0.549541000
6	-0.052645000	0.538565000	0.000128000
8	1.107299000	-0.285859000	0.096895000
6	-1.307272000	-0.250086000	-0.120390000
1	0.023466000	1.240582000	-0.842950000
1	1.104577000	-0.843237000	-0.683100000
1	-0.065068000	1.133084000	0.922924000



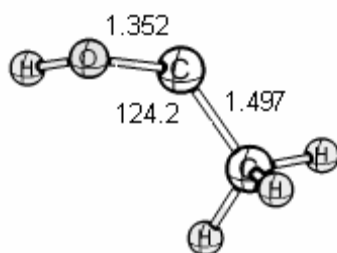
17T

Atomic Number	Coordinates (Angstroms)		
	X	Y	Z
8	1.190407000	-0.361257000	-0.087182000
6	-1.204930000	-0.222498000	-0.021402000
6	0.108205000	0.487645000	0.068350000
1	-1.303374000	-1.204023000	0.429135000
1	-2.065403000	0.247635000	-0.484714000
1	0.160800000	1.347673000	-0.617863000
1	0.265061000	0.907889000	1.089209000



18T

Atomic Number	Coordinates (Angstroms)		
	X	Y	Z
6	0.000000000	1.148720000	-0.225139000
8	0.000000000	0.000000000	0.532072000
6	0.000000000	-1.148720000	-0.225139000
1	-0.029116000	2.046245000	0.381158000
1	0.559302000	1.121496000	-1.158613000
1	-0.559302000	-1.121496000	-1.158613000
1	0.029116000	-2.046245000	0.381158000

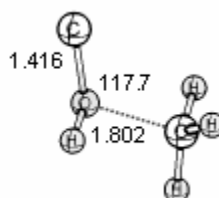


**19T**

Atomic Number	Coordinates (Angstroms)		
	X	Y	Z
6	0.098172000	0.518698000	0.021285000
6	-1.253988000	-0.122828000	0.007620000
8	1.260470000	-0.157113000	-0.116266000
1	-2.028986000	0.646688000	0.061506000
1	-1.399438000	-0.700020000	-0.917047000
1	-1.384590000	-0.806689000	0.860805000
1	1.664155000	-0.258290000	0.751431000

## APPENDIX E

### TRIPLET PES, UCCSD/6-311G(d,p) OPTIMIZED GEOMETRIES AND CARTESIAN COORDINATES OF TRANSITION STRUCTURES IN REACTIONS OF ATOMIC CARBON WITH METHANOL



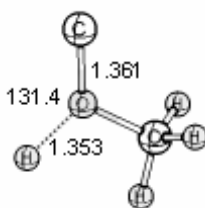
1T/2

Im. Freq. (cm<sup>-1</sup>) = -1364.3879

---

Atomic Number	Coordinates (Angstroms)		
	X	Y	Z
6	-1.289997000	-0.188982000	0.021059000
8	0.385738000	0.453832000	-0.136927000
1	-1.270482000	-0.892777000	-0.804377000
1	-1.294752000	-0.640982000	1.010089000
1	0.407047000	1.077866000	0.605552000
1	-1.937996000	0.674175000	-0.116240000
6	1.458378000	-0.452508000	0.045673000

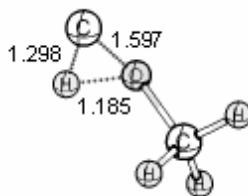
---



**1T/3**

Im. Freq. (cm<sup>-1</sup>) = -2601.2689

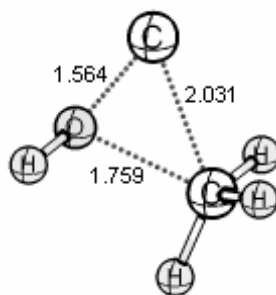
Atomic Number	X	Y	Z
6	1.053374000	-0.226168000	0.000001000
1	1.754129000	0.611073000	-0.000227000
1	1.163657000	-0.833012000	-0.900476000
1	1.163819000	-0.832658000	0.900698000
8	-0.256217000	0.381003000	-0.000004000
6	-1.375532000	-0.393482000	0.000003000
1	-0.098923000	1.724475000	0.000015000



**1T/4T**

Im. Freq. (cm<sup>-1</sup>) = -1346.6098

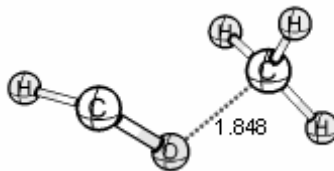
Atomic Number	X	Y	Z
6	-1.440141000	0.376116000	-0.050385000
6	1.079212000	0.216801000	0.016384000
8	-0.138443000	-0.548831000	-0.092063000
1	1.303989000	0.624061000	-0.971618000
1	0.948882000	1.034150000	0.731734000
1	-0.849069000	-0.362535000	0.837743000
1	1.869316000	-0.462530000	0.342653000



**1T/19T**

Im. Freq. (cm<sup>-1</sup>) = -1238.5887

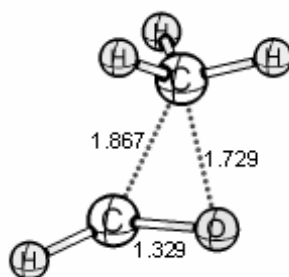
Atomic Number	Coordinates (Angstroms)		
	X	Y	Z
6	-1.034302000	0.084122000	-0.009928000
8	0.561972000	-0.643818000	0.120675000
6	0.829713000	0.889945000	-0.024686000
1	-1.483696000	-0.899491000	-0.183870000
1	-1.255943000	0.462358000	0.981118000
1	-1.276083000	0.778760000	-0.810687000
1	0.747478000	-1.035479000	-0.744275000



**4T/5**

Im. Freq. (cm<sup>-1</sup>) = -957.3543

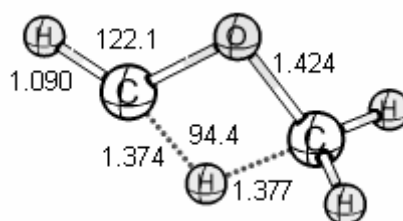
Atomic Number	Coordinates (Angstroms)		
	X	Y	Z
6	1.340329000	0.172496000	0.004457000
8	-0.372124000	-0.520477000	-0.059273000
1	1.390557000	0.592639000	1.005337000
1	1.932504000	-0.722198000	-0.161290000
1	1.339695000	0.892617000	-0.810215000
6	-1.311015000	0.255253000	0.168547000
1	-1.861646000	0.834264000	-0.597678000



**4T/6T**

Im. Freq. (cm<sup>-1</sup>) = -1418.3065

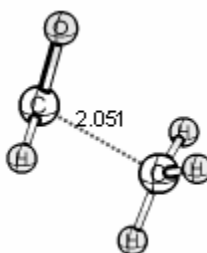
Atomic Number	Coordinates (Angstroms)		
	X	Y	Z
8	0.477406000	0.734405000	0.023441000
6	0.808550000	-0.539941000	-0.154553000
1	1.414442000	-1.129613000	0.543864000
6	-1.008841000	-0.148894000	0.017671000
1	-1.559430000	0.791906000	-0.098489000
1	-1.279159000	-0.814438000	-0.806234000
1	-1.193347000	-0.590084000	0.994624000



**4T/18T**

Im. Freq. (cm<sup>-1</sup>) = -2252.5272

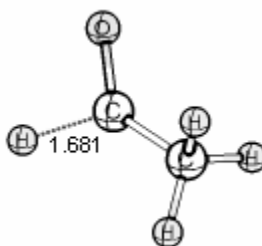
Atomic Number	Coordinates (Angstroms)		
	X	Y	Z
6	0.991380000	-0.224429000	-0.019602000
8	-0.115583000	0.670749000	0.015414000
6	-1.021814000	-0.356304000	0.061675000
1	1.599943000	-0.122427000	-0.918352000
1	1.519710000	-0.309544000	0.929611000
1	0.038480000	-1.213759000	-0.109203000
1	-2.050872000	-0.235863000	-0.277808000



6T/5

Im. Freq. (cm<sup>-1</sup>) = -543.1638

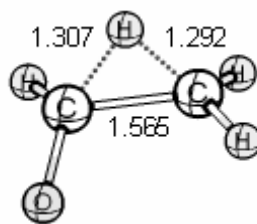
Atomic Number	X	Y	Z
6	-1.40640000	-0.14692000	0.01076200
6	0.51249800	0.55031800	-0.18523800
8	1.23538400	-0.38837900	0.05118900
1	-1.97290900	0.74724000	-0.23684200
1	-1.39305600	-0.93023000	-0.74071200
1	-1.44563200	-0.47818900	1.04516900
1	0.29193400	1.34782900	0.56973400



6T/7

Im. Freq. (cm<sup>-1</sup>) = -1258.7764

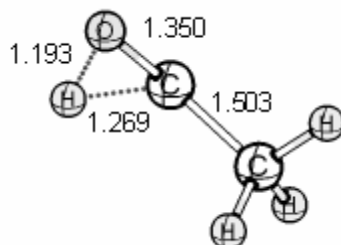
Atomic Number	X	Y	Z
6	-1.18811600	-0.12452400	0.05734900
6	0.24929100	0.26150900	-0.34702900
8	1.24641000	-0.23124900	0.10991700
1	-1.89116500	0.66251300	-0.21719400
1	-1.42400400	-1.03102400	-0.51007300
1	-1.24595000	-0.34084800	1.12924700
1	0.22278200	1.73743900	0.45676400



**6T/17T**

Im. Freq. (cm<sup>-1</sup>) = -1990.3751

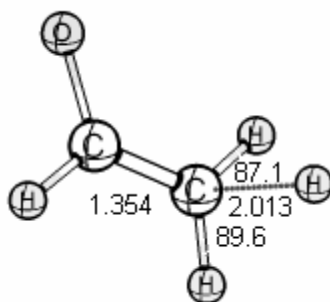
Atomic Number	Coordinates (Angstroms)		
	X	Y	Z
6	1.166594000	-0.209863000	-0.022634000
8	-1.160109000	-0.343309000	-0.066754000
6	-0.210646000	0.524237000	0.098101000
1	0.721833000	0.427645000	1.009128000
1	1.132046000	-1.275236000	0.169985000
1	1.899650000	0.206859000	-0.705271000
1	-0.208345000	1.500962000	-0.392610000



**6T/19T**

Im. Freq. (cm<sup>-1</sup>) = -2170.1007

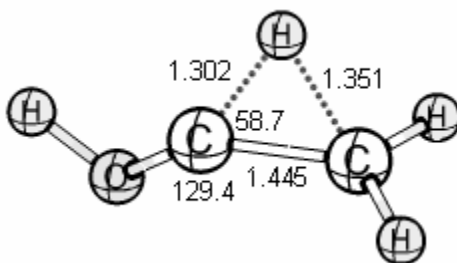
Atomic Number	Coordinates (Angstroms)		
	X	Y	Z
6	-1.243254000	-0.106463000	0.035419000
8	1.297717000	-0.238081000	-0.010583000
6	0.141432000	0.437264000	-0.181162000
1	-1.462534000	-0.852469000	-0.739453000
1	-1.338188000	-0.585754000	1.019304000
1	-1.975609000	0.700981000	-0.042711000
1	1.005532000	0.657081000	0.721984000



6T/20

Im. Freq. (cm<sup>-1</sup>) = -809.4916

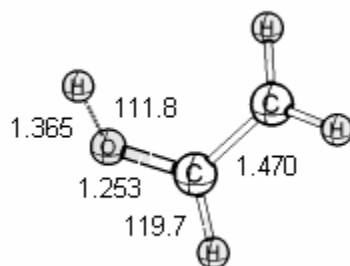
Atomic Number	Coordinates (Angstroms)		
	X	Y	Z
6	-1.089103000	-0.073093000	-0.209957000
6	0.151371000	0.409215000	0.041204000
8	1.280709000	-0.278997000	-0.000044000
1	-1.913894000	0.625685000	-0.260913000
1	-1.224422000	-1.071346000	-0.609853000
1	-1.813082000	-0.781010000	1.529290000
1	0.332125000	1.441915000	0.354344000



13T/19T

Im. Freq. (cm<sup>-1</sup>) = -2195.5977

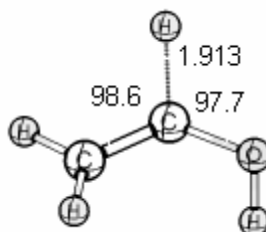
Atomic Number	Coordinates (Angstroms)		
	X	Y	Z
6	-1.293559000	-0.138396000	-0.001391000
6	0.045700000	0.395427000	-0.102433000
1	-1.549187000	-0.746607000	0.867520000
8	1.247630000	-0.253317000	-0.029064000
1	1.899203000	0.392060000	0.253212000
1	-0.874209000	1.001334000	0.591448000
1	-1.969691000	-0.162432000	-0.856722000



**13T/20**

Im. Freq. (cm<sup>-1</sup>) = -2282.6310

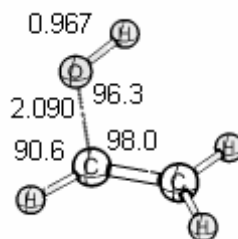
Atomic Number	Coordinates (Angstroms)		
	X	Y	Z
6	-1.227062000	-0.200322000	-0.004302000
6	0.070446000	0.490770000	-0.030845000
1	-2.096304000	0.275446000	0.438902000
8	1.144283000	-0.153699000	-0.076429000
1	1.133049000	-1.220277000	0.775367000
1	0.093726000	1.574588000	0.135792000
1	-1.345043000	-1.142852000	-0.527743000



**13T/21**

Im. Freq. (cm<sup>-1</sup>) = -1121.5471

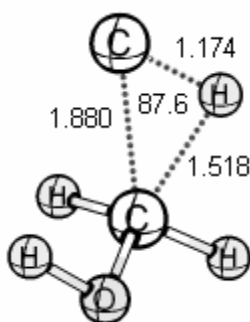
Atomic Number	Coordinates (Angstroms)		
	X	Y	Z
6	-0.013887000	0.303381000	-0.297907000
8	1.216471000	-0.092335000	0.042797000
6	-1.223276000	-0.208085000	0.031376000
1	-0.075207000	1.891808000	0.766724000
1	-2.106709000	0.097754000	-0.516588000
1	1.230280000	-1.054642000	0.048136000
1	-1.357153000	-0.768012000	0.958539000



**13T/24**

Im. Freq. (cm<sup>-1</sup>) = -506.2182

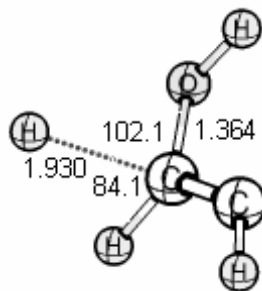
Atomic Number	Coordinates (Angstroms)		
	X	Y	Z
6	-0.436796000	0.724549000	-0.196325000
8	1.439989000	-0.152292000	0.081442000
6	-1.187225000	-0.356958000	0.054904000
1	-0.126313000	1.593206000	0.367176000
1	-1.540925000	-1.004845000	-0.744938000
1	1.291685000	-0.907448000	-0.504606000
1	-1.400233000	-0.668122000	1.079358000



**15T/16T**

Im. Freq. (cm<sup>-1</sup>) = -765.5837

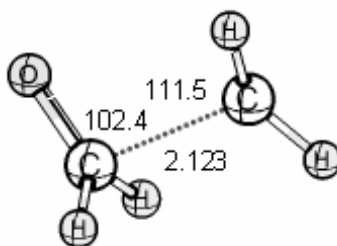
Atomic Number	Coordinates (Angstroms)		
	X	Y	Z
1	1.141155000	0.408582000	-0.764812000
6	-0.100597000	0.598152000	0.087827000
8	-1.061981000	-0.349345000	-0.098784000
6	1.488472000	-0.403338000	0.008258000
1	0.135966000	0.878883000	1.118734000
1	-0.784852000	-1.125298000	0.400495000
1	-0.323667000	1.463709000	-0.540659000



16T/22

Im. Freq. (cm<sup>-1</sup>) = -877.8054

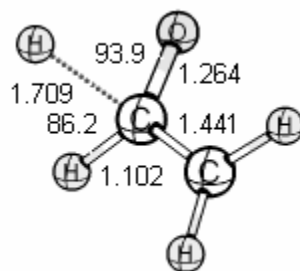
Atomic Number	Coordinates (Angstroms)		
	X	Y	Z
6	-1.218207000	-0.384697000	0.052308000
8	1.176350000	-0.151565000	-0.008871000
6	-0.092574000	0.311473000	-0.197741000
1	-2.275292000	-0.177799000	-0.017158000
1	-0.284622000	1.570136000	1.253342000
1	1.113595000	-0.943013000	0.531127000
1	-0.099793000	1.202539000	-0.823744000



17T/10T

Im. Freq. (cm<sup>-1</sup>) = -489.4942

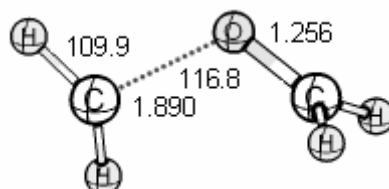
Atomic Number	Coordinates (Angstroms)		
	X	Y	Z
6	0.490603000	0.547953000	0.067850000
8	1.159773000	-0.478386000	-0.067572000
1	0.292875000	0.975391000	1.066964000
1	0.302966000	1.226716000	-0.783620000
6	-1.498246000	-0.184693000	-0.057011000
1	-2.231244000	0.595365000	-0.231057000
1	-1.596929000	-1.149948000	0.423252000



17T/20

Im. Freq. (cm<sup>-1</sup>) = -1099.6941

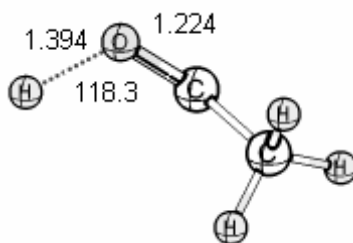
Atomic Number	Coordinates (Angstroms)		
	X	Y	Z
8	1.152191000	-0.349580000	-0.025657000
6	-1.195926000	-0.197677000	0.010208000
6	0.120060000	0.373985000	-0.124666000
1	-1.289593000	-1.208402000	0.392656000
1	-2.085048000	0.380138000	-0.220781000
1	0.190777000	1.358259000	-0.615420000
1	0.421533000	1.208792000	1.335554000



18T/10T

Im. Freq. (cm<sup>-1</sup>) = -847.5473

Atomic Number	Coordinates (Angstroms)		
	X	Y	Z
6	-1.225990000	0.221365000	0.035436000
8	-0.246533000	-0.558701000	-0.066998000
1	-1.699669000	0.648791000	-0.857890000
1	-1.580104000	0.558087000	1.018073000
6	1.473009000	0.212895000	0.067776000
1	1.544210000	1.222658000	-0.325676000
1	2.225709000	-0.565489000	0.082207000



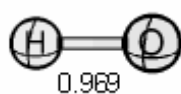
19T/7

Im. Freq. (cm<sup>-1</sup>) = -2097.4689

Atomic Number	Coordinates (Angstroms)		
	X	Y	Z
6	0.133664000	-0.445083000	-0.203348000
6	-1.247878000	0.119789000	0.029305000
8	1.193520000	0.028962000	0.185182000
1	-2.012356000	-0.634422000	-0.165003000
1	-1.335769000	0.495311000	1.055621000
1	-1.390667000	0.956781000	-0.668351000
1	1.875916000	0.902390000	-0.659457000

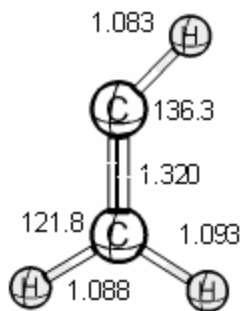
## APPENDIX F

### CCSD/6-311G(d,p) OPTIMIZED GEOMETRIES AND CARTESIAN COORDINATES OF SOME RADICALIC SPECIES IN REACTIONS OF ATOMIC CARBON WITH METHANOL



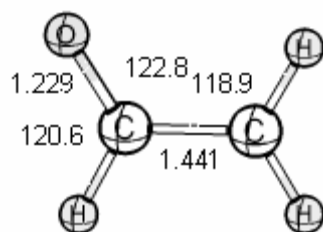
**Singlet OH radical**

Atomic Number	Coordinates (Angstroms)		
	X	Y	Z
8	0.000000000	0.000000000	0.107692000
1	0.000000000	0.000000000	-0.861534000



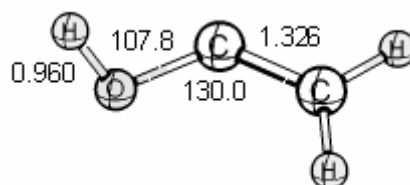
**Doublet CH<sub>2</sub>CH radical**

Atomic Number	Coordinates (Angstroms)		
	X	Y	Z
6	0.050319000	-0.591615000	0.000000000
6	0.050319000	0.727906000	0.000000000
1	-0.881459000	-1.163714000	0.000000000
1	0.975174000	-1.165410000	0.000000000
1	-0.697549000	1.511375000	0.000000000



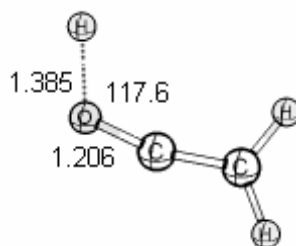
Doublet CH<sub>2</sub>-CHO radical

Atomic Number	X	Y	Z
6	1.054737000	-0.548006000	0.000000000
6	0.000000000	0.433375000	0.000000000
8	-1.191233000	0.130838000	0.000000000
1	2.099337000	-0.252391000	0.000000000
1	0.791421000	-1.601012000	0.000000000
1	0.310687000	1.494483000	0.000000000



Doublet CH<sub>2</sub>-COH radical

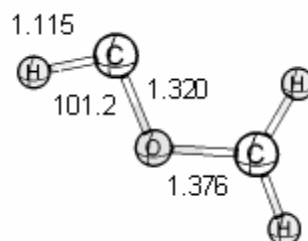
Atomic Number	X	Y	Z
6	-0.027224000	-0.418843000	-0.019522000
8	1.171108000	0.181358000	-0.080095000
6	-1.243288000	0.108717000	0.020143000
1	-2.119418000	-0.523230000	-0.055949000
1	1.747522000	-0.250994000	0.554551000
1	-1.373892000	1.184121000	0.138433000



**TS CH<sub>2</sub>-COH/CH<sub>2</sub>-CO + H**

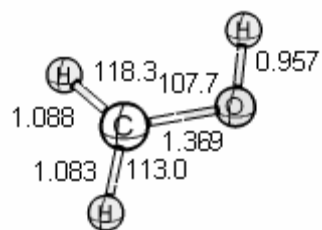
Im. Freq. (cm<sup>-1</sup>) = -2054.2230

Atomic Number	Coordinates (Angstroms)		
	X	Y	Z
6	0.000000000	0.183361000	0.000000000
8	-1.203454000	0.101870000	0.000000000
6	1.291710000	-0.065107000	0.000000000
1	1.625739000	-1.099942000	0.000000000
1	-1.760732000	-1.165805000	0.000000000
1	2.012363000	0.741256000	0.000000000



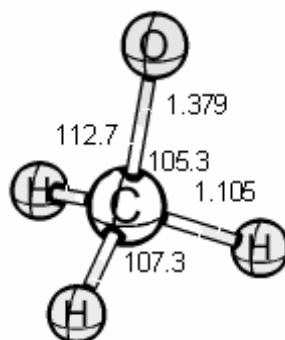
**Doublet CH<sub>2</sub>O-CH radical**

Atomic Number	Coordinates (Angstroms)		
	X	Y	Z
6	-1.123755000	0.157390000	-0.029800000
1	-1.949043000	-0.524193000	0.112660000
1	-1.147601000	1.236447000	0.046976000
6	1.154112000	0.371940000	0.007480000
8	0.114469000	-0.441450000	-0.004787000
1	1.998747000	-0.356634000	0.012580000



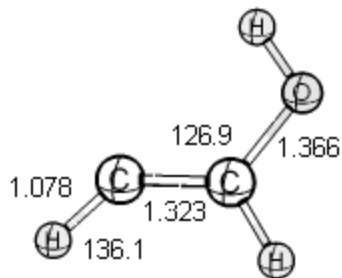
Doublet CH<sub>2</sub>OH radical

Atomic Number	X	Y	Z
6	0.683972000	0.027744000	-0.076644000
8	-0.672462000	-0.124515000	0.028601000
1	1.228577000	-0.889796000	0.111012000
1	1.119812000	0.982344000	0.210171000
1	-1.072524000	0.737111000	-0.090127000



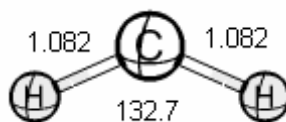
Doublet CH<sub>3</sub>O radical

Atomic Number	X	Y	Z
8	0.009134000	0.797204000	0.000000000
6	0.009134000	-0.582033000	0.000000000
1	-1.056657000	-0.872840000	0.000000000
1	0.464389000	-1.006298000	0.906293000
1	0.464389000	-1.006298000	-0.906293000



Doublet CH-CHOH radical

Atomic Number	X	Y	Z
6	-0.108911000	0.390289000	-0.000408000
8	1.166013000	-0.099906000	0.000135000
6	-1.229653000	-0.312228000	-0.000032000
1	-0.110489000	1.480646000	0.000760000
1	-2.285292000	-0.091785000	0.000758000
1	1.099060000	-1.057975000	0.000049000

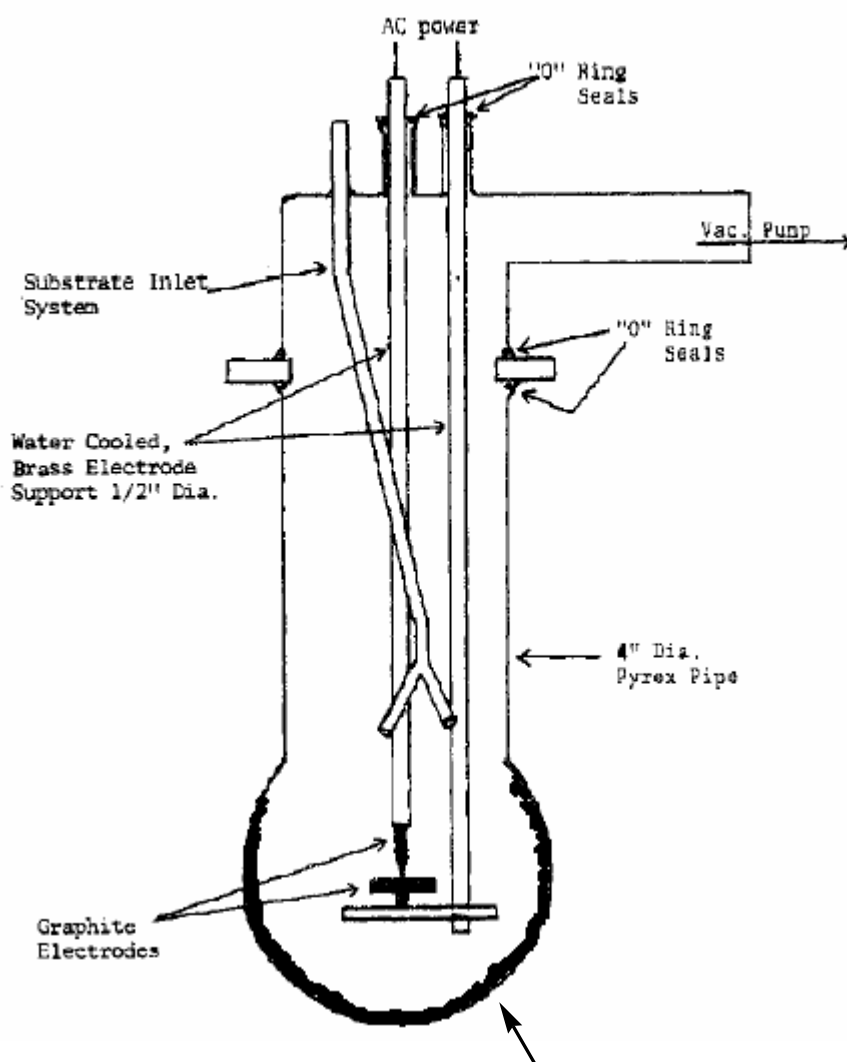


Triplet methylene

Atomic Number	X	Y	Z
6	0.000000000	0.000000000	0.108650000
1	0.000000000	0.991415000	-0.325951000
1	0.000000000	-0.991415000	-0.325951000

## APPENDIX G

### THE APPARATUS USED IN ARC CARBON REACTIONS AS DESCRIBED BY SKELL



Frozen substrate in the inner walls of the chamber kept at 77 K with liquid nitrogen.

*The picture is taken from "Skell, P. S.; Havel, J. J.; McGlinchey, M. J. Acc. Chem. Res. 1973, 6, 97." and modified.*

## CURRICULUM VITAE

Surname: Dede

Name: Yavuz

Date and place of birth: September 6th 1977, Zonguldak.

Email address: dedey@alumni.bilkent.edu.tr

Education:

**Ph.D.:** Middle East Technical University Faculty of Arts and Sciences  
Department of Chemistry 2002 – 2007.

Thesis: Quantum Chemical Investigations of the Reactions of Atomic Carbon (C) with Water and Methanol

Supervisor: Prof. Dr. İlker Özkan

**M.S.:** Middle East Technical University Faculty of Arts and Sciences  
Department of Chemistry 1999 – 2002.

Thesis: Supramolecules for Constructing Nanoscale Devices.

Supervisor: Prof. Dr. Engin Umut Akkaya

**B.S.:** Bilkent University Faculty of Science Department of Chemistry 1995 – 1999. (Full undergraduate scholarship)

Graduation Work: Determination of Trace Element Levels in Human Scalp Hair in Occupationally Exposed Subjects by XRF.

### **Awards and Degrees:**

Bilkent University undergraduate full scholarship 1995 – 1999

Scientific and Technical Research Council of Turkey, Scholarship for students with outstanding performance in the national university entrance examination, 1995 – 1996.

National University Entrance Examination, (8th in ranking in the nationwide exam among ~1,500,000 students), 1995

High School: Milli Piyango Anatolian High School, Ankara (ranking the 2nd in the graduate class of 1995)

### **Publications:**

Y.Dede, H. N. Erten, A. Zararsiz, N.Efe; Determination of trace element levels in human scalp hair in occupationally exposed subjects by XRF, Journal of Radioanalytical and Nuclear Chemistry, Vol.247, No 2 393-397(2001)